Validation of an Air Dispersion Model for Odour Impact Assessment

By
Tamer G. Alexan Gorgy

A Thesis Submitted to the Faculty of Graduate Studies and Research Through the Department of Civil Engineering and Applied Mechanics in Partial Fulfillment of the Requirements for the Degree of Master in Civil Engineering at McGill University

McGill

McGill University
Montreal, Quebec, Canada
July, 2003

Abstract

Odorous emissions can result in physiological and psychological discomfort when released and subsequently perceived by people in the neighbouring community. Regulatory agencies, as well as members of the industrial and agricultural sectors, are obliged to develop methods for mitigating or preventing odorous impacts on communities. It has been proposed that combined application of the Industrial Source Complex-Short Term3 (ISCST3) dispersion model and the Odour Impact Model (OIM) can provide an improved basis for predicting odorous impacts. The objective of this investigation was to validate the use of ISCST3 and the OIM to predict the impact of emissions from a hog farm in rural Quebec in terms of probability of response and degree of annoyance. This was accomplished by predicting the impact through modelling for comparison with on-site field measurements that were conducted on three different occasions.

The ISCST3 dispersion model was used to predict odour concentrations in the region in the immediate vicinity of the farm. Subsequently, the predicted concentrations were used in combination with the dose-response curves of the OIM to predict the probability of response and annoyance that would be experienced in the region surrounding the hog farm. When compared to field measurements, it was concluded that the model resulted in reasonably accurate predictions provided that the predicted one-hour time-averaged concentrations from the dispersion model were first transformed to one-minute time-averaged values. Overall, once this transformation was made, there was a tendency to slightly under predict the probability of response and to slightly over predict the degree of annoyance. The difference in these tendencies may result from differences in the ways that odour are characterized in the laboratory as compared to how they are experienced in the field.

Sommaire

Les émissions odorantes peuvent induire un malaise physiologique et psychologique une fois libérées et peuvent plus tard être perçues par les personnes de la communauté voisine. Les organismes de normalisation, ainsi que les membres des secteurs industriels et agricoles, sont obligés de développer des méthodes pour atténuer ou empêcher les impacts des odeurs sur les communautés. Il est proposé que l'application combinée du modèle de dispersion Industrial Source Complex-Short Term 3 (ISCST3) et du modèle Odour Impact Model (OIM) puisse fournir une meilleure base pour prévoir l'impact des émissions odorantes. L'objectif de cette recherche était de valider l'utilisation d'ISCST3 et de OIM afin de prévoir l'impact des émissions d'une porcherie rurale au Québec en termes de probabilité de réponse et de degré d'inconfort. Ceci a été accompli en simulant l'impact pour le comparer aux mesures sur le terrain qui ont été conduites à trois occasions différentes.

Le modèle de dispersion ISCST3 a été employé pour prédire les concentrations d'odeur dans la région à une proximité immédiate de la ferme. Ensuite, les concentrations prévues ont été utilisées en combinaison avec les courbes de dose-réponse obtenues de OIM pour prévoir la probabilité de réponse et d'inconfort qui serait expérimentée dans la région entourant la porcherie. Une fois comparé aux mesures sur le terrain, il a été conclu que le modèle donnait des prévisions raisonnablement précises à condition que les concentrations prévues par le temps moyen d'une heure obtenu par le modèle de dispersion aient été d'abord transformées en valeurs de temps moyen d'une minute. De façon générale, une fois que cette transformation a été faite, il y a eu une tendance à légèrement sous prévoir légèrement la probabilité de réponse et de sur prévoir le degré d'inconfort. La différence dans ces tendances peut résulter des différences dans les manières dont les odeurs sont caractérisées dans les laboratoires par rapport à la façon dont elles sont expérimentées sur le terrain.

Acknowledgements

Table of Contents

List of Figures

List of Tables

1 Introduction

The rapid development of the industrial and agricultural sectors has brought with it increasing concerns about their impact on the environment. One of these concerns is air quality and the nature of complaints received due to air pollution. In 1994, a survey of regulatory agencies in the USA revealed that almost 60% of the air pollution complaints were related to malodours (Leonardos, 1996). A number of other countries have reported an increase in complaints due to agricultural and industrial related odours. These complaints have increased due to two main reasons: (a) an increase in the number and size of facilities, and (b) an increase in residential development near these types of sources (Mahin, 2001).

An odour is defined as a sensation resulting from the reception of a stimulus by the olfactory sensory system (Sikdar, 2001; Law et al, 2002). Odours can cause long-term adverse physiological and psychological reactions in exposed populations. For example, exposed individuals have claimed that they were forced at times to stay indoors because of tearing eyes, that they suffered from sleep depravation, and were sometimes unable to eat their meals without experiencing nausea (Turk et al., 1979). In addition, individuals have reported that they became "very irritable, upset and nervous" (Turk et al., 1979). With such types of effects and outcomes, regulatory agencies, as well as the industrial and agricultural sectors are obliged to develop methods for mitigating or preventing odorous impacts on communities. One of the approaches that are often taken to serve this purpose is to predict odour levels in a community that arise from a particular odour emission. Such predictions can serve as a basis for establishing whether the emission is likely to cause an adverse impact.

It is common for regulatory agencies to regulate odorous emissions quantitatively. This involves the dilution to threshold (D/T) or odour unit criteria. An odour unit (OU) is a measure of odour concentration describing the number of unit volumes of odourless gas required to dilute one unit volume of odorous gas to reach the odour threshold (Law et al., 2002; Nicell, 1994). The odour threshold is defined as "the odour concentration at

1

which 50% of a panel of odour judges notice a stimulus as being different from odour free samples" (Nicell, 2003). Regulatory agencies can choose to limit the ambient concentration to a maximum of 1 OU at a sensitive receptor (e.g., a residence, apartment building, office building, park, school or mall) or anywhere at or beyond the property line of the plant. Compliance with the one odour unit standard can be established either by measuring the odour concentration in the ambient air or by predicting odour concentrations using an appropriate dispersion modeling technique.

Odorous emissions released into the atmosphere are dispersed and often perceived by people in the neighbouring community. Dispersion modeling has become a popular means for predicting odour concentration levels in the community while taking into account such factors as source odour concentration, gas flow rate, and local geographic and meteorological conditions. The Industrial Source Complex Short Term 3 (ISCST3) model is a widely used dispersion model. It is a steady-state Gaussian plume model that is used to assess air pollutant concentrations from a wide variety of emission types that are associated with industrial or agricultural sources. Emissions can be of point (e.g., stacks and vents), area (e.g., storage piles and lagoons), line and/or volume (e.g., multiple vents, building roof monitors and conveyor belts) types. ISCST3 was developed by the U.S Environmental Protection Agency and, after undergoing extensive field-testing and validation, is now used as a regulatory approved modeling option for air quality guidelines. It has the ability to model multiple sources simultaneously using real time meteorological data to account for the atmospheric conditions that can affect the distribution of the air pollutant.

While dispersion modeling does provide the basis for predicting odour concentration in a neighbourhood, it must be recognized that odour concentration values, in themselves, do not provide sufficient means for evaluating odour impact. That is, numeric values of odour concentration fail to account for the fact that different members of the population have widely differing sensitivities to odours. In addition, odours vary significantly in terms of their offensiveness or tendency to elicit complaint from the population. In order to account for these variables, the Odour Impact Model (OIM) was developed to gauge the response of a panel of odour judges chosen to represent the community population

(Nicell, 1986). The model is used to establish dose-response relationships subjected to a range of dilutions of an odour sample taken from the offending source. This method provides measures of population response to a range of odour concentrations that can be experienced in the field (Tsakaloyannis, 1997; Sikdar, 2001). The population's probability of response and degree of annoyance are two of several dose-response relationships that the OIM can produce (Figure 1.1).
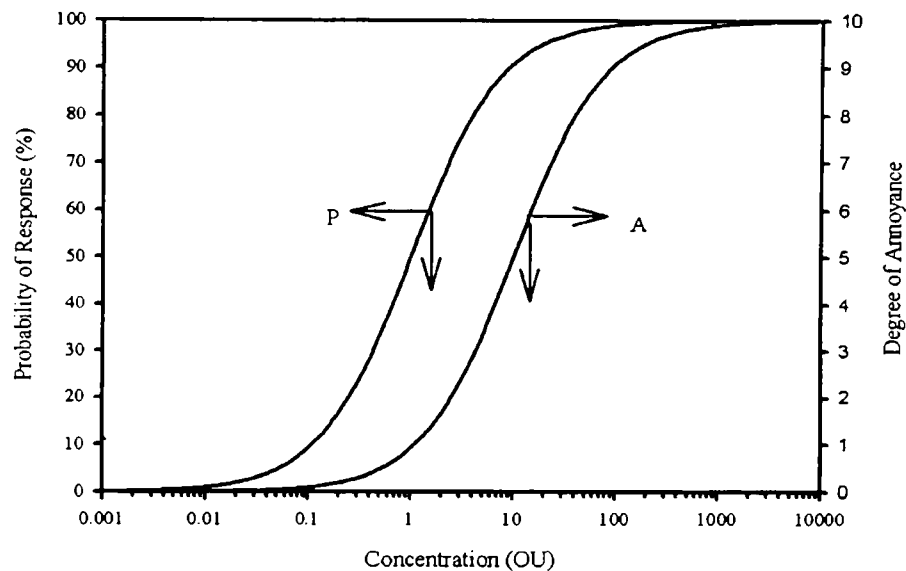
Figure 1.1: A typical odour impact model.

Sikdar (2001) merged the dose-response relationships arising from the OIM with dispersion modeling results to predict spatial variations in population response in the region surrounding the odorous source (Figure 1.2). Sikdar (2001) then used these results as a basis for quantifying the impact of the odour on the population in the exposed region. Several parameters were proposed to serve this purpose (Sikdar, 2001; Henshaw et al., 2002). However, despite the widespread use of dispersion models for odour regulation purposes and, recently, as a basis for the evaluation of odour impact parameters, the reliability of their use for odour impact assessment has not been adequately demonstrated.

3

Probability of response

Degree of annoyance

Dispersion modeling for prediction of odour concentration (OU)

OIM
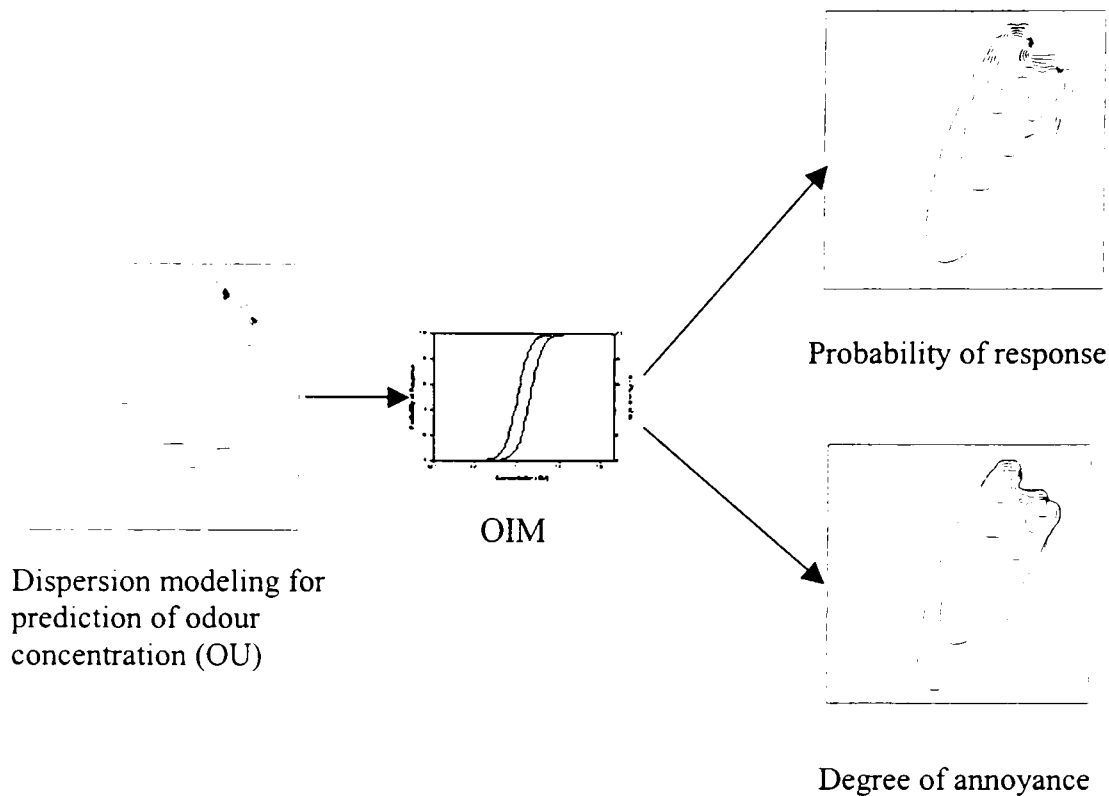
Figure 1.2: Spatial variations in population response arising from the merging of dispersion modeling results with odour impact model dose-response relationships.

Therefore, the primary objective of this research is to validate the ability of the Industrial Source Complex - Short Term (ISCST3) model to predict odour levels in a surrounding area. ISCST3 will be used to predict the impact of emissions from a facility in terms of odour concentration, probability of response and degree of annoyance. The predictive ability of the model will be tested by comparing predicted odour impacts with those measured in the field using a team of volunteers.

For the purpose of this investigation, a hog farm served as the subject of impact assessments. This facility is currently the subject of a larger study in which alternative approaches to regulating odour emissions from livestock facilities are being investigated. The Quebec Ministry of Environment is currently studying the use of air dispersion models in establishing odour-mitigating regulations for livestock facilities - especially hog farms. The importance of such facilities is demonstrated by the fact that Canada experienced an increase of 36% in the number of hogs between 1991 and 2001 (Statistics Canada, 2002). There are about 12,400 hog farms raising almost 13 million heads, with

Quebec having the highest share (19%). In 2001, this industry generated 3.9 billion dollars nationwide from the sale of slaughtered hogs alone. It is therefore considered one of the major contributors in the country's economy. The Quebec Ministry of Environment is currently recommending fixed separation distances for livestock facilities. Separation distances are distances between the odorous source and the community beyond which these emissions are predicted to no longer become sources of complaints. This regulatory approach can be considered arbitrary because it does not take into account local meteorological or geographical characteristics. As an alternative, the use of dispersion models could be used as a basis for regulating such emissions to appropriate levels that safeguard the surrounding communities. However, this alternative requires that the use of dispersion models for odour impact assessment be validated. Thus, the results from the present work will be combined with those of other investigators to study this alternative approach.

2 Literature Review

Dispersion modeling is used to predict odour concentrations in the ambient air surrounding a source. These concentrations can be used to gauge potential population response as a means to assess the impact of odorous emissions. Such an impact assessment will normally require a series of procedures with the intent of measuring odour emission rates, predicting odour concentrations in the surrounding region, and their interpretation to assess odour impact. Source odour concentrations and emission rates are usually quantified based on the application of the dilution-to-threshold principle. And, finally, the impact of these concentrations on the surrounding population can be interpreted in a variety of ways, of which the newest approach is through application of a method called the Odour Impact Model. Each of these procedures will be described below.

2.1 Atmospheric Dispersion Modeling

Dispersion models are tools used by regulatory agencies to determine if the emissions from a specific or proposed source are or will likely be compliant with the ambient air quality criteria. These models are used to predict the downwind concentration under any weather conditions from different types of sources, and across different terrain conditions.

2.1.1 Gaussian Plume Models

Gaussian diffusion models are extensively used in assessing the impacts of existing and proposed sources of air pollution. In these models the crosswind plume concentration distribution are taken to be Gaussian in form (Figure 2.1). The horizontal and vertical dispersion of the plume are normal to the wind direction, also having an increasing cross-section with an increasing downwind distance from the source. The governing equation for this type of model (Equation 2.1) is based on uniform flow with homogenous turbulence, from a continuous source (Arya, 1999; Barrat, 2001; Beychok, 1994).

$$C = \frac{Q}{u\sigma_z\sigma_y 2\pi} e^{\left(-\frac{y^2}{2\sigma_y^2}\right)} \left\{ e^{\left(-\frac{(z-H)^2}{2\sigma_z^2}\right)} + e^{\left(-\frac{(z+H)^2}{2\sigma_z^2}\right)} \right\} \tag{2.1}$$

where

C = concentration of emissions at a receptor point (mass/volume);

Q = source emission rate (mass/time);

u = horizontal wind velocity (length/time);

H = plume centreline height above ground (length);

σ_z = vertical standard deviation of emission distribution (length);

σ_y = horizontal standard deviation of emission distribution (length);

x,y & z = downwind, crosswind and above ground distances respectively (length).
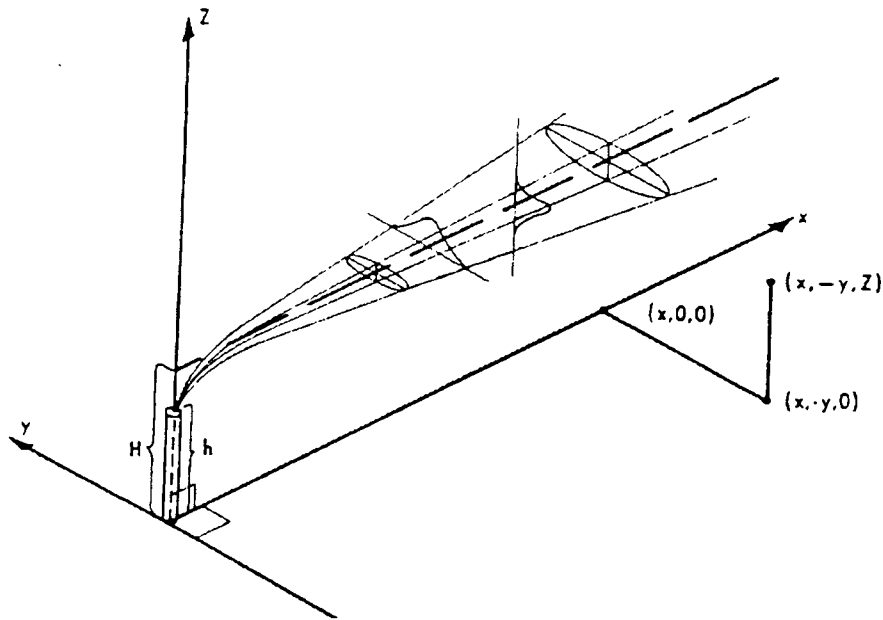
Figure 2.1: Crosswind distribution of plume in Gaussian form (Turner, 1994).

Some assumptions are involved in using the Gaussian plume model for calculating the dispersion of pollutants. The first assumption is that the pollutants are distributed normally and horizontally. The assumption is also made that a continuous emission from the source is at a constant rate, at least for a time equal to or greater than the travel time to the location (receptor) of interest, so that diffusion in the direction of the wind is

negligible. Another assumption is that the material diffused is stable, and none of it is removed through chemical reaction, gravitational settling or deposition. The mass in the plume is conserved, and therefore the continuity equation is satisfied by the Gaussian plume formula described in Equation 2.1. The plume diffusion formula is based on the assumption that the release and sampling times (averaging times) are long compared to the travel time to the receptor, so that the material is spread out in the form of a steady plume (Arya, 1999; Barrat, 2001; Beychok, 1994; Eagleman, 1996; Lyons & Scott, 1990; Ormerod, 2001).

The averaging time is defined as "the time over which a time-series' of sample measurements are averaged (Tsakaloyannis, 1997). For the case of a continuous plume, the duration of the time-averaged period or sampling time determines the effective size of the plume. A longer time average will produce a wider plume, and as the averaging time is reduced, an instantaneous snapshot of the plume is approached (Sykes & Gabruk, 1997). Averaging over a specified period will smooth out some of the variations of air quality (Figure 2.2).

Figure 2.2: Different time-averaging intervals and effect on data (Boubel et al., 1994).

Therefore, averaging conceals peaks that may result from short-term variations in emission rates and meteorological conditions, which are often the case in odour measurement situations. It is common to convert the time-averaged estimates of concentration arising from a particular model (e.g., often 1-hour averages) to shorter time-averaged periods using the following equation:

$$C_2 = C_1 \left(\frac{t_1}{t_2} \right)^n$$

(2.2)

where,

C₁ = concentration for longer averaging time;

C₂ = concentration for shorter averaging time;

t₁ = longer averaging time;

t₂ = shorter averaging time;

n = an empirical exponent.

The exponent n is dependent on the degree of atmospheric turbulence (i.e., stability) and ranges from 0.17 to 0.68 (Beychok, 1994; Venkatram, 2002).

2.1.2 The Industrial Source Complex Model

The Industrial Source Complex (ISC) Model is one of the most commonly used models for assessing pollutant dispersion. It is a steady state Gaussian plume model developed by the U.S. Environmental Protection Agency (USEPA). The model has the ability to analyze concentrations in any type of terrain (Atkinson et al., 1997; Barrat, 2001). There are two versions: the short term version, ISCST, used for averaging period of 24 hours or less, and the long term version, ISCLT, for averaging periods of 30 days or longer.

The ISC short term model (ISCST) provides options to model emissions from a wide range of sources that might be present at a typical industry. Hourly meteorological data records define the conditions for plume rise, transportation, diffusion and deposition (Barrat, 2001).

ISCST allows the user to specify multiple sources and also multiple receptor networks in a single run. The multiple sources include point, volume, area and open pit source types. Source emission rates can be treated as constant throughout the modeling period, or may be varied by month, season, or other optional periods of variation. In a single model run, the user can choose to locate receptors on a Cartesian grid and/or polar grid. The user also has the option to use elevated receptor heights to model the effects of a terrain above

9

or below stack base, and may specify receptor elevation above ground level (Barrat, 2001; Schnelle & Dey, 2000).

2.2 The Dilution-to-threshold Principle

Regulatory agencies apply dispersion model in order to predict ambient odour concentrations. To apply dispersion models, it is necessary to specify the emission rate of the contaminant of interest from each source, typically in units such as g/s. However, most odours result from a complex combination of many different chemical species – many of which may be extremely difficult to quantify. Therefore, an alternative approach is required for specifying odour emission rates that does not rely on specifying the emission rates of individual compounds. Such emission rates are usually quantified based on the application of the dilution-to-threshold principle.

The dilution-to-threshold principle is a common basis for quantifying odour concentrations. This principle is based on the assumption that the concentration of an odour can be quantified simply by measuring the number of unit volumes of odour free air that are needed to dilute a unit volume of a sample of odorous air to a sensory threshold level. The dilution (or concentration) of an odorous gas at which 50% of a panel of odour judges notices a stimulus as being different from odour free blanks is known as detection threshold (D_{50}) (ASTM, 1991). The D_{50} of a sample of odorous gas is usually determined by dynamic olfactometry, as pictured in Figure 2.3.

This procedure involves exposing individual members of a panel of odour judges to a range of dilutions of the original odour sample. The olfactometer is designed to provide streams of odorous air of different concentrations by mixing a controlled flow of odorous sample with odour-free air. The volume ratio of odour free air to odorous air determines the degree of dilution or the concentration of the odour. Each of the diluted odorous streams is presented to the panellists in parallel with one or more streams of odour-free
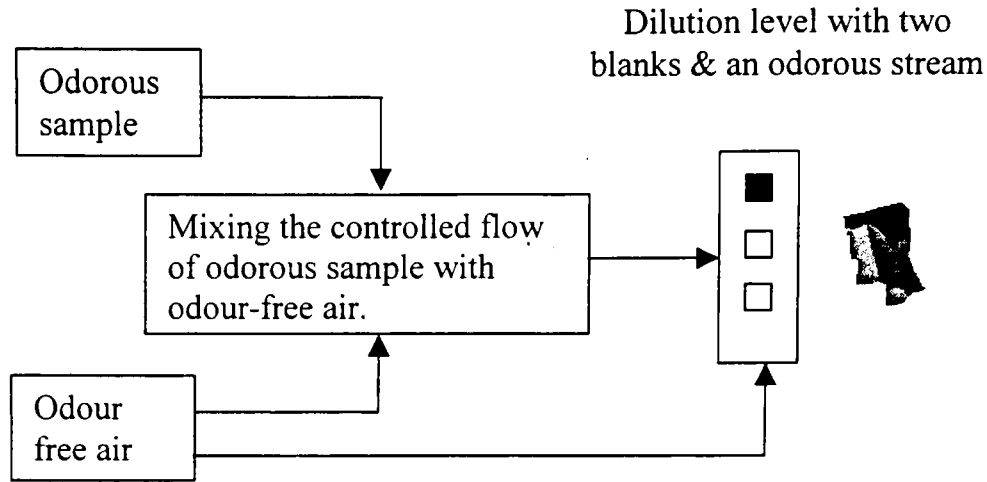
Figure 2.3: Forced choice procedure.

air (Cha, 1998; Nicell, 2003; Schiffman et al., 2001). At each dilution level, the panellist is asked to attempt to identify which of the streams contains the odour. The threshold for that individual is defined as the highest number of dilutions (or lowest concentration) at which the panellist begins to correctly distinguish between odorous streams and odour-free blanks. The D_{50} for the original odour sample is the highest number of dilutions (or lowest concentration) at which 50% of the panellists distinguish the odorous stream from odour-free blanks. The concentration of odour (in OU) is expressed in terms of the number of dilutions that are required to reduce the odour concentration to a sensory threshold level, which is equivalent to the D_{50}. Thus, when an odour is present at its threshold level it is said to have a concentration of one odour unit (1 OU), or when a sample that has a D_{50} of 10 000 dilutions it would be said to have a concentration of 10 000 OU.

The odour emission rate of a source is a function of the odour concentration and the volumetric flow rate of the source and can be calculated using the following equation:

$$ER = Q \times C \tag{2.3}$$

where:

ER = source emission rate (OU · m^3/s);

Q = volumetric flow rate from the source (m^3/s);

C_o = odour concentration at the source (OU)

By inputting an emission rate into a dispersion model, it becomes possible to predict the concentration of odour (in OU) at any receptor in the impacted region.

2.3 The Odour Impact Model

The dilution-to-threshold principle serves as an excellent basis for measuring odour concentration. However, such concentrations are not sufficient to characterize the potential impact of an odour on a population. For example, the acceptability or unacceptability of an odour is probably one of the most important properties in the determination of its impact on a community (Committee On Odours From Stationary and Mobile Sources, 1979). Nor does the concentration reveal any information about what fraction of the population will perceive the odour. According to Nicell (1994), it is important to account for dose-response relationships that relate community impact to odour concentration. This can be accomplished through application of the Odour Impact Model (OIM), which was developed by Poostchi (1985) and refined by Nicell (1986).

This OIM approach relies on the use of olfactometry techniques that are quite similar in practice to those that are used in the evaluation of detection thresholds. However, rather than simply evaluating the particular dilution ratio (or concentration) at which 50% of the population detects the odour (i.e., a threshold), this method involves measuring the responses of the panel of odour judges to a range of odour concentrations extending from above to below the odour threshold level.

At each dilution level, the ability of individual panellists to detect the odour is assessed. This data is then reduced for the whole panel to produce the probability of response curve shown in Figure 2.4. In addition to identifying the ports which are perceived to be emitting odorous gas, the panel of odour judges are also asked to rate their annoyance on a scale of 0 to 10 according to the categories shown in Figure 2.5, as if they were to be exposed to the odour for an average period of 8 hours (Nicell, 1994; Sikdar, 2001; Tsakaloyannis, 1997). At each dilution level, the annoyances expressed by the panellists are averaged to produce an annoyance value. These values serve as the basis for the degree of annoyance curve shown in Figure 2.4.
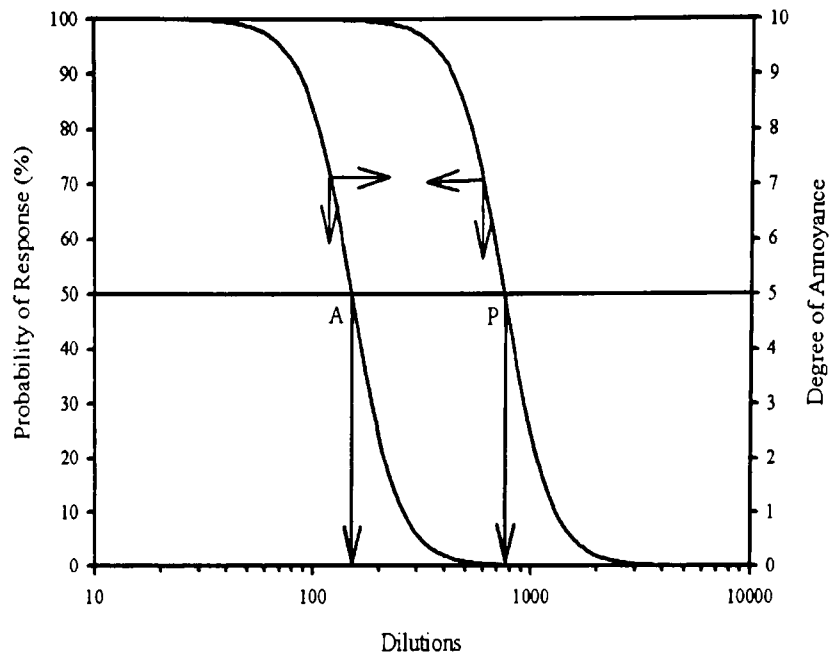
Figure 2.4: Idealized Odour Impact Model, where A=Degree of annoyance and P=Probability of response.

TOLERABLE	UNPLEASANT	VERY UNPLEASANT	TERRIBLE	UNBEARABLE
0 to 2	2 to 4	4 to 6	6 to 8	8 to 10
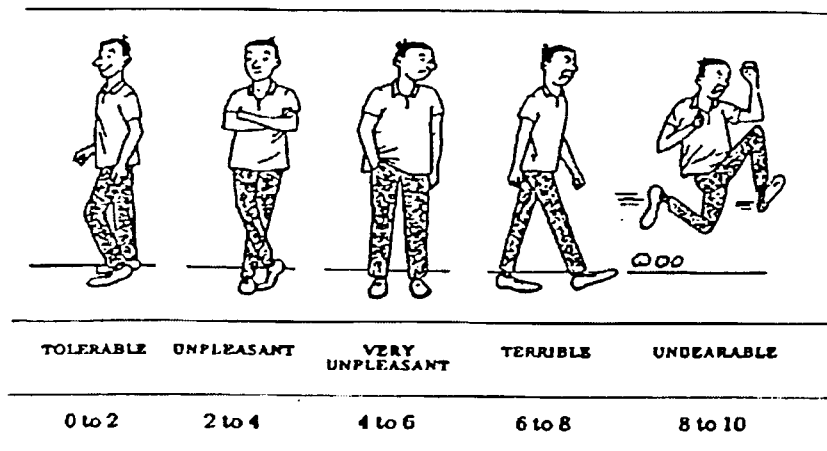
Figure 2.5: Annoyance categories used in OIM (Nicell, 1986).

The results obtained from the Odour Impact Model are used to evaluate the parameters of the following equations that describe the probability of response (Equation 2.4) and degree of annoyance (Equation 2.5) as a function of the number of dilutions of the original odour sample:

13

$$P = \frac{100}{1 + \left(\dfrac{D}{D_{50}}\right)^{\frac{1-p}{p}}}$$ (2.4)

$$A = \frac{10}{1 + \left(\dfrac{D}{D_{A5}}\right)^{\frac{1-a}{a}}}$$ (2.5)

where:

P = Probability of response (%);

A = Degree of annoyance;

D = Number of dilutions (dimensionless);

D_{50} = Dilutions at the threshold (dimensionless);

D_{A5} = Dilutions at which population annoyance is 5 (dimensionless);

p = Persistence of response;

a = Persistence of annoyance.

The persistence values describe the variation in probability of a response or the degree of annoyance as a function of the dilutions of that odour. The values of these parameters are between 0 and 1. If an odour is of low persistence, the probability of response or the degree of annoyance will decline rapidly as the concentration of the odour approaches and drops below the threshold (Sikdar, 2001). If the odour has a high persistence, this reflects an odour that tends to be experienced by a significant fraction of the population over a very wide range of concentrations above and below the threshold value

The ratio of D_{50}/D is equivalent to the number of odour units (C_{OU}) and, hence, the concentration of odour in a sample (Nicell, 2003). Therefore, the probability of response, P, in equation 2.4 can be expressed as:

$$P = \frac{10}{1 + \left(C_{OU}\right)^{\frac{p-1}{p}}}$$

(2.6)

If R shown in Figure 2.6 is defined as the ratio D_{A5}/D_{50}, then the degree of annoyance at any odour concentration is (Nicell, 2003):

$$A = \frac{10}{1 + \left(C_{OU} \cdot R\right)^{\frac{a-1}{a}}}$$

(2.7)
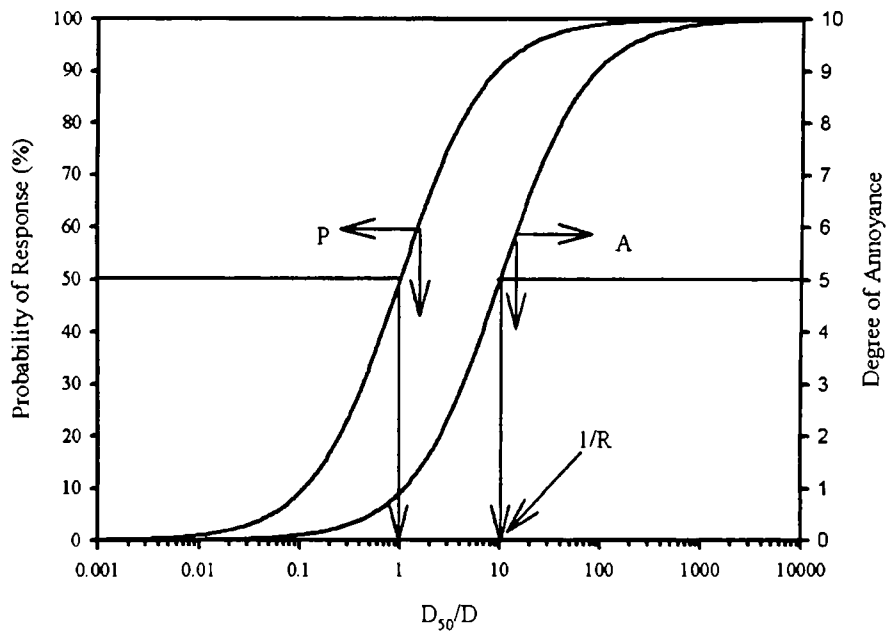
Figure 2.6: Probability of response and degree of annoyance as a function of odour concentration.

2.4 Merging of Odour Impact Model and Dispersion Model Data

The impact of odour emissions on a surrounding community can now be quantified by predicting the ambient odour levels in the neighbourhood using atmospheric dispersion models. The odour concentrations obtained from the dispersion models can be combined with the dose-response relationships represented by the equations discussed above, which are generated from the Odour Impact Model (OIM). This will provide predictions of the

15

probability of response and annoyance that would be expected to be experienced by a population in specific locations throughout the community.

The dispersion of odours from stationary sources is frequently predicted through the use of the Gaussian plume models. The main drawback of using these models for odours is that they calculate a 3-min to 1-hour average concentration (Mahin, 2001), whereas odours can generate community complaints from a series of short detectable exposures (Mussio et al., 2001). The complaints generated by the community mainly arise from the human nose reacting fairly rapidly upon odorous impact. This means that the sampling time relevant to this situation should be very short. These rapid reactions are due to short-term variations in concentrations as depicted in Figure 2.2(a). These variations are caused by the fluctuations of the plume centroid, which if close to the ground, will lead to high concentrations, and if it is high above the ground will lead to low concentrations (Hogstrom, 1974). Therefore, after predicting odour concentrations using an appropriate dispersion model, it is necessary to adjust these concentrations to a suitable averaging time to have a more realistic prediction of the conditions under which the odour will be experienced. The odour concentrations then obtained can be transformed into estimates of population response through Equations 2.6 and 2.7.

Investigations have been conducted to evaluate the reliability of this approach in correctly predicting odour impacts, as they were experienced at various spatial locations surrounding an odour source. Both Tsakaloyannis (1997) and Sikdar (2001) have concluded that odour concentrations predicted by the dispersion model ISCST3 is capable of predicting the location of the downwind zone of odour impact. However, it was also concluded that the model tends to underestimate the concentration (Sikdar, 2001). It remains necessary to assess the ability of the dispersion models, like ISCST3, to predict odour impact parameters, such as probability of response and degree of annoyance, by comparing them with actual field measurements.

3 Methodology

This chapter discusses the general procedures taken to compare predicted odour impact levels from the Industrial Source Complex Short Term Model with those measured on a hog farm. This includes descriptions of the methodology for measuring probability of response and annoyance levels in the field, the reduction of data for the Odour Impact Model, and the application of ISCST3-model as a tool to predict odour levels in the area surrounding the odour source. The methods described in this chapter were applied to the three experiments conducted in this research.

3.1 Field Measurements

This section describes the odour measurements performed on the hog farm. The measurements were conducted as part of a larger study conducted by Consumaj Inc. (Sainte-Hyacinthe, QC), an environmental consulting firm.

3.1.1 Site Preparation

There were three groups of four or five volunteers, each with an assigned colour (red, yellow or blue). The three teams were assigned different locations downwind of the odour-emitting sources. These locations were selected based on the general wind direction at the time that the measurements took place (see Figure 3.1). A smoke-emitting flare was positioned at the ventilator outlets on the two extreme ends of the two barns. The paths of the smoke emissions were used to delineate the general boundary of the area within which the odour measurements were to be performed. Flags of three different colours (red, yellow and blue) marked the locations within this area, each representing a team, and their coordinates were recorded using a GPS device are displayed in Appendix A.
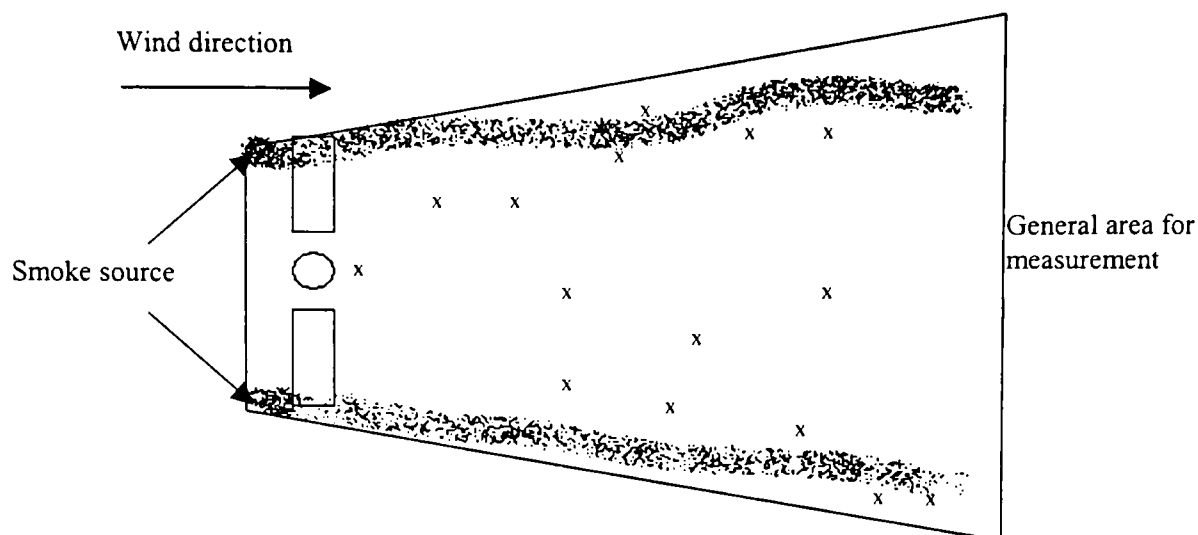
Figure 3.1: Smoke tests to delineate the area within which odour measurements were to take place.

3.1.2 Field Responses

Prior to conducting measurements, each individual was familiarized with the typical smell of the source. At each flag, each individual was required, if an odour was detected, to evaluate the degree of annoyance that he/she experiencing on a 0 to 10 scale.

The method for evaluating the degree of annoyance was explained to the volunteers before they started the measurements. They were shown Figure 2.5 as a means for quantifying their level of annoyance while imagining they were exposed to the same degree of odour for 8 hours.

If an individual was exposed to a continuous source of odour, his/her olfactory senses may become fatigued or adapted to that odour. Also, if he/she were presented with a weaker odour of the same type, he/she might fail to detect it. To overcome these problems in the experiment, each volunteer was required to wear a gas mask to breath odour-free air while moving between the flags and, over the period of the measurements, the teams were required to move upwind into the plume (i.e., approaching the barns). Table 3.1 provides an example of the results from one team during one experiment.

Table 3.1: Example of results from one team during field measurements.
A = Degree of Annoyance (1-10).

Blue flag	Time	UTM coordinates		A of team member #			
				1	2	3	4
3	10:04	683025	5107714	1	2	1	2
4	10:07	683025	5107679	6	2.5	3	3
5	10:10	683028	5107642	1	3	0	3
6	10:13	683029	5107604	0	1	0	3
7	10:17	683028	5107544	0	0	1	4

3.2 Odour Impact Model

To predict the potential impact of an odour on a population using dispersion modeling, certain characteristics related to the odour have to be quantified. The main characteristics that were of concern in this research were parameters that describe trends in probability of response and degree of annoyance. These were determined by performing odour impact modeling on samples obtained from the source.

3.2.1 Sample Collection

The samples were prepared by D. Choiniere, ing., from Consumaj Inc. (Saint-Hyacinthe, QC). There were five samples; two from each barn and one from the manure storage tank (labelled as "fosse").

The samples from the barns were taken by collecting the emissions from the exhaust fans in tedlar bags. Each barn had two samples that were labelled 299 and 300 for the west barn and east barn respectively, and F and C for the east section and west section where the samples labelled F were from the sections closest to the manure storage tank (Figure 3.2). Each sample bag was filled randomly with exhaust air from the fans of the corresponding half of the building.
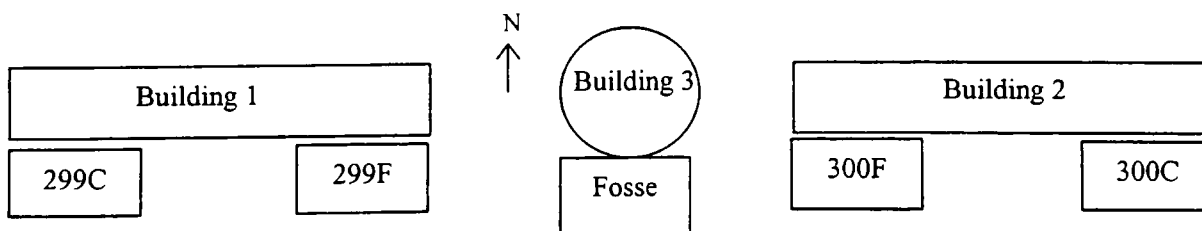
Figure 3.2: Sampling locations

3.2.2 Olfactometry Test

The OIM was prepared from results obtained from the dynamic olfactometry experiments performed at Consumaj Inc, under the supervision of D. Choiniere. The odour was presented to each individual in the panel of odour judges at different dilution levels. The panel consisted of 6 odour judges. They were asked to identify the stream of odour that was among two blank odourless streams and to rate their degree of annoyance on a scale of 0 to 10 (Figure 2.5). The number of dilutions of the original odour that was delivered at each dilution level was evaluated by measuring the volumetric flow rate of the odorous stream and the total flow delivered to the panellist. The odorous gas from the sample was introduced at different volumetric flow rates and mixed with odour free air. This mixture was supplied at a total flowrate, Q_{sample}, of 120,000 mL/min. Table 3.2 shows the various rates at which the odorous air was supplied and the dilution levels calculated using Equation 3.1.

Table 3.2: The calibrated dilutions of odour that were presented in the olfactometry tests.

Volumetric flow rate of odorous air (mL/min)	Total volumetric flow rate (mL/min)	Dilutions
48		2556
96		1236
192		619
384		312
768	120000	157
1536		57
3072		36
6144		19
12288		9

$$Dilutions = \frac{Q_{sample}}{Q_{odour}}$$ (3.1)

where:

Q_{sample} = total volumetric flow rate of odorous air (mL/min);

Q_{odour} = volumetric flow rate of odorous air (mL/min).

The odour was presented to each individual in the panel of odour judges in order of descending dilution levels (i.e., ascending concentration), as shown in Table 3.3. After experiencing the lowest dilution (highest odour concentration), the individual was subjected to some of the same dilutions experienced earlier but in random order.

The results of the olfactometry test were submitted in the format presented in Table 3.3, where a value "1" was assigned to the individual who correctly identified the port emitting the stream of odour and was assigned a "0" if the response was incorrect.

Table 3.3: A sample of the dynamic olfactometery results provided by Consumaj Inc.

Dilutions	Response of panellist #						Annoyance of panellist #					
	1	2	3	4	5	6	1	2	3	4	5	6
2556	0	0	0	0	0	0	0	0	0	0	0	0
1236	0	0	0	0	1	0	0	0	0	0	1	0
619	0	0	1	0	0	0	0	0	1.5	0	0	0
312	1	1	1	1	1	1	1	1	3.5	4	1	3
157	1	1	1	1	1	1	1	2	6	3	1	4
57	1	1	1	1	1	1	5	7	9.5	6	4	6
36	1	1	1	1	1	1	8	9	8.5	7	5	7
19	1	1	1	1	1	1	8	8	8.5	8	6	8
9	1	1	1	1	1	1	8	6	8.5	9	7	9
157	1	1	1	1	0	1	2	1	4	3	0	7
36	1	1	1	1	1	1	5	9	7	5	6	9
57	1	1	1	1	1	1	5	4	6	6	8	9
312	0	0	1	0	0	1	0	0	3	0	0	3

The results were arranged in descending order of dilutions. The dilution levels beyond which the individual continuously correctly identified the odour were given a value of 1, and dilution levels prior to that were given a 0 value (Table 3.4).

Since there were a limited number of panellists, and some dilution levels were used more than once, the repeated dilutions were considered as extra measurements. For example, if there were two 312.5 dilution runs, then the number of measurements made at this dilution level was considered to be 12 instead of 6 (Tables 3.5 and 3.6).

At each dilution, the percentage of the panel of odour judges that detected (i.e., responded to) the odour and the average annoyance were calculated. In order to calculate the percentage of response, the sum of values (i.e., 0's and 1's) at each dilution level was calculated and then divided by number of measurements, as shown in Table 3.5. The degrees of annoyance were determined by dividing the sum of all annoyance values reported at each dilution by the number of measurements (Table 3.6).

Table 3.4: Panellists' response and annoyance arranged in order of descending dilutions (i.e., ascending odour concentration).

Dilutions	Response of panellist #						Annoyance of panellist #					
	1	2	3	4	5	6	1	2	3	4	5	6
2556	0	0	0	0	0	0	0	0	0	0	0	0
1236	0	0	1	0	0	1	0	0	0.5	0	0	1
619	0	0	1	0	0	1	0	0	1	0	0	2
619	0	1	1	0	0	1	0	0.5	1	0	0	1
312	1	1	1	1	0	1	1	0.5	2	1	0	2
312	1	1	1	1	0	1	1	1	3	2	0	7
157	1	1	1	1	0	1	2	1	4	1	2	2
157	1	1	1	1	0	1	1	1	6	3	0	4
157	1	1	1	1	1	1	2	1	5	3	3	5
57	1	1	1	1	1	1	5	4	6.5	5	4	6
57	1	1	1	1	1	1	4	4	8	8	5	10
36	1	1	1	1	1	1	3	6	8	4	5	7
19	1	1	1	1	1	1	5	7	9	8	8	9
9	1	1	1	1	1	1	4	8	10	9	9	10

Table 3.5: Example of method used to calculate probability of response from olfactometry measurements. In this example, panellists were exposed to 3 dilutions levels on two occasions, leading to twice as many measurements as at other dilutions levels. Column (a) is the number of measurements made; column (b) is sum of response values in each row; and column (c) is percentage of panellists identifying the odorous sample at the corresponding dilution, i.e., c = (b/a) × 100%.

Dilutions	Response												a	b	c
1236	0	0	0	0	0	0							6	0	0
619	0	0	1	0	0	1							6	2	33
312	1	0	1	1	0	1	1	0	1	1	0	1	12	8	67
157	1	1	1	1	0	1	1	1	1	1	0	1	12	10	83
57	1	1	1	1	1	1	1	1	1	1	1	1	12	12	100
36	1	1	1	1	1	1							6	6	100
19	1	1	1	1	1	1							6	6	100

Table 3.6: Example of method used to calculate degree of annoyance from olfactometry measurements. In this example, panellists were exposed to 3 dilutions levels on two occasions, leading to twice as many measurements as at other dilutions levels. Column (a) is the number of measurements made; column (b)is the sum of annoyance values in each row; and column (c) is the average degree of annoyance for each dilution i.e., c = b/a.

Dilutions	Degree of Annoyance												a	b	c
1236	0	0	0	0	0	0							6	0	0
619	0	0	1	0	0	1							6	2	0.3
312	1	0	3	1	0	4	1	0	3	0	0	2	12	15	1.3
157	4	0.5	4	2	0	4	1	1	4	2	0	6	12	29	2.4
57	4	4	6	6	2	8	6	6	8.5	8	6	10	12	75	6.2
36	9	6	8	7	8	8							6	46	7.7
19	9	8	9	8	7	10							6	51	8.5

3.2.3 Determination of OIM Parameters

The results from the tables were used to determine the threshold of response and the persistence value for the probability of response for each sample. Plots of the probability of response versus dilution were done in Sigma Plot 8.0 for each sample as shown in Figure 3.3. The non-linear curve-fitting function of Sigma Plot 8.0 was used to fit equation 2.4 to the data, thereby providing estimates of the threshold and persistence of response for the samples.

As mentioned previously, the OIM was done for the three experiments conducted from the same hog farm. It was only in the first experiment that all the olfactometry results of all the 299F, 300C, and 300F samples were combined to give one general threshold and persistence value. This was done because there were no results obtained for the 299C sample. This is shown in Appendix B with all the other OIM results.
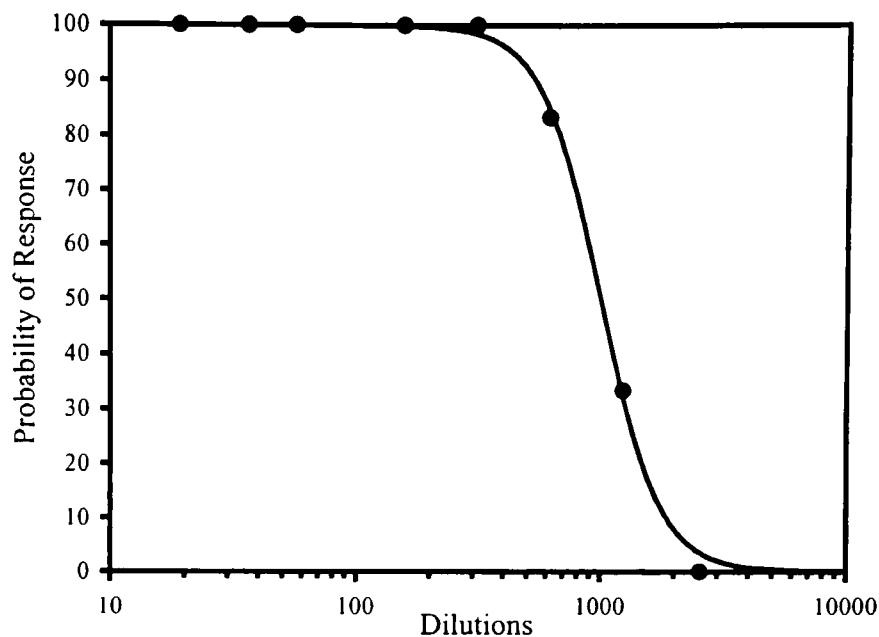
Figure 3.3: Plot of probability of response vs. dilutions.

3.3 Air Dispersion Modeling-ISCST3

This section describes the procedures performed using the Industrial Source Complex Short Term 3 model (ISCST3) to predict the odour concentration levels from the hog barns and manure at the different receptor locations of the area impacted.

3.3.1 Defining the Site and Facility

The ISCST3-model uses the Building Profile Input Program View (BPIP View), which is a graphical user interface, to set-up input data for defining the characteristics of buildings and stacks. These characteristics are used in downwash analysis, which involves the rapid mixing of pollutants emitted from a source toward the ground, resulting in higher ground-level concentrations (The et al., 2000). This is due to the aerodynamic turbulence induced by nearby structure.

BPIP View consists of a Set-up, building, stack and 3-D view sections. In the Set-up section, the name of the project, the output file name, the Universal Traverse Mercator (UTM) chosen as the coordinate system and the site domain were defined. The site domain is the area within which the dispersion of the pollutant is modelled. The area is

defined by its southwest and northwest corners, which were determined according to the average direction of the wind, and must include the region within which the teams of volunteers took their field detection and annoyance measurements.

The building section of BPIP View requires the input of the locations and dimensions of the buildings. The hog facility consisted of two barns with 24 exhaust outlets, and a manure storage tank with an air outlet to regulate the internal pressure. The profile of the barn roofs was triangular in shape. This shape arrangement was represented in BPIP View as set of rectangular tiers (Figure 3.4). The heights of each tier for the two barns are represented in Table 3.7.
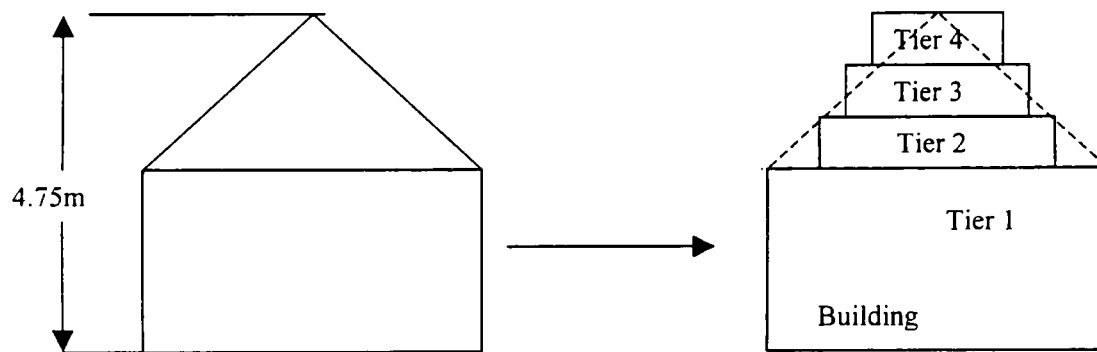
Figure 3.4: Representation of the barn profile in BPIP View.

Table 3.7: Tier heights of the hog two hog barns.

Tier No.	Tier Height (m)
1	2.74
2	3.11
3	3.88
4	4.75

The manure storage tank had a dome shaped cover. This cover was represented in BPIP View as a series of concentric cylinders stacked on top of each other as depicted in Figure 3.5.

Side view

Plan
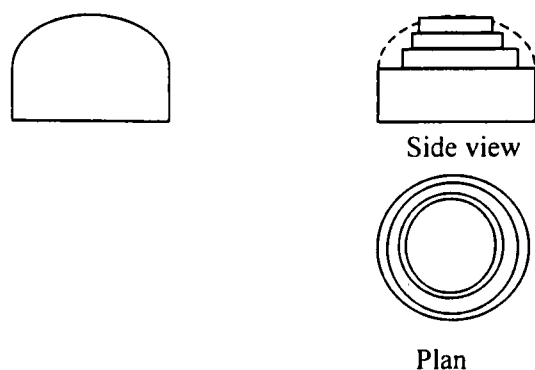
Figure 3.5: Manure storage tank representation in BPIP View.

The locations of the hog barns, and the manure storage tank were represented as UTM coordinate system (Tables 3.8, 3.9 and 3.10).

In the stack section of the model, the source type, source ID, UTM coordinates and the description must be specified. The base elevation of all stacks (0 m), their heights (m), emission rates (OU· m^3/s), stack gas exit temperatures (K), stack gas velocities (m/s) and the stack inside diameters at release points are also required. The calculation of the emission rates is described in Section 3.3.2.2. The above parameters are only required if the sources chosen are of point type. This is due to the inability of BPIP View to calculate downwash for emissions from other source types such as line sources or area sources.

In the 3-D View section, the whole set-up of the buildings and the stacks can be viewed in three-dimensional perspective.

Table 3.8: Building 1 (Barn) coordinates.

Tier 1		
	x-coordinate (m)	y-coordinate (m)
Corner1	682529.40	5107389.32
Corner2	682538.00	5107398.00
Corner3	682595.39	5107341.11
Corner4	682586.79	5107332.43
Tier 2		
	x-coordinate (m)	y-coordinate (m)
Corner1	682530.45	5107390.39
Corner2	682536.94	5107396.93
Corner3	682594.34	5107340.05
Corner4	682587.85	5107333.50
Tier 3		
	x-coordinate (m)	y-coordinate (m)
Corner1	682532.29	5107392.24
Corner2	682535.11	5107395.08
Corner3	682592.50	5107338.19
Corner4	682589.68	5107335.35
Tier 4		
	x-coordinate (m)	y-coordinate (m)
Corner1	682532.99	5107392.95
Corner2	682534.40	5107394.37
Corner3	682591.80	5107337.48
Corner4	682590.39	5107336.06

Table 3.9: Building 2 (Barn) coordinates.

Tier 1		
	x-coordinate (m)	y-coordinate (m)
Corner1	682658.40	5107261.32
Corner2	682667.00	5107270.00
Corner3	682724.39	5107213.11
Corner4	682715.79	5107204.43
Tier 2		
	x-coordinate (m)	y-coordinate (m)
Corner1	682660.59	5107263.53
Corner2	682664.81	5107267.79
Corner3	682722.20	5107210.90
Corner4	682717.98	5107206.42
Tier 3		
	x-coordinate (m)	y-coordinate (m)
Corner1	682661.29	5107264.24
Corner2	682664.11	5107267.08
Corner3	682721.50	5107210.19
Corner4	682718.68	5107207.35
Tier 4		
	x-coordinate (m)	y-coordinate (m)
Corner1	682662.00	5107264.95
Corner2	682663.40	5107266.37
Corner3	682720.80	5107209.48
Corner4	682719.39	5107208.06

Table 3.10: Manure storage tank location and dimensions.

Tier	Tier height (m)	Radius (m)	Centre	
			x-coordinate (m)	y-coordinate (m)
1	2.44	16	682626.89	5107301.22
2	3.11	11.68	682626.89	5107301.22
3	3.88	7.19	682626.89	5107301.22
4	4.75	4.28	682626.89	5107301.22

3.3.2 Defining the Input Parameters of the Sources

The model requires certain parameters (Table 3.11) to be defined in order to calculate the predicted ambient concentrations downwind of the odorous source. One of the parameters required is the odour emission rate. This value is a function of the source volumetric flow rate and the dilution-to-threshold of the odorous air emitted from the source.

27

Table 3.11: Input parameters required for the different source types in ISCST3.

Parameter	Source type		
	Point	Area	Volume
Emission rate	x	x	x
x,y coordinates	x	x	x
Base elevation	x	x	x
Release height	x	x	x
Stack gas exit temperature	x		
Stack gas velocity	x		
Stack inside diameter	x		

3.3.2.1 Volumetric Flow Rate

The volumetric flow rate is the volume of air released at the source per unit time. This value depends on the velocity of air emitted and the cross-sectional area of the source, which is determined by the type of source.

To determine the exit air velocity for each source, a simple mass balance was performed between the inlet air flow rate, which was measured, and the exiting air flow rate from the exhaust fans which were the sources emitting the odorous air. The air entered the barn through a 20-cm wide grill running along the upper part of north wall of each barn (of 80.81 m length) at an average velocity that was measured (Figure 3.6). The total volumetric flow rate, Q_{in}, of the air entering each barn is:

$$Q_{in} = v \times A \tag{3.2}$$

where:

v = the velocity of the air entering (m/s);

A = surface area of the grill through which air enters (m^2).
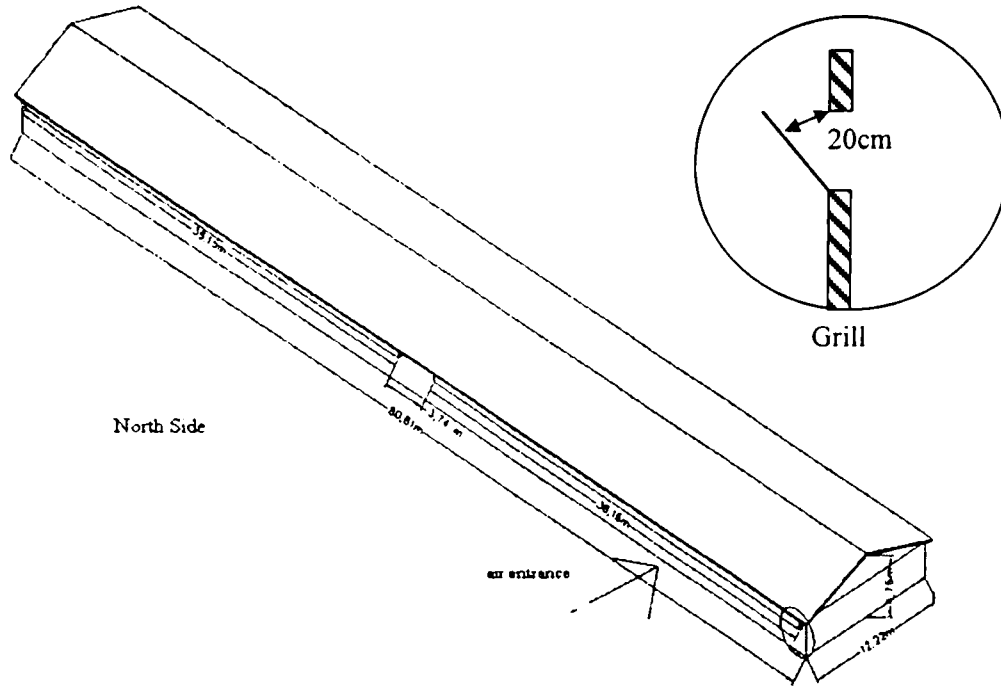
Figure 3.6: A typical north side of the barns on the hog farms and the grill configuration.

The air exiting the barns mainly flowed from 24 ventilation fans on the south-side of the building (Figure 3.7). There are eight 16-inch, 21-inch and 24-inch diameter fans in each barn, with nominal flow capacities of 2200 cubic feet per minute (cfm), 3500 cfm, and 4170 cfm, respectively. Therefore, the ratios of the flow capacities of the fans were 1:1.6:1.9 respectively. In order to estimate the flow exiting from each fan, the total flow of air entering the barns was assumed to exit each fan in proportion to its capacity and the total number of fans operating. For example, by performing a mass balance on the total flow rate entering and that leaving using the ratios established gave:

$$Q_{in} = 8(q) + 8(1.6)(q) + 8(1.9)(q) \qquad (3.3)$$

where q was the flow rate for the 16-inch fan. Using the above equation, for a known inlet flowrate, Q_{in}, the volumetric flow rate and the emission rate of each fan were calculated.
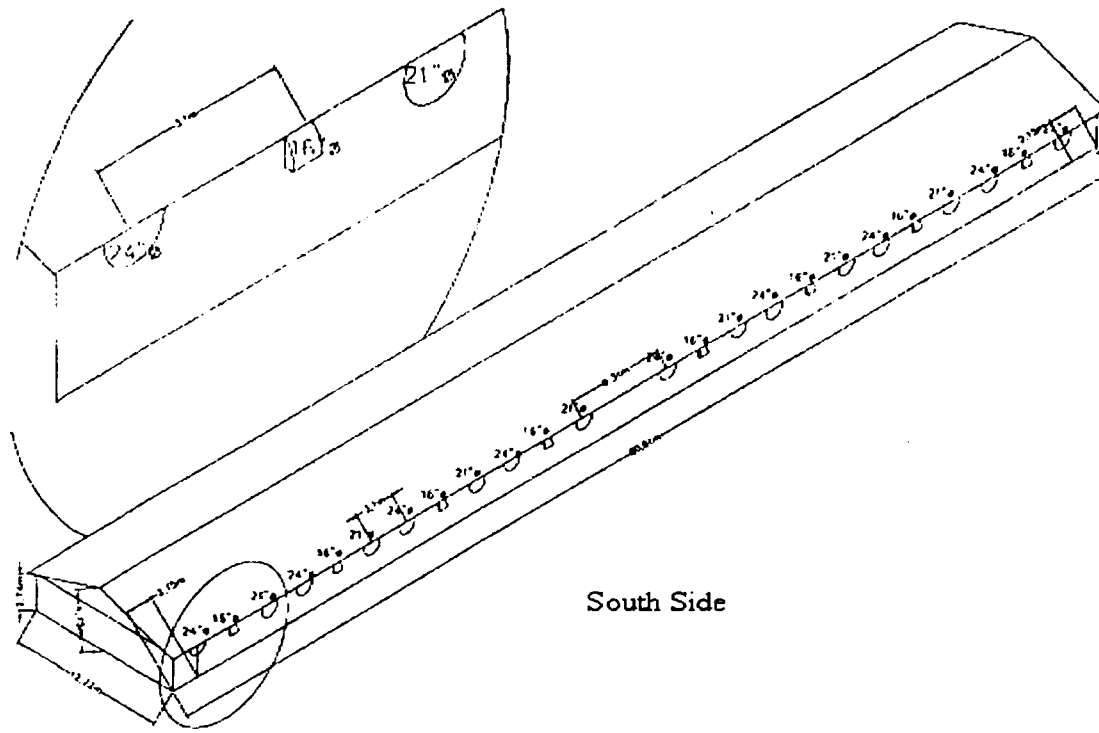
Figure 3.7: South side of barn having 24 air exhaust fans.

3.3.2.2 Calculating the Emission Rate

The ISCST3 model represents the concentrations of a certain compound at a receptor in unit mass per unit volume. In this study, it was necessary to predict the concentration at any receptor point in odour units (OU). In order to obtain such a result, the emission rates had to be entered in a form that would result in the desired concentration unit.

For point sources, the emission rate was calculated as the product of the source concentration (in OU) and the volumetric flowrate. The source concentration, expressed in OU, is numerically equivalent to the number of dilutions required to reduce the odour intensity to the sensory threshold level, i.e., the D_{50}. For example, a sample with a D_{50} of 100 dilutions, is said to have an odour concentration of 100 OU. Thus, the emission rate for point sources may be calculated as follows:

$$ER = D_{50} \times Q \times \frac{1 \ OU}{dilution} \tag{3.4}$$

30

where ER is the emission rate (in $OU \cdot m^3/s$) and Q is the volumetric flowrate (m^3/s) from the point sources.

When modelling area sources, the ISCST3 model requires an emission rate to be specified as a mass per unit area per unit time. In this study, the emissions were modeled as being emitted from 40 area sources (20 at each barn) of equal size. The emission rate, M, from each area was calculated using:

$$M = \frac{(Q_{in})(D_{50})}{S \times A_s} \times \frac{1 \, OU}{dilution} \tag{3.5}$$

where:

M = emission rate from each sub-area ($OU \cdot m/s$);

Q_{in} = flowrate of air entering the barn (m^3/s);

D_{50} = sensory threshold (dilutions);

S = total number of equal sized sub-areas of the barn to be modelled (specified as 20 in this study);

A_s = Surface area of each sub-area (m^2).

In the case of the modelling of volume sources, the emission rate must be entered into the software as a mass per unit time. Therefore, the same equation used for calculating emission rates of point sources was utilized for this type of source. The only difference was that the total volumetric flow rate of each barn was divided by the number of sources, which was four (one on each side of the barn).

For the first experiment, the odour concentrations for all the sources on the two barns were set as being equal to the D_{50} of the combined OIM results for the 200F, 300C, and 300F sample. For the second and third experiments, the odour concentration for each source emission was the D_{50} of the sample that was from the same side of the barn where that source was located. For example, a source on the 299C side was said to have an odour concentration equivalent to the D_{50} of the 299C sample.

The emission rates and other necessary input parameters for all the sources are summarized in Appendix C.

3.3.2.3 Coordinates of Sources

The ISCST3-model can model point, area, and volume source emissions. In the case of the barns under study, some of the exhaust fans emit the air horizontally, and others emit the air vertically towards the ground. Since the exhaust air is then reflected from the ground, it was assumed that this situation can be approximated as though the sources were at ground level. In this study, all source types were tested for their ability to predict odour concentrations experienced in the field. In addition, different release heights for each source type were tested. The range of modelling conditions that were examined are summarized in Table 3.12.

The centre of each point source was determined relative to the corners of the barns of known coordinates. If the sources were assumed to be at ground level then the height above ground of the center (z-coordinate) had a value of 0 m. The x, y coordinates for the sources were specified according to their type shown in Table 3.13. In the case when it was assumed that the emissions were released at a height above ground level, then the release height was equal to the height of the corresponding fan above the ground indicated in Table 3.14.

Table 3.12: The three types of sources considered in modelling
the dispersion of the odorous emissions using ISCST3 model,
and the release heights considered.

Source type	Release heights tested
Point	Ground level
	Release heights of fans
Area	Ground level
	Release at average heights of fans
Volume	Ground level release height
	Release at average heights of fans

Table 3.13: Location for the X and Y coordinates.

Source type	Location for the x & y coordinates
Point	Centre of the source
Area	Southwest corner
Line source	First point defined for the line source

Table 3.14: The height of each fan.

Fan	Height above ground (m)
16"	2.14
21"	2.17
24"	2.22

For the area sources, the x, y coordinates of the vertex that is in the southwest quadrant of the source, as well its dimensions and orientation angle were required. The dimensions of the source were defined in ISCST3 as length of side X and length of side Y. Side X is the side of the area source that is counter clockwise along the perimeter from the defined vertex, and side Y is the side clockwise along the perimeter from the vertex (Figure 3.8). The orientation angle is the angle in degrees from the North.
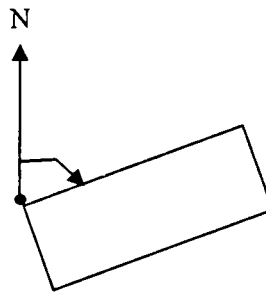
Figure 3.8: Parameters of an area source (The et al., 2000).

The hog farm arrangement consisted of area sources along the barn wall, and a circular area source representing the manure storage tank. Figure 3.9 is a general layout of the

location and arrangement of the area sources for each barn present on the hog farm. The shaded area represents the area sources. The overall length of each side was 34.1 m, which was divided into 10 segments, each of 3.4 m in length. The width for each source was estimated to be equal to the average diameter of the three types of ventilation fans present, which was 0.516 m.

Length along which area sources
are located

682538,
5107398

682595,
51073411

8.31 m

682529,
5107389

682586,
5107333

2.15 m

34.1m

34.1m

2.15 m

80.81 m
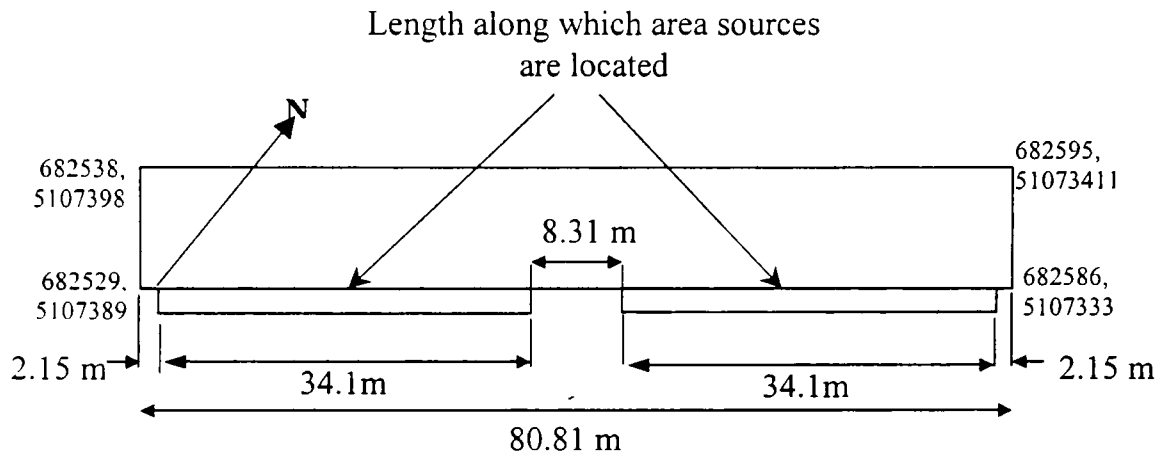
Figure 3.9: Sketch of the lengths along which area sources cover on each side of the barn.

The location, i.e., the x,y coordinates of the vertex, and the angle of orientation of each area source were determined by interpolating their location with respect to the known coordinates of the four corners of the barn. The coordinates of the vertex of each area source are found in Appendix C.

The manure storage tank was also considered to be a circular area source. The area source was simply described in the model by inputting the location of the centre of the circular shape (682626.89, 5107301.22), as well as the radius, which was equal to 16 m. ISCST3 approximates a circular area source as a polygon having the same area as the circular source that is to be represented. The model requires that the number of vertices be specified to represent the source. A value of 20 was specified, which is the maximum number allowed in the model.

34

The area sources were assumed to have an average release height of 2.18 m in the case where the emissions were modeled as being released above the ground. This value was the average of the elevations of the three fans.

The ISCST3 model represents line sources as a series of volume sources. As shown in Figure 3.10, the location of the line source is defined by specifying the coordinates of nodes that are along the centreline of the line source, at the intersection of two line segments (The et al., 2000) . If the line source is only one segment, then the nodes are located at the ends of the centre line.
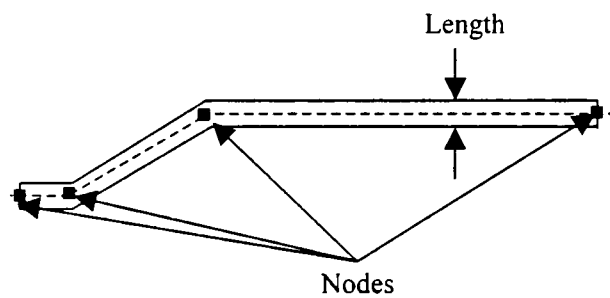
Figure 3.10: Line source parameters.

Four line sources were used to represent barn emission conditions, with each barn having a line source running on each side. Therefore, there were only 4 line segments defined by the length of the source, two nodes representing the two ends of the line, and the release height. The length, which represented the width of the source, was assumed to be the average of the three fan diameters, which was 0.516 m. The node coordinates, which are in Appendix C, were determined by interpolating their position relative to the known coordinates of the 4 corners of the barns. When a release height was specified, it was equal to the average height of the fans, which is the same as that specified when modelling area sources.

3.3.3 Meteorological Data

The meteorological data were recorded each time the field measurements were performed. A weather station was erected in the hog farm to record the ambient

temperature, wind speed, wind direction, average wind speed and peak wind speed at a one-minute time average as shown in Table 3.15.

Table 3.15: Example of format of meteorological data file at hog farm.

Time	Inside temp. (°C)	Outside temp. (°C)	Wind chill (°C)	Wind direction (degrees from North)	Wind Speed (m/s)	Avg. wind speed (m/s)	Peak wind speed (m/s)
8:08	30.1	30.0	29.3	263	4.5	4.5	4.5
8:09	30.2	30.3	30.1	259	2.7	3.7	4.5
8:10	30.2	30.2	29.7	259	3.6	3.1	4.5
8:11	30.4	29.3	28.6	259	3.6	3.6	4.5

temp. = temperature

The ISCST3-model has the ability to process 1-hour time-averaged meteorological data. The model can only process the data that is in the following order: year; month; day; hour; wind direction (degrees, with respect to the North); wind speed (m/s); ambient temperature (K); stability class (using the ranges specified in Table 3.16); urban mixing height (assumed to be 550 m); rural mixing height (assumed to be 550 m).

Table 3.16: Atmospheric stability categories based on wind speed (Barrat, 2001; Beychok, 1994).

Wind speed (m/s)	Stability class
<2	A-B
2-3	B
3-5	B-C
5-6	C-D
>6	D

Normally, ISCST3 requires that meteorological data be entered as 1-hour averages and uses dispersion coefficients to predict one-hour average concentrations. This approach is based on the assumption that over the one-hour period, the pollutant achieves a steady-state concentration at each receptor for each meteorological condition. However, the

meteorological data collected in this study was available in one-minute increments and revealed substantial variations in wind speed and direction over short periods of time. In order to predict the average concentrations at receptors in the study region during the study period, it was decided that the one-minute data would be input into the model and that the model would be instructed to determine average concentrations over the entire modelled period. This was done in an attempt to incorporate as much as possible the variations in meteorological conditions that affect the dispersion process. This approach would result in the calculation of 1-hour time averaged concentrations over the modelled period, since the extent of dispersion is still calculated based on dispersion coefficients developed for one-hour time averages.

The accuracy of the predicted average concentrations using 1-minute meteorological data depends to some extent on whether the steady-state assumption mentioned above is true. This would not be the case if the dispersion of the emissions was being modelled over a large area where the time between release of the contaminant and its arrival at a receptor is long. However, in this study, all field measurements were conducted in a region that was very close to the source. Thus, the travel time for the odour would be short and would be very nearly achieved within a one-minute time frame.

3.3.4 Receptors

The ISCST3-model allows the user to define Cartesian grid receptor networks and/or polar grid receptor networks, with either uniform or non-uniform grid spacing, and to also define discrete Cartesian receptors. In addition to defining the grid network, the height of the receptors can also be specified. In this study, receptors were specified in Cartesian coordinates at two different heights. That is, as is normally done in many odour impact studies, receptors were first defined at ground level. However, it was also recognized that the individuals who conducted the field measurements were actually experiencing the odour at nose level, i.e., approximately at a 1.5 m height. In most impact studies, there would not likely be a large difference between concentrations modelled at these two heights. However, in this field study, the dispersion of odours was modelled in a very

small region near the source. This might result in large variations in odour concentration over small distances or release heights.

The uniform Cartesian grid was used to define a regular grid of receptors which could be used for developing contours of odour concentration throughout the study region. The discrete Cartesian grid was used to define specific receptors at points that represented the location of the teams of volunteers who performed field detection and annoyance measurements.

3.3.5 Transformation of Predicted Odour Concentrations

3.3.5.1 Time Averaging

The ISCST3 model produces 1-hour time-average concentrations during the period specified. The one-hour average concentrations would mask the higher concentrations that would be experienced by persons in the field who would be exposed to the odours for much shorter periods. Given that each measurement of response and annoyance in the field was conducted over a 1-minute period (see Table 3.1), Equation 2.2 was used to convert the 1-hour average concentrations to 1-minute average concentrations

The exponent used in Equation 2.2 is a function of the atmospheric stability. In this study, n was chosen based on the values provided the USEPA and are presented in Table 3.17. The stability class was determined from the average wind speed, according to the categories shown in Table 3.16, which had been calculated from the data obtained during the period in which the field study was conducted. During this study, the stability was either B or C, and thus the exponent always had a value of 0.52.

Table 3.17: Exponent, n, as a function of atmospheric stability (Beychok, 1994).

Stability class	n (USEPA)
A	0.65
B	0.52
C	0.52
D	0.32
E	n/a
F	n/a

n/a = not available

3.3.5.2 Probability of Response and Degree of Annoyance

After the odour concentrations were converted to 1-minute time-averages, they were used to calculate the probability of response and degree of annoyance using Equations 2.6 and 2.7, respectively. In order to use these equations to translate predicted field odour concentrations into response and annoyance values, it was assumed that all odours emitted from the barns are of similar characteristic. This assumption was necessary because it is currently not known how to predict how populations will respond to mixed odours of very different characteristics. Thus, it must be assumed that all odours emitted from the hog operations have the same persistence values. If this is the case, the method proposed by Nicell (2003) can be used to estimate the persistence values for odours of same characteristic (i.e., odours of similar origin and relative concentrations of certain chemical species that are odorous), but different concentrations. This is accomplished by normalizing the response data for each sample by its threshold. This causes all odour response curves to collapse onto a single curve, which can be described by a particular value of persistence. This procedure is shown in Figure 3.11, where the data arising from 4 odour samples have been normalized. A curve described by Equation 2.4 was fit to the data for all the samples and the overall persistence of response value, p, was determined. This overall persistence value was then used with Equation 2.6 to transform predicted odour concentrations in OU into probability of response.

A similar approach, as described by Nicell (2003), was used to estimate the parameters, R and a, that were needed in Equation 2.7 to transform odour concentration into degree of annoyance. In this approach, the annoyance data are normalized with respect to their thresholds and tend to collapse onto a single annoyance curve as shown in Figure 3.12. This normalized data was then fit to Equation 2.5 in order to estimate an overall persistence of annoyance value, a, and D_{A5}. The value of R, as described in section 2.3.1 and in Figure 2.6, was then calculated from D_{50} and D_{A5}.
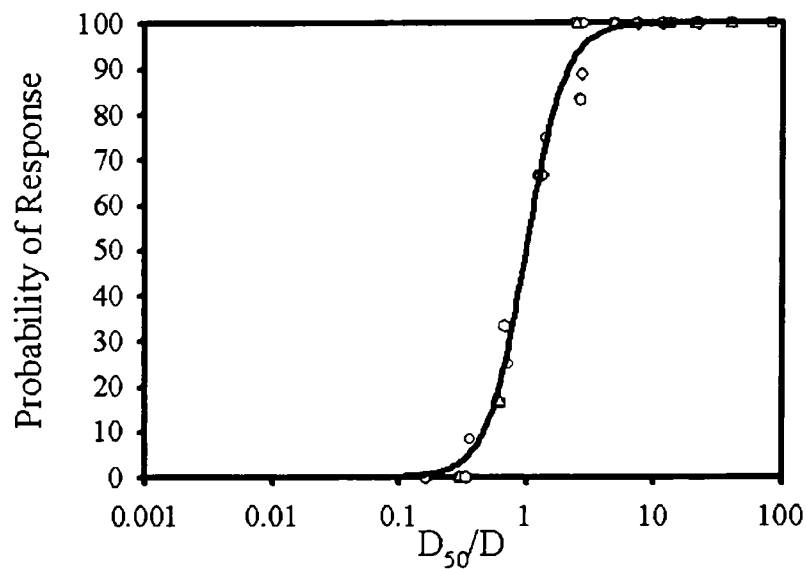
Figure 3.11: Normalized probability of response curve.
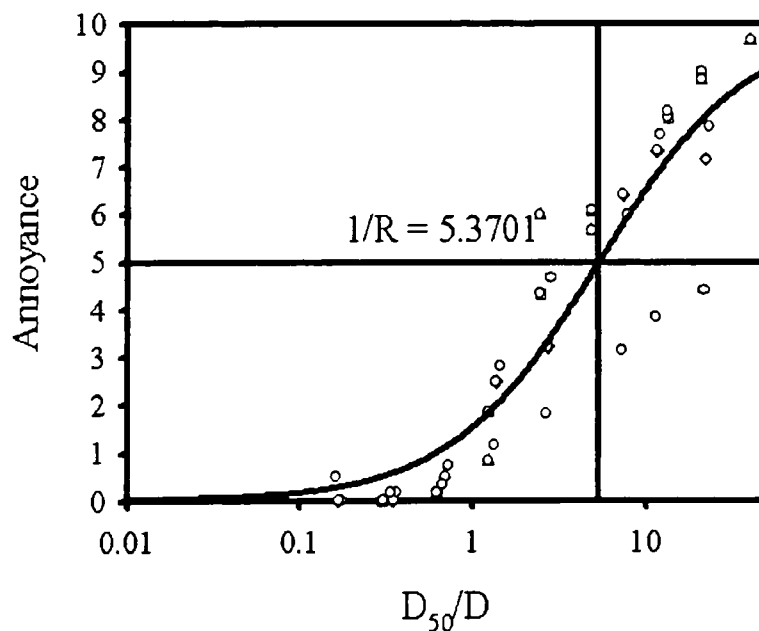
Figure 3.12: Normalized degree of annoyance curve.

40

4 Results and Calculations

4.1 Field Measurement Results

All results for field measurements that were collected as described in Section 3.1.2 are contained in Appendix A.

4.2 Olfactometry Results

Raw olfactometry data arising from the analysis of odour samples using the methodology described in Section 3.2.2 are contained in Appendix B. Table 4.1 shows the reduced data that were used to create OIM curves, which are also shown in Appendix B. This data was then fit to Equations 2.4 and 2.5, resulting in the OIM parameters shown in Table 4.2. Also listed in the latter table are the adjusted regression coefficients (r^2) that reflect the goodness-of-fit of these equations to the data.

Table 4.1: Average probability of response and degree of annoyance for all samples. D = response of panellists and A= average degree of annoyance.

	Dilutions	299C		299F		300C		300F		Fosse	
		D	A	D	A	D	A	D	A	D	A
First Experiment	2556	Not available		0	0	0	0	Not available		Not available	
	1236			0	0	41.67	0.13	0	0	0	0
	619			16.67	0.25	83.33	0.92	33.33	0.33	0	0
	312			33.33	1.04	83.33	1.71	66.67	1.25	41.67	1.17
	157			100	2.83	88.89	2.44	83.33	2.38	50	1.83
	57			100	6.29	100	5.79	100	6.21	58.33	4
	36			100	7.13	100	5.50	100	7.67	83.33	6.79
	19			100	7.75	100	7.67	100	8.5	100	8
	9			100	7.92	100	8.33	100	9	Not available	
Second Experiment	2556	0	0	0	0	0	0	Not available		0	0.5
	1236	8.33	0.17	16.67	0.17	16.67	0.17	0	0	0	0.17
	619	25	0.75	66.67	1.88	66.67	0.83	0	0	33.33	0.33
	312	75	2.83	100	4.33	100	6	33.33	0.5	66.67	1.17
	157	100	4.67	100	6.08	100	5.67	66.67	2.5	83.33	1.83
	57	100	6	100	8.04	100	8.17	88.89	3.22	100	3.17
	36	100	7.67	100	9	100	8.83	100	6.42	100	3.83
	19	100	7.83	100	0	100	9.67	100	7.33	100	4.42
	9	Not available		100	0	Not available		100	7.17	Not available	

Table 4.1 (continued): Average probability of response and degree of annoyance for all samples. D = response of panellists and A= average degree of annoyance.

	Dilutions	299C		299F		300C		300F		Fosse	
		D	A	D	A	D	A	D	A	D	A
Third Experiment	2556	0	0	0	0	0	0	0	0	0	0
	1236	50	0.67	33.33	0.5	16.67	0.17	16.67	0.08	0	0
	619	83.33	1.83	83.33	3.5	91.67	3	66.67	1.42	11.11	0.17
	312	100	4	100	6.17	100	5.5	100	3.58	38.89	0.72
	157	100	5.83	100	6.73	100	6.75	100	5.33	88.89	2.17
	57	100	7.25	100	8	100	7.67	100	6.33	100	3.33
	36	100	7.83	100	8.6	100	8	100	7.17	100	4.67
	19	100	8	100	9	100	8.17	100	8.17	100	4.83

Table 4.2: Threshold (D_{50}), persistence (p) and adjusted r^2 values from the probability of response curve of the OIM.

Sample	First Experiment			Second Experiment			Third Experiment		
	D_{50}	p	r^2	D_{50}	p	r^2	D_{50}	p	r^2
299C	Not available			445	0.24	0.99	1001	0.23	0.98
299F	278	0.16	0.98	765	0.22	0.99	1174	0.22	0.99
300C	1044	0.27	0.95	765	0.22	0.99	936	0.15	0.99
300F	414	0.31	0.99	425	0.3	0.99	765	0.22	0.99
Fosse	133	0.46	0.86	414	0.31	0.99	279	0.23	0.99

As mentioned in Section 3.2.3, the olfactometry results for the 299F, 300C and 300F of the first experiment were combined as though they were one sample to provide a single dose response curve and hence one threshold, and persistence value. The dose response curve shown in Figure B.5 in Appendix B gave an overall response threshold of 423 dilutions, an overall p of 0.34, with an adjusted r^2 is 0.99.

Based on the D_{50} values shown in Table 4.2 and the volumetric emission rates of the sources in the barns, emission rates were estimated for each source as described in Section 3.3.2.2. The emission rates that were used in dispersion modelling for all the sources in the three experiments may be found in Appendix C.

4.3 Normalized Response and Annoyance

Normalized response and annoyance curves were generated in order to determine overall values of the persistences of annoyance and response and R. The dilutions values found in Table 4.1 for each curve were normalized by dividing them by their D_{50}. As described in Section 3.3.5.2, this causes all curves to collapse onto a single curve from which the overall OIM parameters can be extracted. The normalized curves for all three experiments are shown in Appendix D. Table 4.3 contains a summary of the results obtained from the normalized curves.

Table 4.3: Values of OIM parameters (R, p and a) used to describe overall trends in probability of response and degree of annoyance curves.

	R	Normalized Response		Normalized Annoyance	
		Persistence (p)	r^2	Persistence (a)	r^2
First Experiment	0.17	0.34	0.94	0.51	0.83
Second Experiment	0.19	0.26	0.99	0.50	0.85
Third Experiment	0.18	0.21	0.99	0.52	0.90

The values of R shown in Table 4.3 are very consistent, with only a 7% difference between the lowest and highest values. These values are on the high end of the range of R values observed by Nicell (2003). Odours with high values of R would tend to have greater impact than those with low values since the annoyance of the population would be observed at odour concentrations that are close to the threshold. The persistences of response and annoyance fall within the range of those observed by Nicell (2003) with ranges of 0.21 to 0.45 and 0.41 to 0.59 for response and annoyance, respectively.

43

4.4 Predicted Odour Concentrations, Probability of Response & Annoyance

Dispersion modelling was conducted for all experiments using the emission rates and source parameters listed in Appendix C. This resulted in predictions of 1-hour time-averaged odour concentrations (in OU) in the regions surrounding the barns. The 1-hour average odour concentrations were converted to 1-minute averages as explained in Section 3.3.5.1. The probability of response and degree of annoyance for both time averages were calculated using Equations 2.6 and 2.7, respectively.

The predicted values were then compared with the field responses and degrees of annoyance summarized in Appendix A. This was done by plotting the predicted response and annoyance at each location versus the observed values. The plots were done for all combinations of different source types (point, area and volume sources), emission heights (ground level and estimated emission height), and receptor height (ground level and 1.5 m). Table 4.4 summarizes the correlation coefficients for all modelled situations. Plots for the best correlations (as identified in bold-italicized font in Table 4.4) for each experiment with 1-hour and 1-minute averaging times are shown in Appendix E.

Table 4.4: Correlation coefficients of all the modelling situations for the predicted probability of response and degree of annoyance. Values in bold italics are the best and worst correlation coefficients for each experiment and averaging time.

			First Experiment			
			Probability of Response		Degree of Annoyance	
			1hr averaging	1 min. averaging	1hr averaging	1 min. averaging
Point Sources	G.L Sources	G.L Receptors	0.2876	0.2902	0.5616	0.6569
		1.5m Receptors	0.2902	*0.5174*	0.5779	*0.6622*
	Sources with release ht.	G.L Receptors	0.2882	0.5172	0.5818	0.6563
		1.5m Receptors	0.2907	0.5173	0.5946	0.6617
Area Sources	G.L Sources	G.L Receptors	0.3570	*0.2417*	0.5984	0.5303
		1.5m Receptors	*0.3573*	0.2419	*0.6079*	0.5318
	Sources with release ht.	G.L Receptors	0.3232	0.5139	*0.1312*	*0.0728*
		1.5m Receptors	0.3521	0.2832	0.4454	0.4450
Volume Sources	G.L Sources	G.L Receptors	0.2506	0.4031	0.4147	0.4329
		1.5m Receptors	0.2505	0.4180	0.4503	0.4482
	Sources with release ht.	G.L Receptors	0.2508	0.4174	0.4521	0.4454
		1.5m Receptors	*0.2502*	0.4170	0.4454	0.4450

Table 4.4 (continued): Correlation coefficients of all the modelling situations for the predicted probability of response and degree of annoyance. Values in bold italics are the best and worst correlation coefficients for each experiment and averaging time.

Second Experiment						
Point Sources	G.L Sources	G.L Receptors	0.3244	0.5487	0.4168	0.4381
		1.5m Receptors	0.3230	0.5477	0.4201	0.4381
	Sources with release ht.	G.L Receptors	0.3113	0.5432	0.4119	0.4321
		1.5m Receptors	0.3113	0.5432	0.4119	0.4321
Area Sources	G.L Sources	G.L Receptors	*0.4449*	0.6458	0.5431	0.6158
		1.5m Receptors	0.4277	0.6019	0.4372	0.4564
	Sources with release ht.	G.L Receptors	0.4409	0.5845	0.5404	0.5774
		1.5m Receptors	0.4409	0.6349	0.5404	0.5804
Volume Sources	G.L Sources	G.L Receptors	*0.1056*	*0.1209*	*0.0944*	*0.1304*
		1.5m Receptors	0.3903	0.6127	0.5189	*0.6116*
	Sources with release ht.	G.L Receptors	0.3735	*0.6682*	0.5343	0.5954
		1.5m Receptors	0.3703	0.5991	*0.5575*	0.6081
Third Experiment						
Point Sources	G.L Sources	G.L Receptors	0.1363	0.5614	0.4844	0.5369
		1.5m Receptors	0.1353	0.5608	0.4858	0.5367
	Sources with release ht.	G.L Receptors	0.1360	*0.5614*	0.4850	*0.5371*
		1.5m Receptors	0.1351	0.5609	0.4864	0.5369
Area Sources	G.L Sources	G.L Receptors	*0.1679*	0.5415	0.4713	0.5251
		1.5m Receptors	0.1668	0.5410	0.4729	0.5247
	Sources with release ht.	G.L Receptors	0.1658	0.5405	0.4748	0.5369
		1.5m Receptors	0.1647	0.5401	0.4759	0.5369
Volume Sources	G.L Sources	G.L Receptors	0.1298	0.5509	*0.4680*	0.5255
		1.5m Receptors	0.1287	0.5503	0.4697	0.5251
	Sources with release ht.	G.L Receptors	0.1276	0.5496	0.4718	0.5249
		1.5m Receptors	*0.0016*	*0.1704*	*0.0239*	*0.0482*

Contour lines for the 50% probability of response and an annoyance of 5 were generated from four situations selected from all experiments that had the highest correlations between predicted and field results (see Table 4.4); i.e., 2 cases where the correlations between field and predicted results were highest for probability of response and 2 cases where correlations were highest for annoyance. These predicted contour lines were then compared with contour lines generated from the field measurements, as shown in Figures 4.1 to 4.4. The 50% contour of response line was used to identify the region within which 50% of the group of odour judges was expected to be able to respond the odour. This contour also exactly corresponds to the contour line where the odour concentration is 1 OU. This contour line and the annoyance contour of 5 (corresponding to a "very

unpleasant" odour, as shown in Figure 2.5) were chosen as the means for visualizing the spatial extent of the impact zone of the odorous emissions and to determine if the model was under- or over-predicting the size of the impacted region.
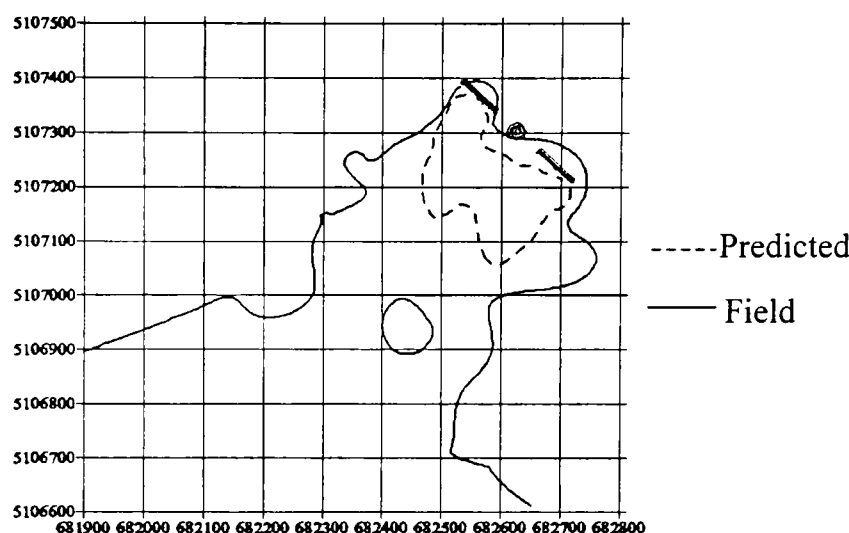
Figure 4.1: Impact zones (defined by the area in which there was 50% or greater response) generated from field data and 1-hour time-averaged dispersion-modelling results for the second experiment with modelling of emissions as area sources at ground-level and with ground-level receptors (i.e., the scenario in which there was the highest correlation between measured and predicted probabilities of response).
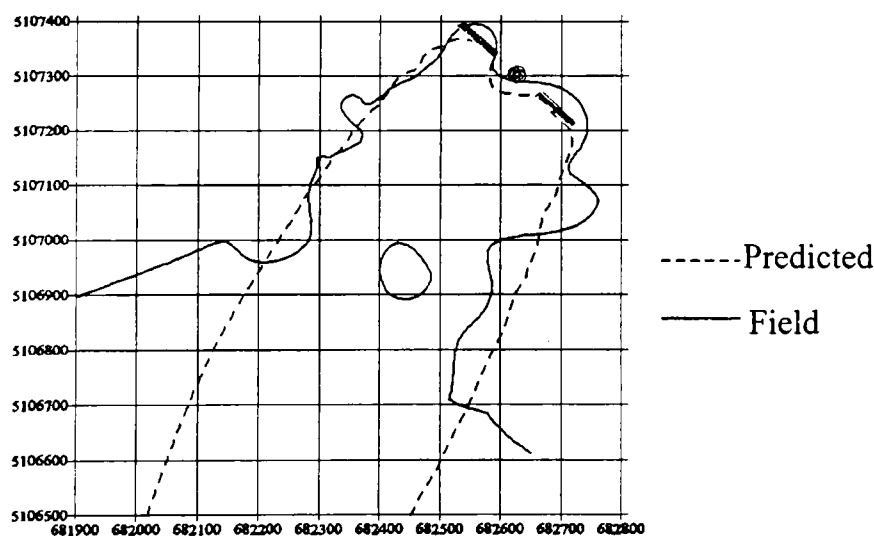
Figure 4.2: Impact zones (defined by the area in which there was 50% or greater response) generated from field data and 1-minute time-averaged dispersion-modelling results for the second experiment with modelling of emissions as volume sources with a release height and with ground-level receptors (i.e., the scenario in which there was the highest correlation between measured and predicted probabilities of response).

46
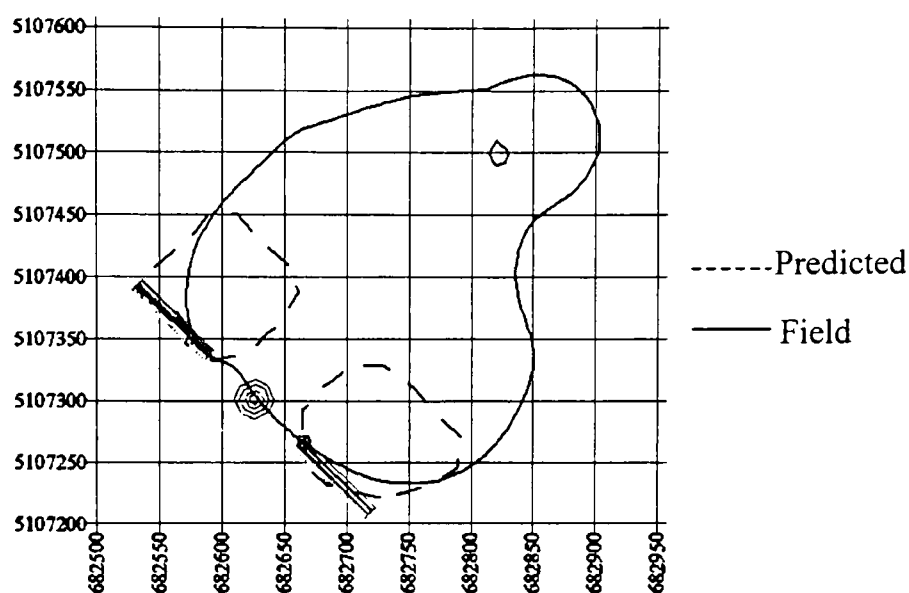
Figure 4.3: Impact zones (defined by the area in which there was a degree of annoyance of 5 or greater) generated from field data and 1-hour time-averaged dispersion-modelling results for the first experiment with modelling of emissions as area sources at ground-level and with receptors at 1.5 m (i.e., the scenario in which there was the highest correlation between measured and predicted degrees of annoyance).
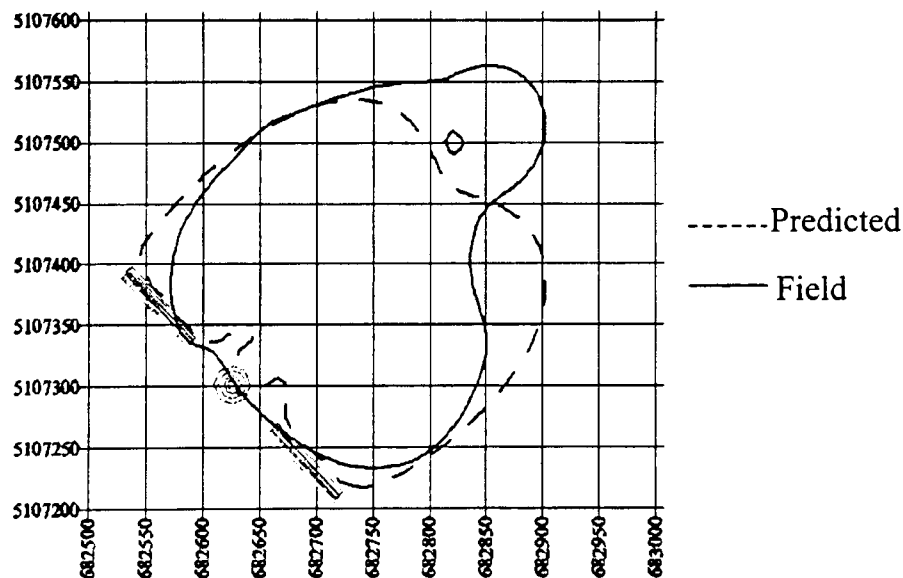
Figure 4.4: Impact zones (defined by the area in which there was a degree of annoyance of 5 or greater) generated from field data and 1-minute time-averaged dispersion-modelling results for the first experiment with modelling of emissions as ground-level point sources and with receptors at 1.5 m (i.e., the scenario in which there was the highest correlation between measured and predicted degrees of annoyance).

Detailed analyses were conducted to compare model predictions with field results for the case where the emissions were modelled as point sources released at ground level and with receptors at a 1.5 m height. In addition to the correlations already presented in Table 4.4, spatial analyses of the extent of the predicted zones of 50% probability of response (Figures 4.5 to 4.10) and a degree of annoyance of 5 (Figures 4.4 and 4.11 to 4.15) were compared with those of the field measurements. The results of all field and predicted responses and annoyances from all experiments were combined to provide an overall view of how well the model predictions correlate with field results (Figures 4.16 to 4.19). In addition, histograms (Figures 4.20 to 4.23) were constructed to reflect the magnitude and frequency of differences between the predicted and field measurements of response and annoyance for all three experiments.
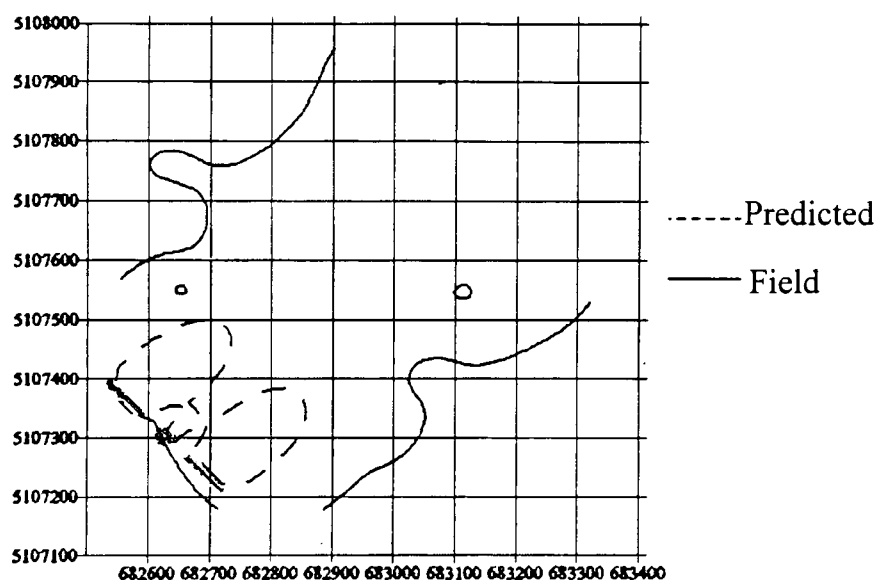
Figure 4.5: Impact zones (defined by the area in which there was 50% or greater response) generated from field data and 1-hour time-averaged dispersion-modelling results for the first experiment with modelling of emissions as point sources with a ground-level release height and with receptors at 1.5 m.

48
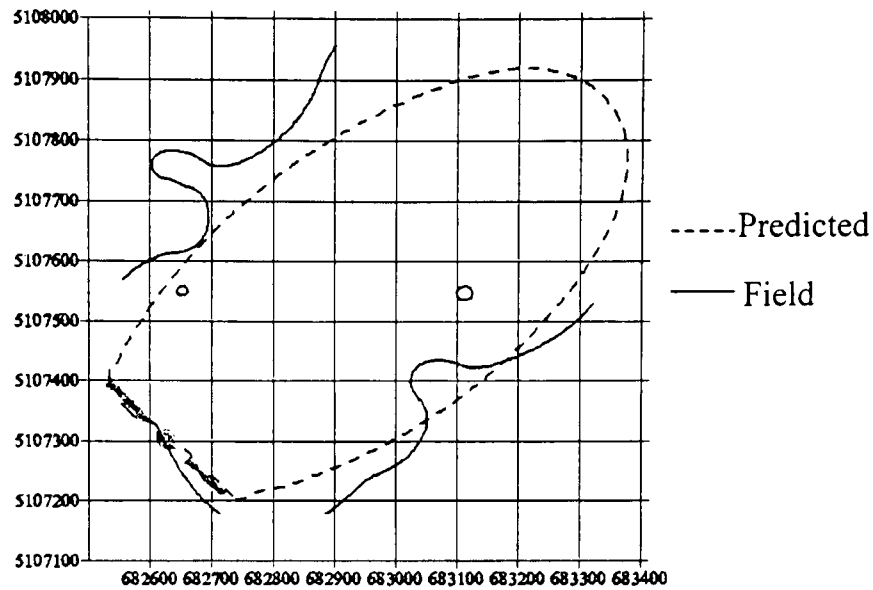
Figure 4.6: Impact zones (defined by the area in which there was 50% or greater response) generated from field data and 1-minute time-averaged dispersion-modelling results for the first experiment with modelling of emissions as point sources with a ground-level release height and with receptors at 1.5 m.
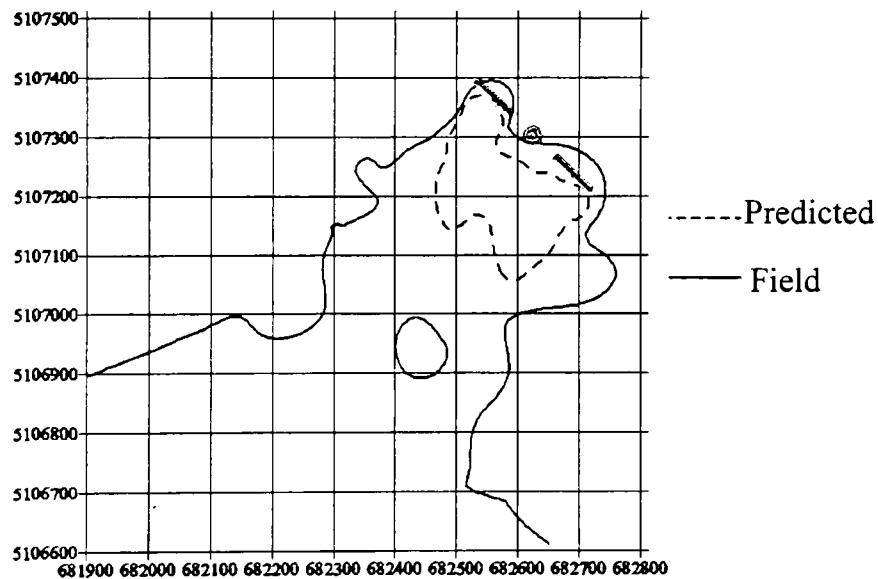
Figure 4.7: Impact zones (defined by the area in which there was 50% or greater response) generated from field data and 1-hour time-averaged dispersion-modelling results for the second experiment with modelling of emissions as point sources with a ground-level release height and with receptors at 1.5 m.
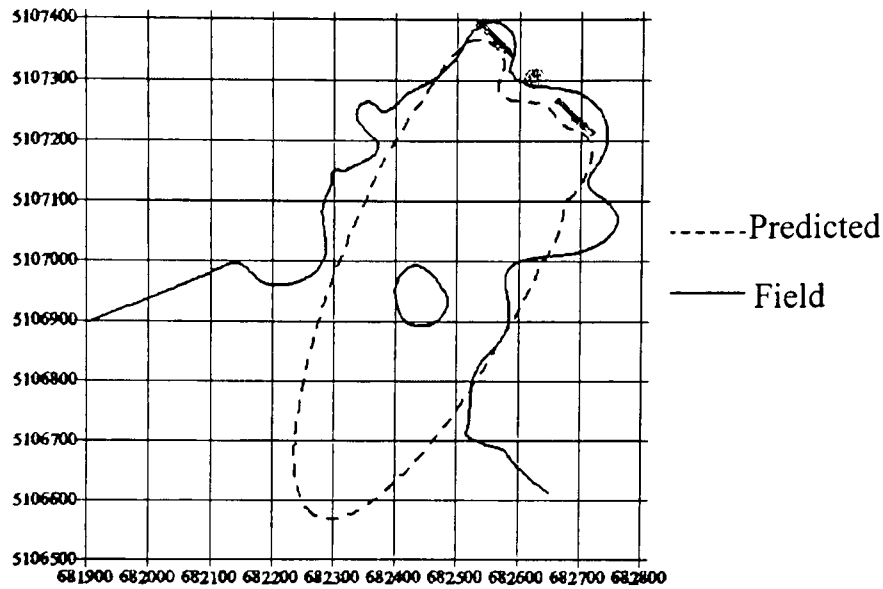
Figure 4.8: Impact zones (defined by the area in which there was 50% or greater response) generated from field data and 1-minute time-averaged dispersion-modelling results for the second experiment with modelling of emissions as point sources with a ground-level release height and with receptors at 1.5 m.
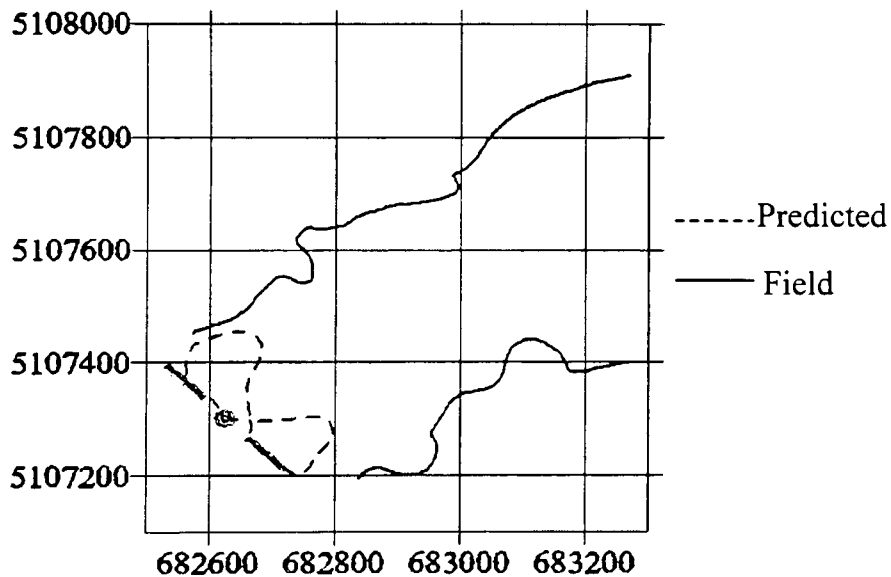
Figure 4.9: Impact zones (defined by the area in which there was 50% or greater response) generated from field data and 1-hour time-averaged dispersion-modelling results for the third experiment with modelling of emissions as point sources with a ground-level release height and with receptors at 1.5 m.
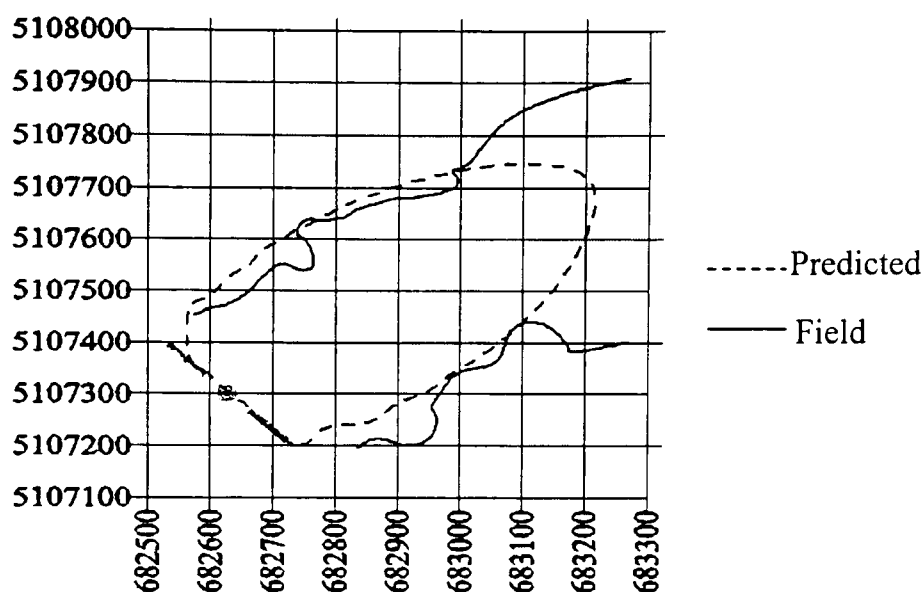
Figure 4.10: Impact zones (defined by the area in which there was 50% or greater response) generated from field data and 1-minute time-averaged dispersion-modelling results for the third experiment with modelling of emissions as point sources with a ground-level release height and with receptors at 1.5 m.
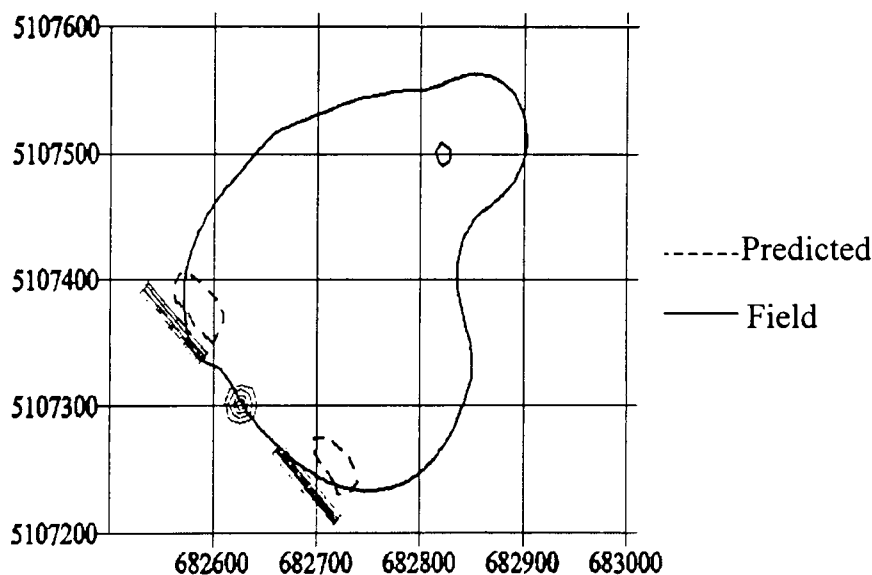
Figure 4.11: Impact zones (defined by the area in which there was a degree of annoyance of 5 or greater) generated from field data and 1-hour time-averaged dispersion-modelling results for the first experiment with modelling of emissions as point sources with a ground-level release height and with receptors at 1.5 m.
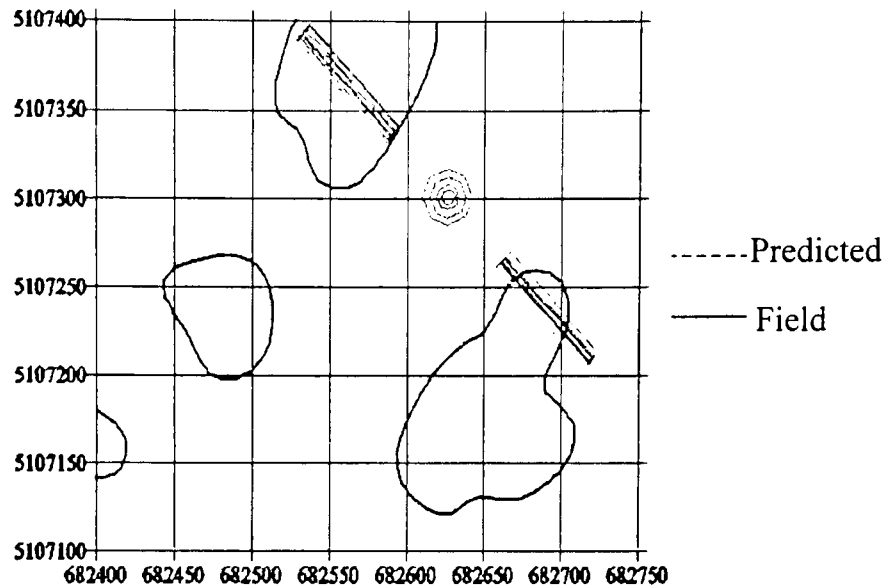
Figure 4.12: Impact zones (defined by the area in which there was a degree of annoyance of 5 or greater) generated from field data and 1-hour time-averaged dispersion-modelling results for the second experiment with modelling of emissions as point sources with a ground-level release height and with receptors at 1.5 m. Note: in this scenario, no region in which annoyance was equal to or exceeded 5 was predicted.
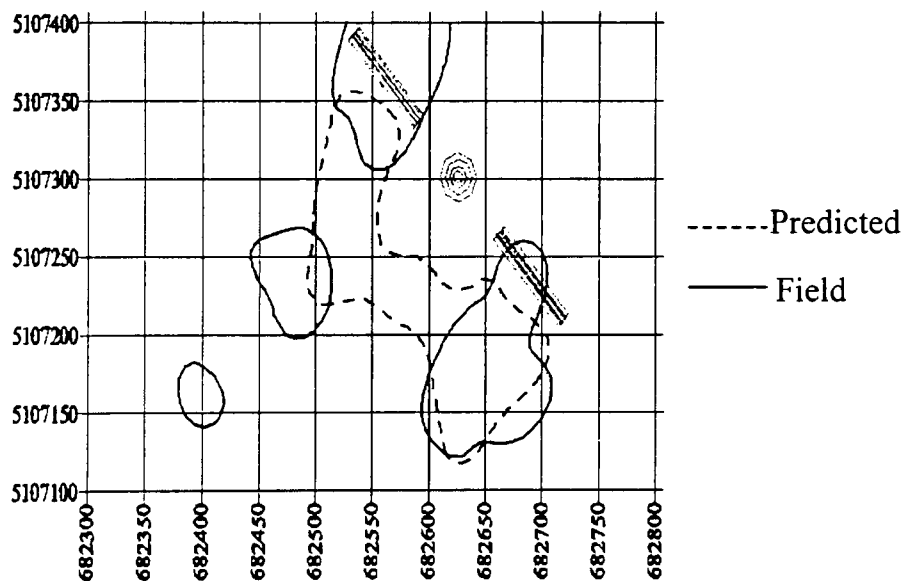
Figure 4.13: Impact zones (defined by the area in which there was a degree of annoyance of 5 or greater) generated from field data and 1-minute time-averaged dispersion-modelling results for the second experiment with modelling of emissions as point sources with a ground-level release height and with receptors at 1.5 m.
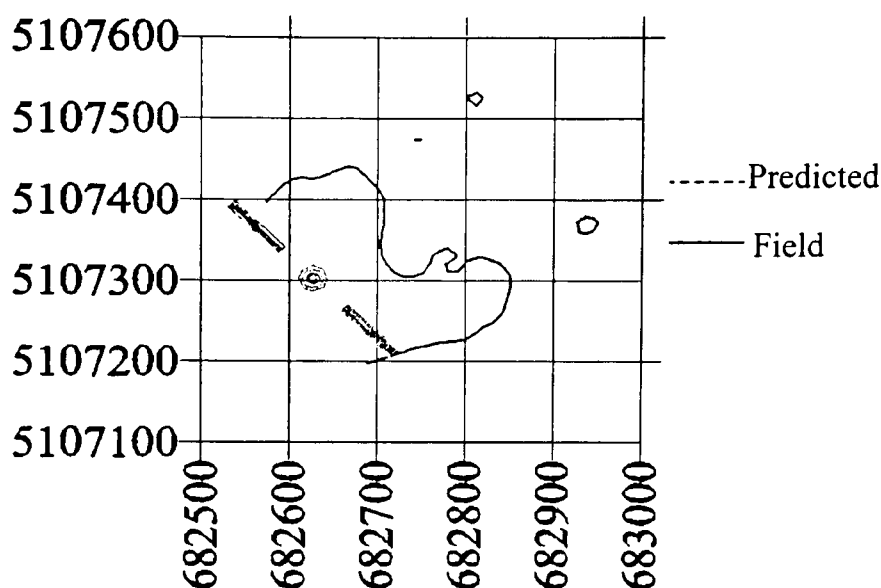
Figure 4.14: Impact zones (defined by the area in which there was a degree of annoyance of 5 or greater) generated from field data and 1-hour time-averaged dispersion-modelling results for the third experiment with modelling of emissions as point sources with a ground-level release height and with receptors at 1.5 m. Note: in this scenario, no region in which annoyance was equal to or exceeded 5 was predicted.
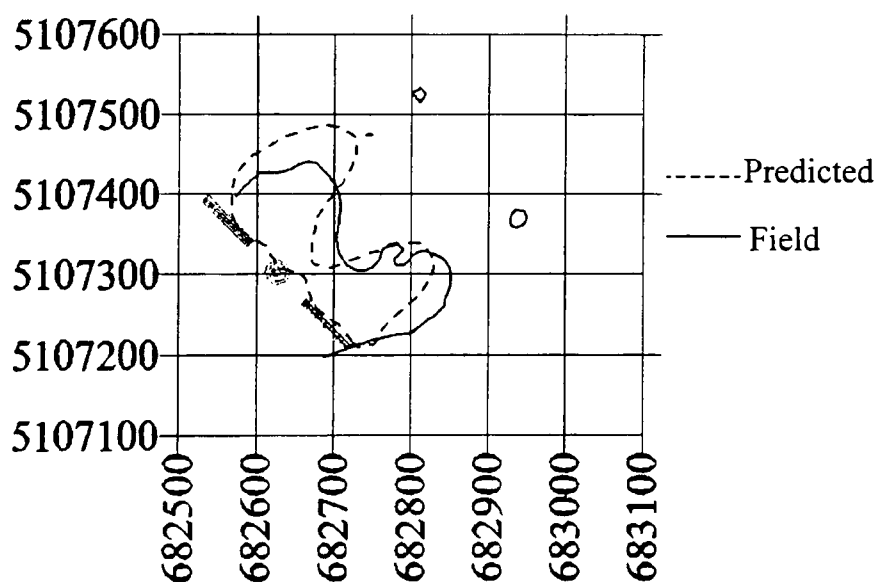
Figure 4.15: Impact zones (defined by the area in which there was a degree of annoyance of 5 or greater) generated from field data and 1-minute time-averaged dispersion-modelling results for the third experiment with modelling of emissions as point sources with a ground-level release height and with receptors at 1.5 m.
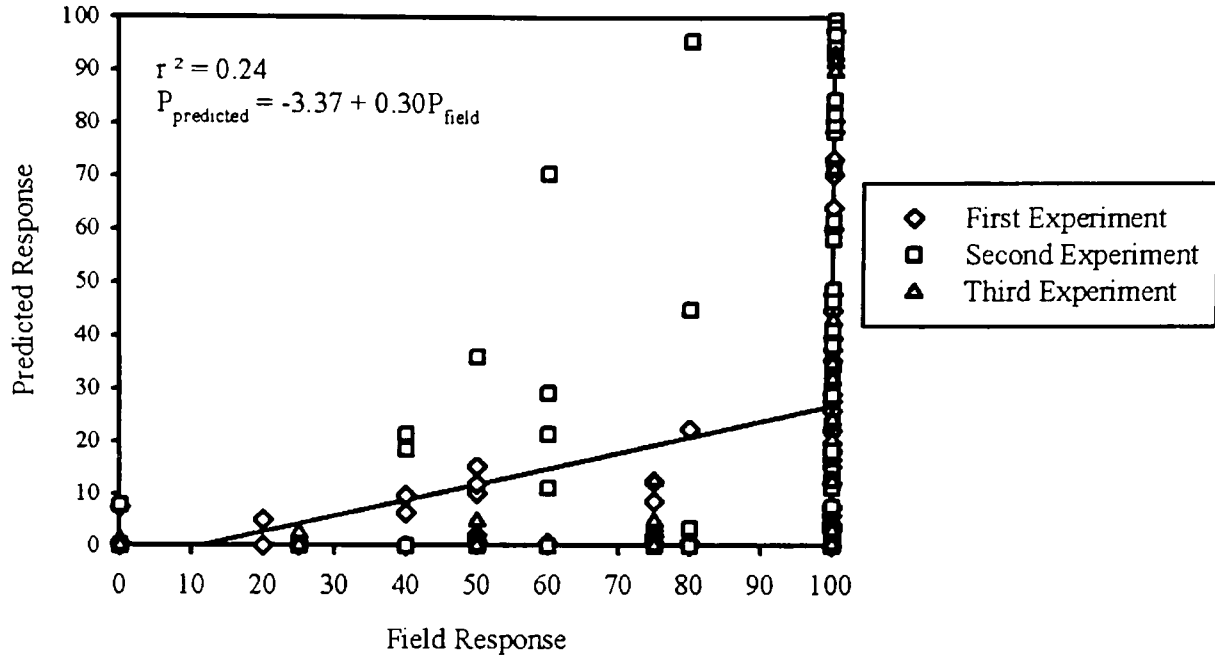
Figure 4.16: Combined results of field and predicted 1-hour time-averaged responses from all experiments to provide an overall view of how well the model predictions correlate with field results. Predictions were made using ISCST3 with modelling of emissions as point sources with a ground level release height and with receptors at 1.5 m.
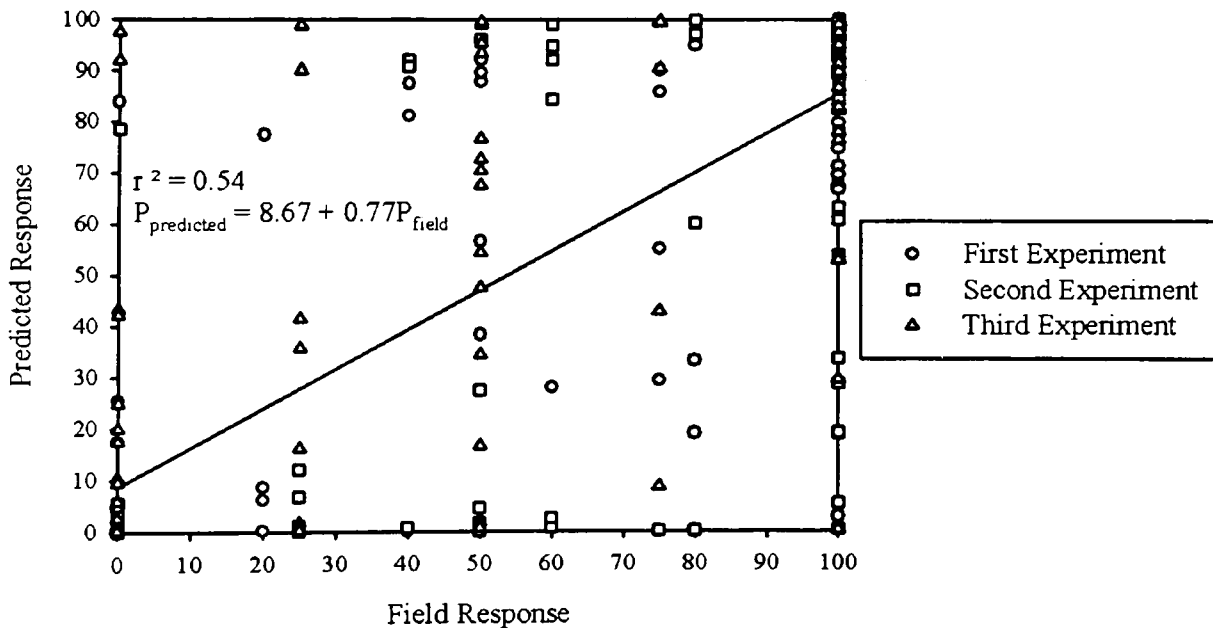
Figure 4.17: Combined results of field and predicted 1-minute time-averaged responses from all experiments to provide an overall view of how the model predictions correlate with field results. Predictions were made using ISCST3 with modelling of emissions as point sources with a ground level release height and with receptors at 1.5 m.
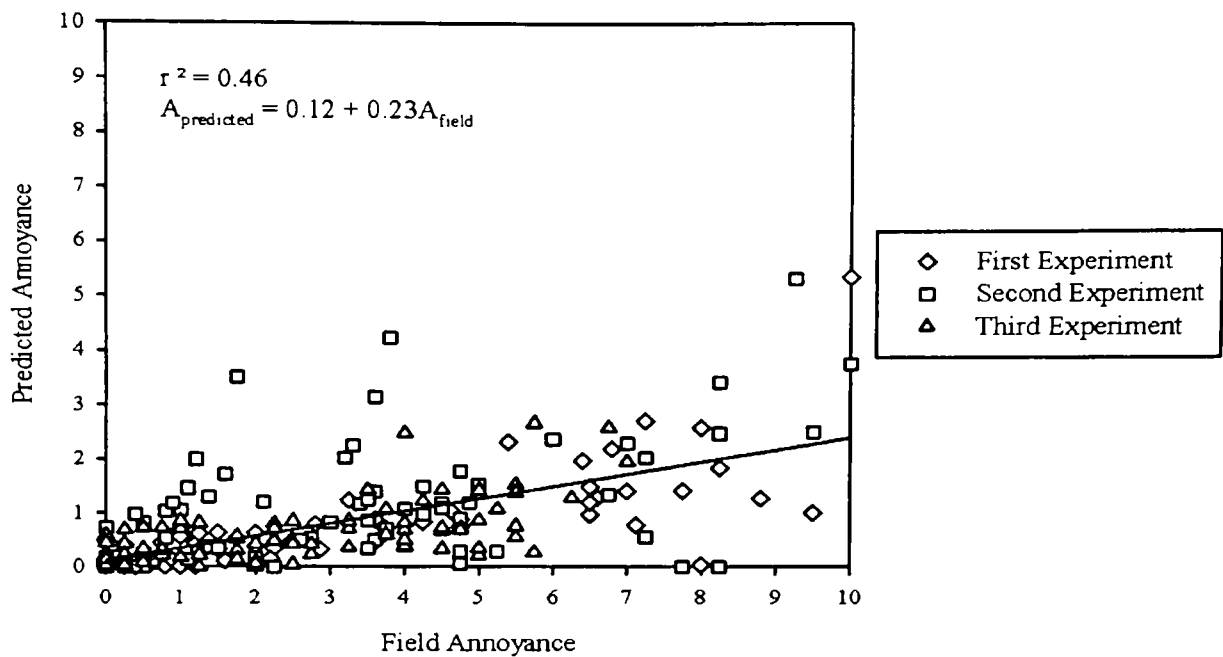
Figure 4.18: Combined results of field and predicted 1-hour time-averaged annoyances from all experiments to provide an overall view of how the model predictions correlate with field results. Predictions were made using ISCST3 with modelling of emissions as point sources with a ground level release height and with receptors at 1.5 m.
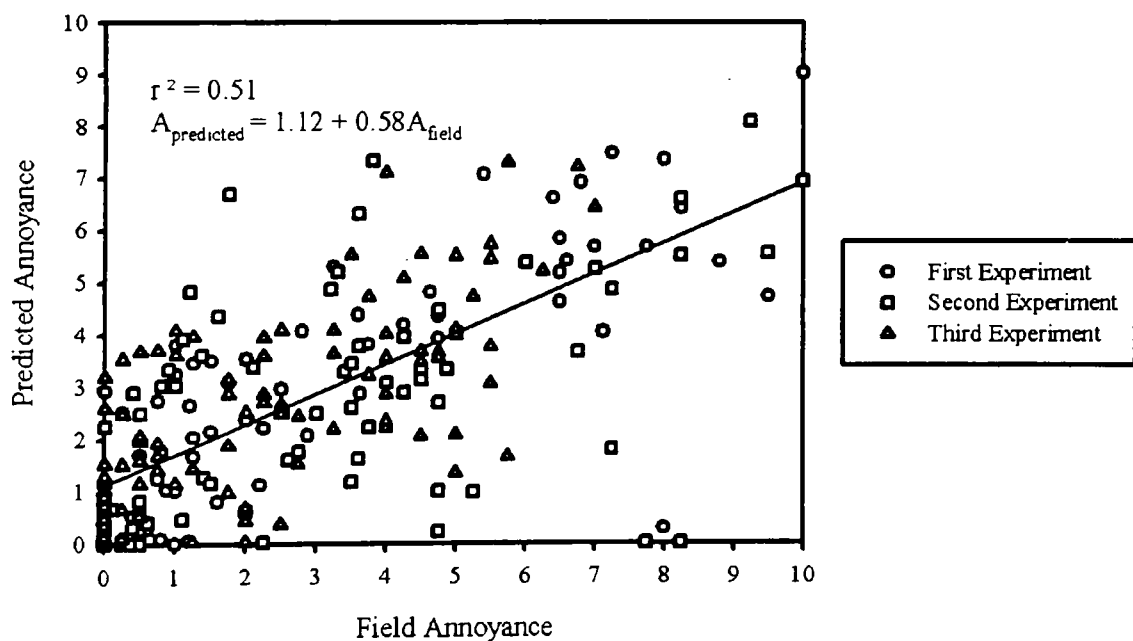
Figure 4.19: Combined results of field and predicted 1-minute time-averaged annoyances from all experiments to provide an overall view of how the model predictions correlate with field results. Predictions were made using ISCST3 with modelling of emissions as point sources with a ground level release height and with receptors at 1.5 m.
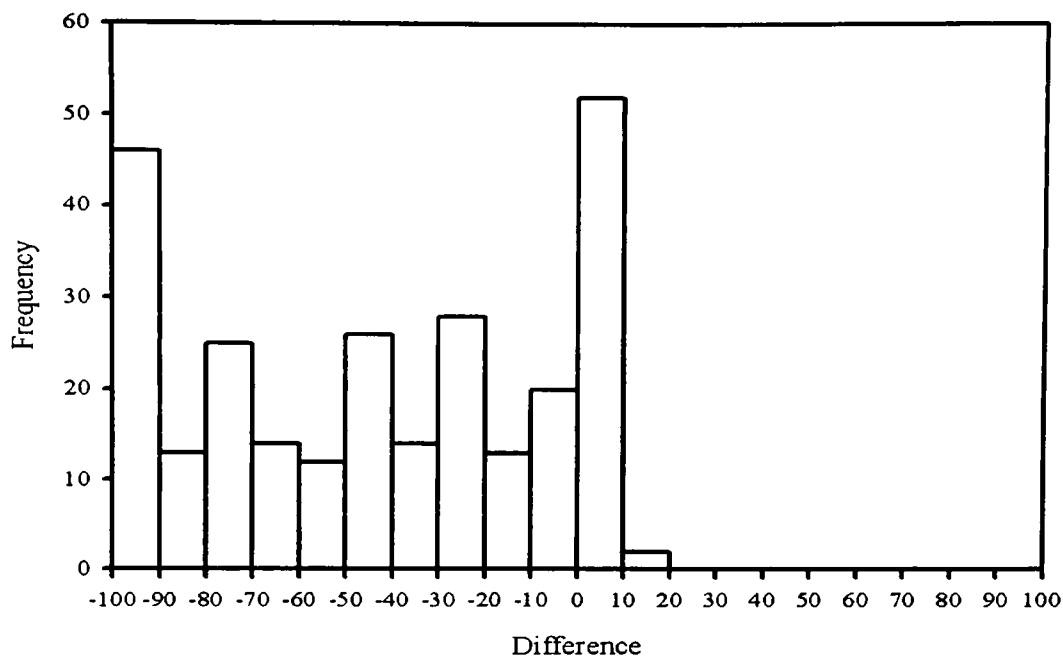
Figure 4.20: Frequency of the magnitude of differences between measured and predicted 1-hour averaged responses at receptors for all 3 experiments. Predictions were made using ISCST3 with modelling of emissions as point sources with a ground-level release height and with receptors at 1.5 m.
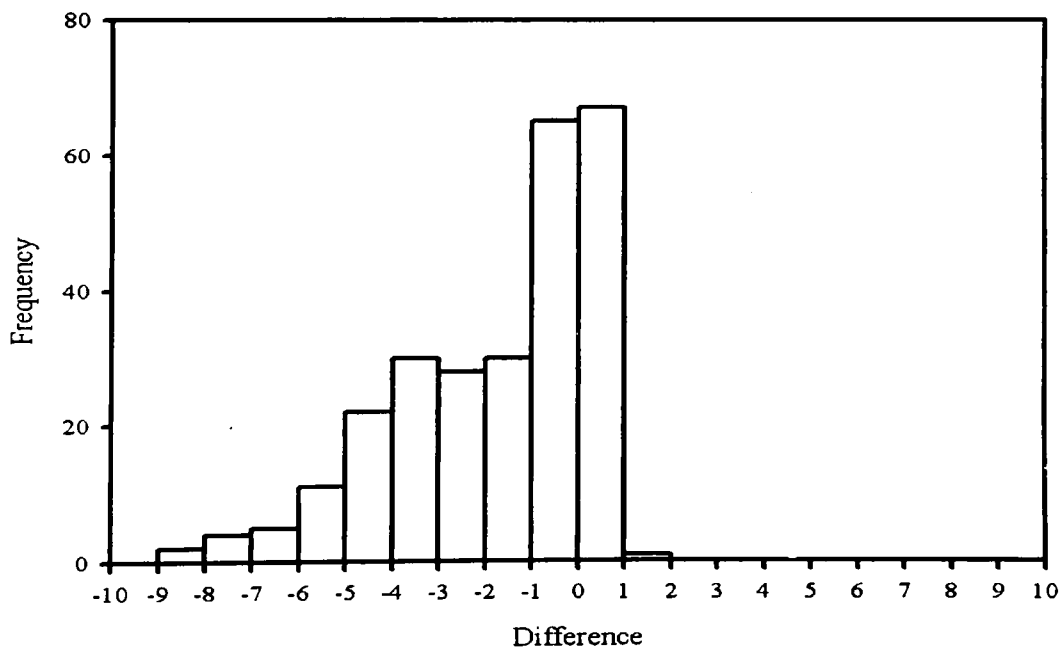
Figure 4.21: Frequency of the magnitude of differences between measured and predicted 1-minute averaged responses at receptors for all 3 experiments. Predictions were made using ISCST3 with modelling of emissions as point sources with a ground-level release height and with receptors at 1.5 m.
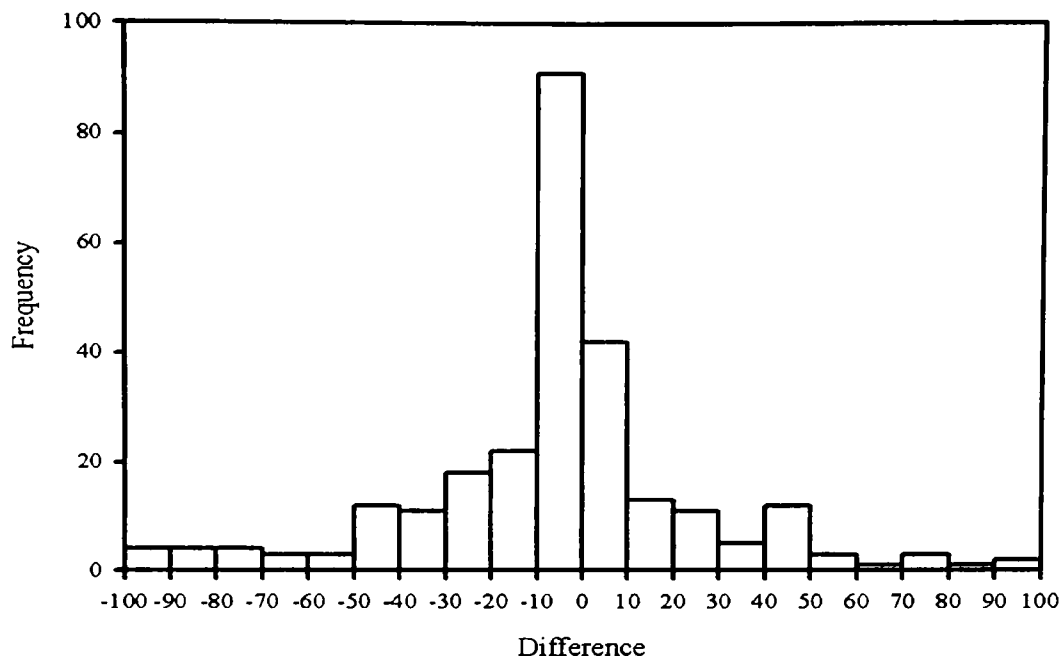
Figure 4.22: Frequency of the magnitude of differences between measured and predicted 1-hour averaged annoyances at receptors for all 3 experiments. Predictions were made using ISCST3 with modelling of emissions as point sources with a ground-level release height and with receptors at 1.5 m.
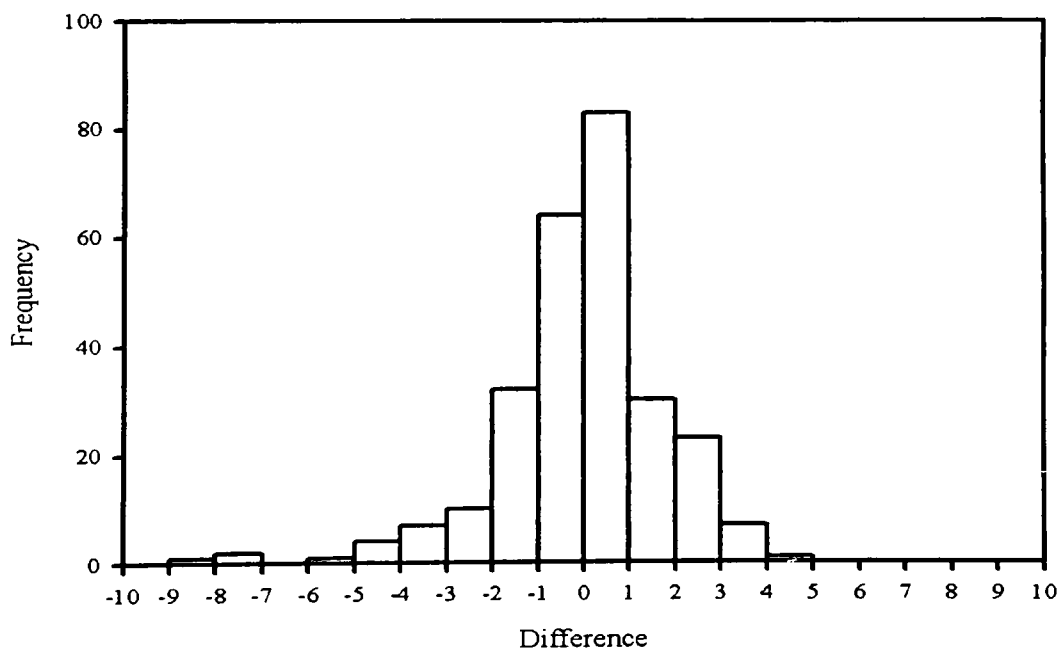
Figure 4.23: Frequency of the magnitude of differences between measured and predicted 1-minute averaged annoyances at receptors for all 3 experiments. Predictions were made using ISCST3 with modelling of emissions as point sources with a ground-level release height and with receptors at 1.5 m.

5 Discussion

5.1 OIM & Normalized Response and Annoyance

When modelling odours emitted from multiple sources, it is necessary to assign and emission rate from each source based on the threshold and volumetric flow rates from those sources. In doing this, it is inherently assumed that all odours are of similar characteristics such that the odour concentration being dispersed from each source can be arithmetically added together at each receptor. If the odours are of similar characteristic (but of different concentrations), then they should produce normalized probability of response and annoyance curves that overlap (Nicell, 2003). As a result, Nicell (2003) claimed that odours of similar characteristic would have similar R and persistence values.

The persistence of response values, p, presented in Table 4.2 for the first experiment lie within a wide range of 0.16 to 0.46. For the second and third experiments these values are within narrower ranges of 0.22 to 0.31 and 0.15 to 0.23, respectively. The wide range of persistence values in the first experiment probably arose from experimental error as the odour judges gained experience both in the laboratory and the field. This was evident in the inconsistent responses that were recorded from the panellists as they conducted the first series of odour analyses. This initial inexperience is reflected in the high degree of scatter in the normalized probability of response curves in Figure D.1 and the lower r^2 value for this experiment shown in Table 4.3. In contrast, the results for the second and third experiment had less scatter (Figures D.4 and D.5) and better correlation coefficients (Table 4.3) and, for the most part, the annoyance curves collapsed onto each other (Note: the higher scatter in the annoyance curves results from the subjective nature of the evaluation of annoyance). These observations appear to support the assumption that these odours were of similar characteristics.

This assumption is further supported by the values of R shown in Table 4.3, which are quite similar between experiments. Also, when all data from all experiments are put on the same graph, as shown in Figures 5.1 and 5.2 below, the results from the barn samples (299C, 299F, 300C, and 300F) tend to collapse onto a single curve. However, the "fosse"

sample from the manure storage tank appears to have different probability of response and annoyance curves, as reflected by substantially different values of p, a and R as compared to the barn emissions (see Figures 5.1 and 5.2). This leads to the conclusion that the odours emitted from the manure storage tank are of different character than the barn odours. While this would invalidate the initial assumption about the similar characteristics of the odours, thereby introducing error in the modelling results, it should be noted that the emission rate and odour concentration from the manure storage pit are the lowest of all sources. Thus, manure storage tank emissions contribute minimally to the overall odour impact. In fact, when the ISCST3 model was run for the condition that produced the results shown in Figure 4.11, but with the manure storage pit eliminated as a source, virtually the same contours resulted. Thus, the manure storage pit did not contribute significantly to the odour impacts observed in this study and the assumption that all odours that were emitted were of similar characteristic is justified.
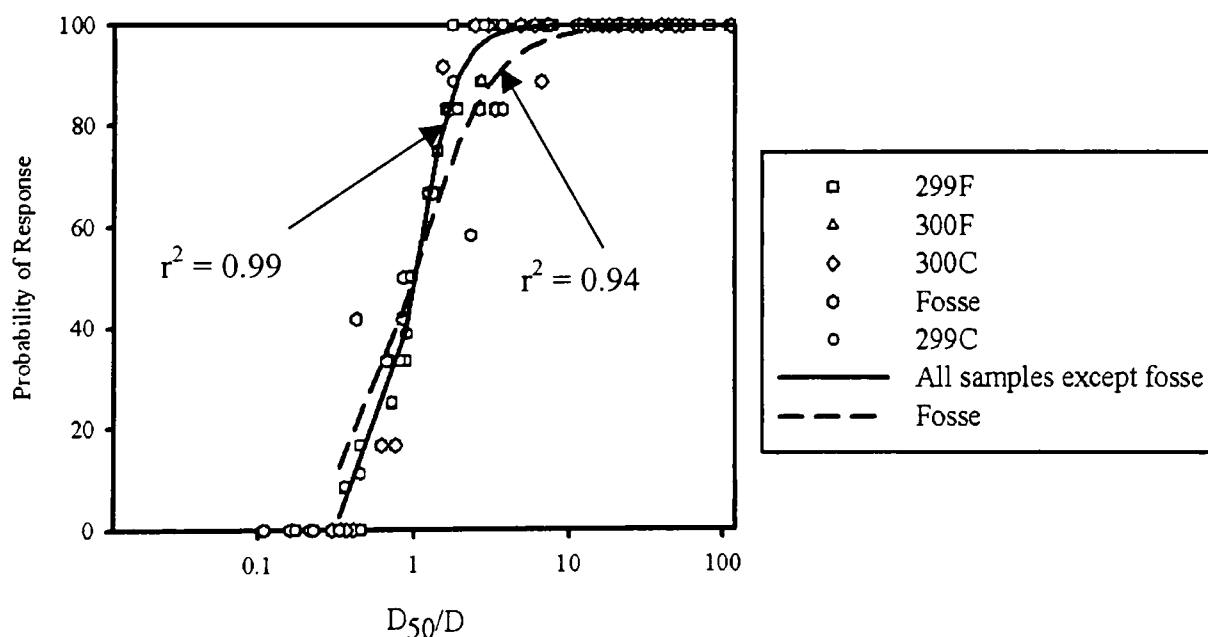
Figure 5.1: Overlapping normalized probability of response curves for all samples of the three experiments.
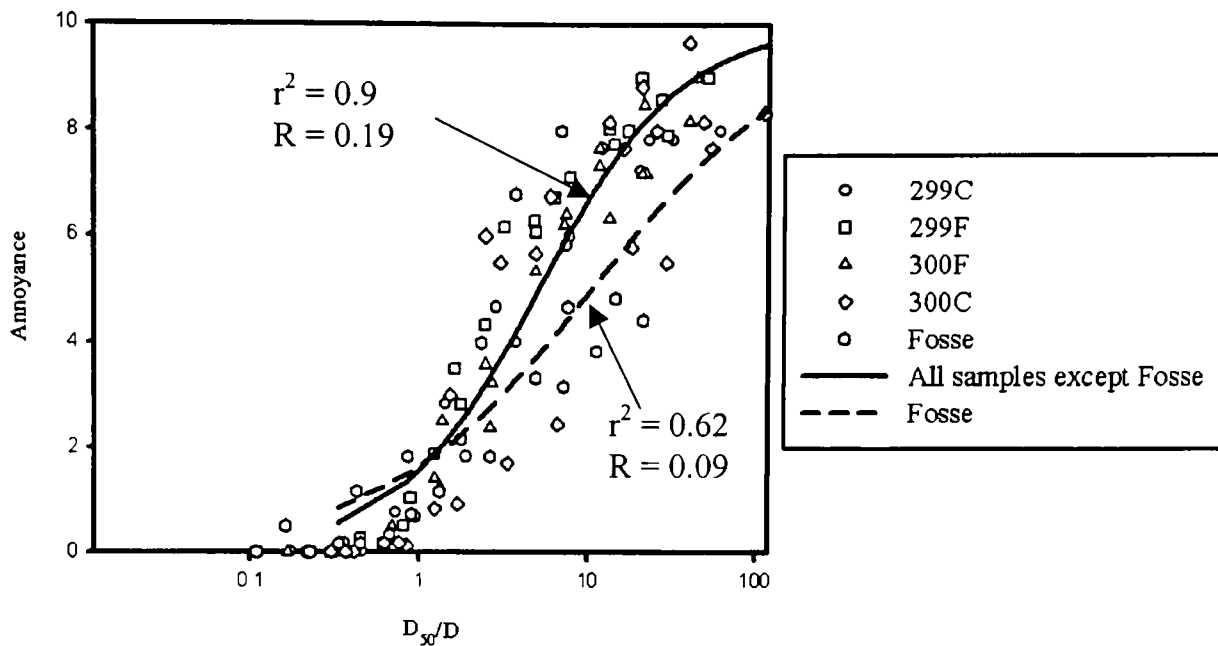
Figure 5.2: Overlapping normalized annoyance curves for all samples of the three experiments.

5.2 Selection of the Best Modeling Scenario

As revealed in this study, when modelling the dispersion of contaminants from a source, the modeller must make decisions about the type of source, the release height, the receptor height and an appropriate averaging time. Table 4.4 reveals that the emissions from the barns can be modelled in many different ways that can produce correlations to different degrees between field measurements and predicted results. Ultimately, however, only one modelling scenario must be selected for detailed study.

The ISCST3 model predicts receptor concentrations that are widely accepted as being 1-hour time-averaged concentrations. When the field observations were plotted against predicted probability of response and annoyance, the 1-hour values were poorly correlated (see Table 4.4) and the predicted values were consistently substantially lower than measured values (see 1-hour results in Appendix E). In addition, the zones of odour impact defined by the areas enclosed inside the 50% response contour or the annoyance contour of 5 tended to be very small relative the measured zones (e.g., see Figures 4.1 and 4.3), even for those cases where there was the highest correlation between results. All

60

of these observations support the conclusion that a 1-hour averaging time is inappropriate. The latter conclusion is not unexpected since the odour was experienced over shorter time intervals in the field.

Given that field observers were required to assess the odour over a 1-minute period before judging the odour, it was decided that the 1-hour average concentrations should be converted to 1-minute values. Table 4.4 shows that, in general, the use of 1-minute values improved the correlations between predicted and field measurements. The 1-minute averaging results in Appendix E also show that the 1-minute averaged results are closer to field measurements, but occasionally under- and over-predict measured values. In addition, the sizes of the predicted zones of impact tended to be nearer in size to the measured regions (e.g., see Figures 4.2 and 4.4).

When a 1-minute averaging time is selected, the correlation coefficients resulting from modelling using different sources types (point, volume and area), emission height (ground level and specified emission height) and receptor heights (ground level and 1.5 m) are quite similar, though with a few low outliers (see Table 4.4). This reveals that the model is not highly sensitive to these choices. However, out of the three types of sources modelled, point sources resulted in some of the best correlations; i.e. in 2 out of 3 experiments, the modelling of emissions as point sources tended to produce the highest and/or most consistent correlations. Also, the majority of the best correlations arose when the odorous emissions were modelled as being released from ground level. The modelling of receptors at a 1.5 m height also produced the most highly correlated results. From these observations, it can be concluded that the modelling of emission from the barns to predict impact in the field should be done using ground level point sources and receptors receiving the dispersion of the odorous emissions at a 1.5 m height. This scenario is also justified logically by the actual case present in the hog farm facility. The exhaust fans emitted the air from the barns vertically downward; therefore the emitted air was reflected from the ground before it was dispersed, hence the odorous emissions are considered to be emitted from the ground. The individuals who participated in this study experienced the odour at nose level, which was approximately 1.5 m high from the

ground; therefore the heights of the receptors should be specified in the ISCST3 model as that of the average nose level.

5.3 Predicted Probability of Response and Annoyance from Best Modelling Scenario

The predicted responses and annoyances calculated from modelling ground level point odorous releases and receptors at 1.5 m above the ground were compared with the field results. Results are shown for 1-hour and 1-minute time-averaging in order to assess the importance of time averaging in predicting odour impact.

As mentioned above, the 50%-response contours for 1-hour time-averages (Figures 4.5, 4.7 and 4.9) show that the predicted impact zones are smaller than what would be generated from the field results. This is also true for the 1-hour time-average annoyance contour of 5 (Figures 4.11, 4.12, and 4.14). In fact, in some cases, the annoyance contour lines generated from the predicted values were not present because the predicted values were always less than 5, such as in the second and third experiment represented in Figures 4.12 and 4.14, respectively. In contrast, the sizes of impact zones from the 50% response contours (Figures 4.6, 4.8, and 4.10) and contours of annoyance of 5 (Figures 4.4, 4.13 and 4.15) that were generated from the 1-minute time-averaged values are almost equal to or slightly larger in area than the zones generated from the field measurements.

The correlation coefficients obtained from the 1-hour time-averaged results were poorer than those obtained from 1-minute averages. Combined plots of all predicted 1-hour averaged responses against the field responses from the three experiments resulted in a correlation coefficient of 0.24 (see Figure 4.16) as compared to 0.54 for the predicted 1-minute time-averaged responses (see Figure 4.17). The correlation coefficient of the 1-hour time-averaged annoyance from Figure 4.18 was 0.46, which was lower than that of the 1-minute averaged correlation with the field results ($r^2 = 0.51$), as shown in Figure 4.19.

The histograms shown in Figure 4.20 and 4.22 demonstrate that the responses of the population to odours are consistently under predicted when 1-hour time-averaged concentrations are used. The differences in probability of response that were generated from the modelled and field responses are concentrated on the negative side of the histogram with differences that are fairly evenly distributed between 0 and -100%. In contrast, when the predicted responses were adjusted to 1-minute time-averaged responses, the histogram (Figure 4.21) became bell-shaped with a sharp peak near 0% difference. The majority of the predicted responses are within 10% of field responses, with other differences distributed on both sides. However, the distribution of differences was slightly asymmetric and skewed toward the negative side. This indicates that the calculated 1-minute time-average responses are still slightly under predicted. Therefore, there is a slight tendency for the ISCST3 model to under predict the responses from odour concentrations at different receptor locations. Similarly, Figure 4.22 clearly shows that 1-hour averaged annoyances were under predicted although the highest frequency of differences is in the 0 to 1 range. Figure 4.23 shows that the predicted 1-minute time-averaged degrees of annoyance were much closer to the field results than the 1-hour time-averages and had a bell-shaped curve with a well-defined peak, with differences between the predicted and field annoyances covering both the negative and positive sides of the histogram. Collectively, these results reflect the vastly improved predictions when 1-minute time-averaging is used. Thus, the influence of time averaging is very strong and must be accounted for in modelling odour impact.

As with the probability of response results in Figure 4.21, the annoyance histogram shown in Figure 4.23 was also somewhat asymmetrical. However, in contrast to the probability of response results, which tended to be slightly under predicted, the annoyance distribution was slightly skewed towards the positive side. Given that the probability of response results tended to be slightly under predicted and the annoyance results tended to be slightly over predicted, this would appear to indicate that the values of R that are used in predicting annoyance as a function of odour concentration were over estimated. Thus, the annoyances reported by panellists exposed to the odour in the laboratory tended to be higher than those reported in the field for a given concentration of

odour. This could be due to (1) error in measurement of odour impact model data and parameters or (2) differences arising from the manner in which the odour is experienced and perceived in the field versus the laboratory (i.e., an odour stream emitted from a tube versus odour present in the ambient air).

Modeling the dispersion of odorous releases from ground level point sources and 1.5 m receptors using ISCST3 has provided acceptable predictions. Although correlations between the predicted and field results were between 0.50 and 0.54, the ability of the model to produce such predictions should not be under rated. This is due to the fact that the quality of the olfactometry results could have been improved if there were a larger number of well-trained panellists. Despite the use of only 6 panellists per olfactometry test and teams of only 4 to 5 members in the field studies, the impact zones generated using odour impact model data and 1-minute time-averaged odour concentrations were very similar in size and location to those generated from the field results. In addition, histograms of the distribution of differences between predicted and field results were bell-shaped with sharp peaks around zero. These observations demonstrate that ISCST3 can be used to accurately predict odour impacts, provided that predicted odour concentrations are first transformed to account for time-averaging effects.

It is suggested that the quality of results could be improved beyond those observed in the present study. This is due to the fact that the emissions rate in ISCST3 is a function of the threshold of response of the odorous emission, which is determined through olfactometry. In addition, the equations describing the probability of response and degree of annoyance are expressed in terms of the concentration of an odour and the parameters obtained from the OIM curves, such as the ratio R that describes the characteristics of an odour, and the persistence of response, p, and annoyance, a. To improve the results of the OIM, it is suggested that the panel of odour judges in the olfactometry tests should be selected to properly represent the sensitivities of the population being exposed to the odorous emissions (Nicell, 1986; Nicell, 2003). This would imply that panels should be larger in size than those used in the present study. It is recommended that future research focus on establishing an appropriate manner for panellist selection and training and to determine an appropriate panel size that should be used to accurately reflect overall population

response to odours. In addition, samples from the sources should be collected using representative sampling techniques, rather than grab samples, conducted during the field test. This would ensure that the odour impact model data generated in the olfactometry tests accurately reflects the odour being experienced in the field. These suggestions might improve the predicted odour concentration calculated by ISCST3 at the different receptors within the region and will also allow a better prediction of the probability of response and degree of annoyance experienced at these receptor locations.

6 Conclusion

The objective of this research was to validate the ability of the Industrial Source Complex - Short Term (ISCST3) model to predict odour levels in a surrounding area. ISCST3 was used to predict the concentration of odour in a region surrounding an odour-emitting facility. Odour impact models were developed to characterize the odours and to provide estimates of probability of response and annoyance as a function of odour concentration. By combining the dispersion modelling results with odour impact model data, the impact of emissions from the facility were predicted in terms of probability of response and degree of annoyance. The predictive ability of the model was tested by comparing predicted odour impacts with those measured in the field using a team of volunteers.

In previous reports, it had been stated that the ISCST3 model tended to under-predict odour concentration. In this study, the ISCST3 model was used in combination with the odour impact model to quite accurately predict the probability of response and annoyance that were experienced in the region surrounding a hog farm. However, this was only true provided that the predicted concentrations from the dispersion model were first transformed to account for time-averaging effects. Following transformation, there was only a slight tendency to under predict probability of response and a slight tendency to over predict degree of annoyance. The difference in these tendencies may result from differences in the ways that odour are experienced and perceived in the laboratory as compared to the field. Future work should concentrate on establishing appropriate olfactometry procedures to ensure that odour impact model data accurately reflect the manner in which odours will be perceived in the ambient air.

References

2001 Census of Agriculture. Statistics Canada, from the World Wide Web. http://www.statcan.ca/english/freepub/95F0301XIE/quality.htm. 2002.

Arya, S. P. Air Pollution Meteorology and Dispersion. New York. Oxford University Press, Inc. 1999.

ASTM. *"Standard Practice for Determination of Odor and Taste Thresholds by a Forced Choice Ascending Concentration Series Method of Limits E 679-91"*, *Annual Book of Standards.* Philadelphia, PA. American Society for Testing Materials. 1991.

Atkinson, D. G., Bailey, D. T., Irwin, J. S., & Touma, J. S. *"Improvements to the EPA Industrial Source Complex Dispersion Model".* Journal of Applied Meteorology, vol.*36*, pp 1088-1095. 1997.

Barrat, R. Atmospheric Dispersion Modeling-An Introduction to Practical Applications (First ed.). Sterling, Virgina. Earthscan Publications Ltd. 2001.

Beychok, M. R. Fundamentals of Stack Gas Dispersion (Third ed.). Irivine, California. Published by Milton R. Beychok. 1994.

Boubel, R. W., Fox, D. L., Turner, D. B., & Stern, A. C. Fundamentals of Air Pollution (Third ed.). San Diego, California. Academic Press, Inc. 1994.

Cha, S. S. *Sensory Test Methods.* In Odor and VOC Control Handbook, H. J. Rafson (Ed.) (New York, NY. McGraw-hill Companies, Inc. 1998.

Choiniere, D., & Chapman, A. Validation d' un Modele de Dispersion des Odeurs Provenant de Batiment Agricoles. St. Hyacinthe, Quebec. Consumaj Inc. 2003.

Committee On Odors From Stationary and Mobile Sources, Odors From Stationary and Mobile Sources. Washington, D.C. National Academy of Sciences. 1979.

Eagleman, J. R. Air Pollution Meteorology (Second ed.). Lenexa, Kansas. Trimedia Publishing Company. 1996.

Henshaw, P. F., Nicell, J. A., & Sikdar, A. *A New Method for Odour Impact Assessment Based on Spatial and Temporal Analyses of Community Response.* Proceedings of 2002 Joint CSCE-EWRI International Conference on Environmental Engineering, Niagara Falls, ON. (on CD ROM). (July 21-24, 2002).

Hogstrom, U. *Transport and Dispersal of Odors*. In <u>Human Responses to Environmental Odors</u>, A. Turk & J. James W. Johnston & D. Moulton (Eds.) (pp. 164-198. New York, NY. Academic Press, Inc. 1974.

Law, S., Loney, A., & Reusing, G. *Ambient Air Odor Regulations In Canada And The United states*. Proceedings of 2002 Joint CSCE-EWRI International Conference on Environmental Engineering, Niagara Falls, Ontario. (on CD ROM). (July 21-24, 2002).

Leonardos, G. *Review of Odor Control Regulations in the USA*. In <u>Odors, Indoor and Environmental Air, Proceedings of a Specialty Conference</u>, pp. 73-84. Bloomington, MN. Air and Waste Management Association, Pittsburgh, PN. 1996.

Lyons, T. J., & Scott, W. D. <u>Principles of Air Pollution Meteorology</u>. Boca Raton, Florida. CRC Press. 1990.

Mahin, T. D. *"Comparison of Different Approaches Used To Regulate Odours Around the World"*. Water Science and Technology, vol.*44*(9), pp 87-101. 2001.

Mussio, P., Gnyp, A. W., & Henshaw, P. F. *"A Fluctuating Plume Dispersion Model for the Prediction of Odour-Impact Frequencies from Continuous Stationary Sources"*. Atmospheric Environment, vol.*35*, pp 2955-2962. 2001.

Nicell, J. A. *Preliminary Assessment of the Odour Impact Model as a Regulatory Strategy*. Thesis of Master of Applied Science, University of Windsor, Windsor, Ontario. 1986.

Nicell, J. A. *"Development of the Odour Impact Model as a Regulatory Strategy"*. International Journal of Environment and Pollution, vol.*4*(1), pp 124-138. 1994.

Nicell, J. A. *"Expressions to Relate Population Responses to Odor Concentration"*. pp (in press). 2003.

Ormerod, R. *"Improving Odour Assessment by Using Better Dispersion Models: Some Examples"*. Water Science and Technology, vol.*44*(9), pp 149-156. 2001.

Poostchi, E. B. M. *Development of a Strategy for Quantifying the Impact of odorous Emissions from Stationary Sources on Surrounding Communities*. Ph.D. Dissertation, University of Windsor, Windsor, Ontario. 1985.

Schiffman, S. S., Bennett, J. L., & Raymer, J. H. *"Quantification of Odors and Odorants from Swine Operations in North Carolina"*. Agricultural and Forest Meteorology, vol.*108*, pp 213-240. 2001.

Schnelle, K. B., & Dey, P. R. Atmospheric Dispersion Modeling Compliance Guide. New York, NY. McGraw-Hill Companies, Inc. 2000.

Sikdar, A. *An Objective Method for the Assessment of the Impacts of Odorous Emissions from Stationary Sources*. Thesis of Master of Applied Science, University of Windsor, Windsor, Ontario, Canada. 2001.

Sykes, R. I., & Gabruk, R. S. *"A Second-Order Closure model for the Effect of Averaging time on Turbulent Plume Dispersion"*. Journal of Applied Meteorology, vol.*36*, pp 1038-1045. 1997.

The, J. L., The, C. L., & Johnson, M. A. *ISC-AERMOD View-User's Guide*. Waterloo, Ontario. Lakes Environmental. 2000.

Tsakaloyannis, M. K. *Development of a Regulatory Strategy for Odour Impact Assessment*. Thesis of Master of Engineering, McGill University, Montreal, Canada. 1997.

Turk, A., Burns, J. C., & Flesh, R. D. *An Evaluation of Community Problems Caused by Industrial Odors*. In Human Responses to Environmental Odors, A. Turk & J. James W. Johnston & D. G. Moulton (Eds.) (pp. 33-45. New York, New York. Academic Press, Inc. 1974.

Turner, T. D. Workbook of Atmospheric Dispersion Estimates: An Introduction to Dispersion Modelling (2nd ed.). Boca Raton, Florida. CRC Press Inc. 1994.

Venkatram, A. *"Accounting for Averaging Time in Air Pollution Modeling"*. Atmospheric Environment, vol.*36*, pp 2165-2170. 2002.

Appendix A

Field Results

Table A.1: Individual responses for blue flag team in the 1ˢᵗ experiment.

Blue Flag	UTM coordinates (m)		Annoyance of team member:			
	Easting	Northing	1	2	3	4
3	683025	5107714	1	2	1	2
4	683025	5107679	6	2.5	3	3
5	683028	5107642	1	3	0	3
6	683029	5107604	0	1	0	3
7	683028	5107544	0	0	1	4
8	682984	5107536	0	1	0	4
9	682953	5107521	2	5	2	5
10	682912	5107510	7	5	2	5
11	682854	5107505	8	7	4	7
12	682823	5107499	4	5.5	2	7
13	682783	5107488	8	7	3	8
14	682740	5107472	9	5	3	9
15	682695	5107477	10	8	5	10
16	682713	5107440	9	7.5	2	10
17	682721	5107404	9	7	2	10
1	683020	5107798	1	1	1	2
18	682712	5107368	9	9	4	10
2	683018	5107753	4	1	1	2
19	682635	5107331	10	10	8	10

Table A.2: Individual responses for red flag team in the 1st experiment.

Red Flag	UTM coordinates (m)		Annoyance of team member:			
	Easting	Northing	1	2	3	4
16	682904	5107912	4	1	1	2
49	682860	5107928	0	0	2	0
16	682834	5107935	0	0	0	0
27	682790	5107944	0	0	0	0
39	682733	5107956	0	0	0	0
28	682700	5107925	0	0	0	0
20	682670	5107899	1	0	0	0
9	682647	5107859	0	0	0	0
6	682639	5107833	0	0	0	2
38	682633	5107796	0	0	0	0
41	682633	5107771	2	1	1	2
26	682628	5107725	2	0	2	0
40	682625	5107695	0	1	1	0
7	682633	5107635	1	0	2	0
46	682638	5107591	2	0	3	2
4	682654	5107547	0	1	4	0
48	682658	5107526	5	4	5	4
42	682666	5107508	7	7	7	6
34	682673	5107475	7	8	8	7
44	682670	5107463	6	7	7	7
3	682670	5107419	8	8	8	7
45	682669	5107396	3	5	9	8
23	682631	5107325	8	9	9	10
8	682598	5107344	10	10	10	10
47	682598	5107322	0	0	0	0
50	682555	5107350	4	1	0	0

Table A.3: Individual responses for yellow flag team in the 1st experiment.

Yellow flag	UTM coordinates (m)		Annoyance of team member:			
	Easting	Easting	1	2	3	4
33	683321	5107531	2	0	0	1
15	683264	5107557	2	1	0	2
43	683193	5107578	2	1	2	4
49	683085	5107608	2	2	2	4
36	683117	5107549	2	0	0	1
6	683146	5107480	3	1	1	1
40	683192	5107380	0	0	0	0
18	683133	5107422	1	0	0	1
32	683024	5107491	2	1	1	2
21	682981	5107540	5	4	2	4
11	683016	5107468	4	1	0	3
14	683048	5107393	0	0	1	0
16	683088	5107308	0	0	0	0
9	683020	5107339	0.5	1	5	5
38	682950	5107366	5	4	4	6
46	682881	5107396	4	2	3	4
48	682914	5107328	5	4	3	5
22	682946	5107260	1	1	2	0
50	682970	5107179	0	1	0	0
23	682880	5107237	0	1	2	0.5
31	682793	5107286	7	7	7	8
12	682704	5107330	8	7	7	9
24	682633	5107324	10	10	10	10
17	682574	5107342	10	10	10	10

Table A.4: Probability of response and degree of annoyance for the 1ˢᵗ experiment.

UTM Coordinates (m)		Response (%)	Annoyance	UTM Coordinates (m)		Response (%)	Annoyance
x	y			x	y		
682904	5107912	80	1.6	682654	5107547	40	1
683321	5107531	50	0.75	682854	5107505	100	6.5
682860	5107928	20	0.4	683048	5107393	20	0.25
683264	5107557	75	1.25	682658	5107526	80	3.6
682834	5107935	0	0	682823	5107499	100	4.625
682790	5107944	0	0	683088	5107308	0	0
683193	5107578	100	2.25	682666	5107508	100	6.6
682733	5107956	0	0	683020	5107339	100	2.875
683025	5107714	100	1.2	682783	5107488	100	6.5
683085	5107608	100	2.5	682673	5107475	100	6.4
682700	5107925	0	0	682950	5107366	100	4.75
683025	5107679	100	3.625	682670	5107463	100	6.8
682670	5107899	20	0.002	682740	5107472	100	6.5
683117	5107549	40	0.75	682881	5107396	100	3.25
682647	5107859	0	0	682670	5107419	100	8
683028	5107642	75	1.75	682914	5107328	100	4.25
683146	5107480	100	1.5	682669	5107396	100	5.4
682639	5107833	20	0.4	682695	5107477	100	8.25
683029	5107604	50	1	682946	5107260	60	1
683192	5107380	0	0	682713	5107440	100	7.125
682633	5107796	20	0.4	682970	5107179	25	0.25
682633	5107771	80	1.2	682721	5107404	100	7
683028	5107544	50	1.25	682880	5107237	75	0.875
683133	5107422	50	0.5	682631	5107325	100	8.8
682628	5107725	40	0.8	683020	5107798	100	1.25
682984	5107536	50	1	682712	5107368	100	8
682625	5107695	40	0.4	682793	5107286	100	7.25
683024	5107491	100	1.5	682598	5107344	100	10
682953	5107521	100	2.8	683018	5107753	100	2
682633	5107635	20	0.6	682598	5107322	0	0
682981	5107540	100	3.75	682635	5107331	100	9.5
682912	5107510	100	4.75	682704	5107330	100	7.75
682638	5107591	80	2.2	682555	5107350	40	1
683016	5107468	75	2				

Table A.5: Individual responses for blue flag team in the 2nd experiment.

Blue Flag	UTM Coordinates (m)		Annoyance of team member:			
	Easting	Northing	1	2	3	4
1	681894	5107239	0	0	0	0
2	681970	5107174	0	0	0	0
3	682058	5107099	0	0	0	0
4	682127	5107050	0	0	0	0
5	682222	5106997	0	0	0	0
6	682190	5107064	0	0	0	0
7	682121	5107141	0	0	0	0
8	682150	5107178	0	0	0	0
9	682195	5107215	0	0	0	0
10	682239	5107174	0	0	0	2
11	682280	5107139	0	0	0	2
12	682329	5107100	3	4	3	4
13	682312	5107145	0	0	1	1
14	682282	5107197	0	0	0	0
15	682257	5107245	0	0	0	0
16	682233	5107282	0	0	0	0
17	682295	5107247	0	0	0	0
18	682332	5107218	0	0	0	2
19	682365	5107194	0	0	0	2
20	682393	5107171	8	8	8	5
21	682381	5107206	3	7	7	4
22	682359	5107245	3	5	6	5
23	682336	5107280	0	0	0	1
24	682313	5107318	0	0	0	0
25	682295	5107342	0	0	0	0
26	682339	5107323	0	0	0	0
27	682371	5107304	0	0	0	0
28	682401	5107283	0	0	0	0
29	682424	5107264	4	5	6	4
30	682461	5107235	7	7	7	6
31	682488	5107221	7	8	7	7
32	682464	5107274	6	4	5	2
33	682447	5107314	0	0	0	0
34	682418	5107362	0	0	0	0
35	682398	5107401	0	0	0	0
36	682442	5107382	0	0	0	0
37	682478	5107372	0	0	0	0
38	682527	5107348	8	9	8	8
39	682569	5107330	8	10	10	9

Table A.6: Individual responses for red flag team in the 2nd experiment.

Red Flag	UTM Coordinates (m)		Annoyance of member:				
	Easting	Northing	1	2	3	4	5
1	682518	5107008	2	1.5	1	0	0
4	682431	5106986	2	0	1	1	0
6	682581	5107334	9		9	8	7
10	682570	5107203	1	3	0	0	2
11	682483	5107293	3	5	4	3	3
13	682536	5107236	2	3.5	4	3	4
14	682376	5107251	0	1	0	0	1
17	682489	5107358	0	0	0	0	0
19	682650	5107231	4	6	2	2	5
20	682144	5106989	0	0	1	1	1
22	682362	5107121	1	5	1	3	3
23	682452	5107324	0	0	0	0	0
24	682527	5107154	2	1.5	1	0	1
25	682698	5107193	1	0	1	3	2
27	682255	5106926	1	2	1	2	1
29	682386	5106860	0	0.5	1	0	1
31	682302	5107148	1	2.5	2	0	0
33	682586	5107095	1	4	1	1	1
34	682526	5107338	3	5	3	4	3
35	682596	5107321	0	0	0	0	0
38	682677	5107235	8	0	9	7	7
40	682421	5107000	2	2	0	0	1
41	682647	5107123	2	4	4	3	3
42	682282	5106901	4	6	2	2	4
45	682382	5107058	3	4	3	2	3
46	682582	5107290	2	5	1	1	1
47	682450	5107222	3	3	3	4	4
49	682440	5107064	2	2.5	1	3	2
50	682405	5107201	1	1	1	0	1

Table A.7: Individual responses for yellow flag team in the 2nd experiment.

Yellow Flag	UTM Coordinates (m)		Annoyance of member:			
	Easting	Northing	1	2	3	4
1	682702	5107017	1	1	0	0
4	682647	5107054	2	5	3	4
5	682549	5107027	0.5	5	0	0
7	682607	5107079	3	7	5	4
11	682601	5107024	2	5	3	4
14	682650	5106613	0.5	0.5	0	0
16	682577	5106687	2	0.5	0	0
17	682652	5106948	0	0	0	0
19	682672	5107211	10	10	10	10
20	682389	5106781	6	5	1	3
21	682514	5106709	0	1	0	5
22	682544	5106924	4	5	4	6
23	682656	5107083	4	4	4	4
26	682598	5106815	0.5	0	0	0
30	682649	5107148	8	9	8	8
31	682723	5107130	0	2	0	0
32	682560	5107111	4	8	3	5
33	682692	5107173	9	10	9	10
34	682484	5107042	2.5	6	6	5
35	682615	5107159	5	8	6	9
39	682562	5107080	5	3	6	3
41	682612	5106980	0	0	0	0
42	682285	5106849	4	2	3	2
43	682762	5107072	0	0.5	1	0
46	682632	5107130	4	8	5	7
47	682682	5107129	4	4	5	5
49	682717	5107100	0	4	3	2
50	682531	5106995	3	6	5	4

Table A.8: Probability of response and degree of annoyance for the 2nd experiment.

UTM Coordinates		Response %	Annoyance	UTM Coordinates		Response %	Annoyance
x	y			x	y		
681894	5107239	0	0	682461	5107235	100	6.75
681970	5107174	0	0	682464	5107274	100	4.25
682058	5107099	0	0	682476	5106934	40	0.4
682121	5107141	0	0	682478	5107372	0	0
682127	5107050	0	0	682483	5107293	100	3.6
682144	5106989	60	0.6	682484	5107042	100	4.875
682150	5107178	0	0	682488	5107221	100	7.25
682190	5107064	0	0	682489	5107358	0	0
682195	5107215	0	0	682514	5106709	50	1.5
682222	5106997	0	0	682518	5107008	60	0.9
682233	5107282	0	0	682526	5107338	100	3.6
682239	5107174	25	0.5	682527	5107154	80	1.1
682255	5106926	100	1.4	682527	5107348	100	8.25
682257	5107245	0	0	682531	5106995	100	4.5
682280	5107139	25	0.5	682536	5107236	100	3.3
682282	5106901	100	3.6	682544	5106924	100	4.75
682282	5107197	0	0	682549	5107027	50	1.375
682285	5106849	100	2.75	682560	5107111	100	5
682295	5107247	0	0	682562	5107080	100	4.25
682295	5107342	0	0	682569	5107330	100	9.25
682302	5107148	60	1.1	682570	5107203	60	1.2
682312	5107145	50	0.5	682577	5106687	50	0.625
682313	5107318	0	0	682581	5107334	80	8.25
682329	5107100	100	3.5	682582	5107290	100	2
682332	5107218	25	0.5	682586	5107095	100	1.6
682336	5107280	25	0.25	682596	5107321	0	0
682339	5107323	0	0	682598	5106815	25	0.125
682359	5107245	100	4.75	682601	5107024	100	3.5
682362	5107121	100	2.6	682607	5107079	100	4.75
682365	5107194	25	0.5	682612	5106980	0	0
682371	5107304	0	0	682615	5107159	100	7

Table A.8 (continued): Probability of response and degree of annoyance for the 2nd experiment.

UTM Coordinates		Response %	Annoyance	UTM Coordinates		Response %	Annoyance
x	y			x	y		
682376	5107251	40	0.4	682632	5107130	100	6
682381	5107206	100	5.25	682647	5107054	100	3.5
682382	5107058	100	3	682647	5107123	100	3.2
682386	5106860	60	0.5	682649	5107148	100	8.25
682389	5106781	100	3.75	682650	5106613	50	0.25
682393	5107171	100	7.25	682650	5107231	100	3.8
682398	5107401	0	0	682652	5106948	0	0
682401	5107283	0	0	682656	5107083	100	4
682405	5107201	80	0.8	682672	5107211	100	10
682418	5107362	0	0	682677	5107235	80	7.75
682421	5107000	60	1	682682	5107129	100	4.5
682424	5107264	100	4.75	682692	5107173	100	9.5
682431	5106986	40	0.8	682698	5107193	80	1.75
682440	5107064	100	2.1	682702	5107017	50	0.5
682442	5107382	0	0	682717	5107100	75	2.25
682447	5107314	0	0	682723	5107130	25	0.5
682450	5107222	100	3.4	682762	5107072	50	0.375
682452	5107324	0	0				

Table A.9: Individual responses for blue flag team in the 3rd experiment.

Blue Flag	UTM Coordinates (m)		Annoyance of member:			
	Easting	Northing	1	2	3	4
1	682637	5108216	0	0	0	0
2	682664	5108172	0	0	0	0
3	682700	5108123	0	0	0	0
4	682725	5108089	0	0	0	0
5	682752	5108054	0	0	0	0
6	682789	5108009	0	0	0	0
7	682838	5107957	0	0	0	0
8	682874	5107907	0	0	0	0
9	682901	5107861	0	0	0	0
11	682935	5107772	0	0	0	0
12	682949	5107732	0	0	0	0
13	682906	5107759	0	1	1	0
14	682856	5107781	0	0	0	0
15	682807	5107802	0	0	0	0
16	682755	5107827	0	0	0	0
17	682778	5107774	0	0	0	0
18	682813	5107732	0	0	0	0
19	682840	5107688	0	0	0	0
20	682848	5107640	3	2	4	4
21	682860	5107618	3	2	0	3
22	682816	5107644	1	0	0	1
23	682769	5107666	0	0	0	0
24	682721	5107687	0	0	0	0
25	682682	5107710	0	0	0	0
26	682707	5107651	1	0	0	0
27	682732	5107612	0	2	0	1
28	682747	5107558	0	0	0	0
29	682778	5107523	3	0	1	5
30	682721	5107534	4	4	6	5
31	682688	5107553	1	0	0	0
32	682653	5107570	0	0	0	0
33	682608	5107587	0	0	0	0
34	682637	5107543	0	0	0	0
35	682656	5107509	0	0	0	1
36	682675	5107472	5	5	7	3
37	682633	5107492	2	0	0	0
38	682598	5107505	0	0	0	0
39	682573	5107514	0	0	0	0
40	682591	5107471	0	0	0	0
41	682616	5107426	5	6	5	7
42	682640	5107397	7	7	6	7

Table A.10: Individual responses for red flag team in the 3rd experiment.

Red Flag	UTM Coordinates (m)		Annoyance of member:			
	Easting	Northing	1	2	3	4
4	682784	5107323	6	3	5	4
5	682765	5107369	0	2	1	2
6	682839	5107466	5	2	2	7
8	682671	5107514	0	0	1	2
10	682821	5107428	0	0	2	2
11	682945	5107566	3	0	0	4
13	682859	5107410	4	2	4	8
14	682865	5107701	0	0	1	0
17	682663	5107402	9	3	8	8
20	682684	5107485	5	2	5	5
21	682708	5107373	7	2	3	8
23	682748	5107472	7	3	4	7
24	682940	5107815	0	0	0	0
25	682818	5107607	5	2	1	2
26	682883	5107558	3	1	1	2
27	682706	5107448	7	1	2	4
28	682741	5107403	7	3	2	4
31	682703	5107497	0	2	5	8
32	682756	5107643	0	0	1	2
33	682909	5107628	4	2	1	4
35	682783	5107563	4	3	2	6
36	682741	5107346	7	0	2	4
37	682982	5107735	1	1	0	0
38	682619	5107431	8	2	2	4
39	683013	5107676	0	1	1	0
40	682782	5107452	0	0	3	1
41	682805	5107524	7	2	5	8
42	682595	5107460	7	1	2	0
44	683048	5107598	6	2	4	4
48	682962	5107514	6	2	3	5
49	682972	5107638	5	1	2	2
50	682911	5107678	0	1	2	0

Table A.11: Individual responses for yellow flag team in the 3rd experiment.

Yellow Flag	UTM Coordinates (m)		Annoyance of member			
	Easting	Northing	1	2	3	4
4	682952	5107274	0	7	1	0
5	682987	5107212	0	5	0	0
7	682963	5107511	1	5	2	1
9	683042	5107453	4	6	4	2
12	682865	5107294	4	8	4	3
13	683163	5107366	0	2	0	0
14	682993	5107494	2	4	2	2
16	682806	5107291	5	10	6	1
17	682888	5107402	0	8	1	0
18	682985	5107462	0	8	1	0
20	682905	5107347	2	10	4	2
21	682805	5107228	6	8	4	2
22	682813	5107315	8	7	5	2
23	683010	5107328	0	4	0	0
30	683131	5107683	1	6	0	0
31	683178	5107573	8	8	5	2
32	682925	5107247	1	7	1	1
34	682863	5107197	0	8	0	0
35	683065	5107306	0	8	0	0
37	683098	5107414	0	5	0	0
39	682852	5107418	2	6	3	2
42	683017	5107387	5	8	3	2
43	683085	5107763	3	7	0	1
44	683234	5107476	0	5	1	1
46	682938	5107371	6	10	5	1
47	682840	5107252	5	10	4	1
48	682778	5107331	7	10	6	2
49	683268	5107319	0	1	0	0

Table A.12: Probability of response and degree of annoyance for the 3rd experiment.

UTM Coordinates (m)		Response %	Annoyance	GPS Coordinates		Response %	Annoyance
x	y			x	y		
682637	5108216	0	0	682905	5107347	100	4.5
682664	5108172	0	0	682805	5107228	100	5
682700	5108123	0	0	682813	5107315	100	5.5
682725	5108089	0	0	683010	5107328	25	1
682752	5108054	0	0	683131	5107683	50	1.75
682789	5108009	0	0	683178	5107573	100	5.75
682838	5107957	0	0	682925	5107247	100	2.5
682874	5107907	0	0	682863	5107197	25	2
682901	5107861	0	0	683065	5107306	25	2
682935	5107772	0	0	683098	5107414	25	1.25
682949	5107732	0	0	682852	5107418	100	3.25
682906	5107759	50	0.5	683017	5107387	100	4.5
682856	5107781	0	0	683085	5107763	75	2.75
682807	5107802	0	0	683234	5107476	75	1.75
682755	5107827	0	0	682938	5107371	100	5.5
682778	5107774	0	0	682840	5107252	100	5
682813	5107732	0	0	682778	5107331	100	6.25
682840	5107688	0	0	683268	5107319	25	0.25
682848	5107640	100	3.25	682784	5107323	100	4.5
682860	5107618	75	2	682765	5107369	75	1.25
682816	5107644	50	0.5	682839	5107466	100	4
682769	5107666	0	0	682671	5107514	50	0.75
682721	5107687	0	0	682821	5107428	50	1
682682	5107710	0	0	682945	5107566	50	1.75
682707	5107651	25	0.25	682859	5107410	100	4.5
682732	5107612	50	0.75	682865	5107701	25	0.25
682747	5107558	0	0	682663	5107402	100	7
682778	5107523	75	2.25	682684	5107485	100	4.25

Table A.12 (continued): Probability of response and degree of annoyance for the 3rd experiment.

UTM Coordinates (m)		%-Response	Annoyance	UTM Coordinates (m)		%-Response	Annoyance
x	y			x	y		
682721	5107534	100	4.75	682708	5107373	100	5
682688	5107553	25	0.25	682748	5107472	100	5.25
682653	5107570	0	0	682940	5107815	0	0
682608	5107587	0	0	682818	5107607	100	2.5
682637	5107543	0	0	682883	5107558	100	1.75
682656	5107509	25	0.25	682706	5107448	100	3.5
682675	5107472	100	5	682741	5107403	100	4
682633	5107492	25	0.5	682703	5107497	75	3.75
682598	5107505	0	0	682756	5107643	50	0.75
682573	5107514	0	0	682909	5107628	100	2.75
682591	5107471	0	0	682783	5107563	100	3.75
682616	5107426	100	5.75	682741	5107346	75	3.25
682640	5107397	100	6.75	682982	5107735	50	0.5
682952	5107274	50	2	682619	5107431	100	4
682987	5107212	25	1.25	683013	5107676	50	0.5
682963	5107511	100	2.25	682782	5107452	50	1
683042	5107453	100	4	682805	5107524	100	5.5
682865	5107294	100	4.75	682595	5107460	75	2.5
683163	5107366	50	0.5	683048	5107598	100	4
682993	5107494	100	2.5	682962	5107514	100	4
682806	5107291	100	5.5	682972	5107638	100	2.5
682888	5107402	50	2.25	682911	5107678	50	0.75
682985	5107462	50	2.25				

Appendix B

Odour Impact Model Results

First Experiment

Table B.1: Determination of probability of response and annoyance for each dilution of sample 299F in the first experiment.

Probability of Response															
Dilutions	1	2	3	4	5	6	7	8	9	10	11	12	Total	No. of measurements	%
2556	0	0	0	0	0	0							0	6	0
1236	0	0	0	0	0	0							0	6	0
619	0	0	1	0	0	0							1	6	16.67
312	0	0	1	0	0	1	0	0	1	0	0	1	4	12	33.33
157	1	1	1	1	1	1	1	1	1	1	1	1	12	12	100
57	1	1	1	1	1	1	1	1	1	1	1	1	12	12	100
36	1	1	1	1	1	1	1	1	1	1	1	1	12	12	100
19	1	1	1	1	1	1							6	6	100
9	1	1	1	1	1	1							6	6	100
Annoyance															
Dilutions	1	2	3	4	5	6	7	8	9	10	11	12	Total	No. of measurements	Average
2556	0	0	0	0	0	0							0	6	0
1236	0	0	0	0	0	0							0	6	0
619	0	0	1.5	0	0	0							1.5	6	0.25
312	0	0	3.5	0	0	3	0	0	3	0	0	3	12.5	12	1.04
157	1	2	6	3	1	4	2	1	4	3		7	34	12	2.83
57	5	7	9.5	6	4	6	5	4	6	6	8	9	75.5	12	6.29
36	8	9	8.5	7	5	7	5	9	7	5	6	9	85.5	12	7.13
19	8	8	8.5	8	6	8							46.5	6	7.75
9	8	6	8.5	9	7	9							47.5	6	7.92

Figure B.1: Probability of response and dilution-to-threshold of the 299F sample in the first experiment..

Table B.2: Determination of probability of response and annoyance for each dilution of fosse sample in the first experiment.

Probability of Response																					
Dilution	1	2	3	4	5	6	7	8	9	10	11	12	13	14	15	16	17	18	Total	No. of measurements	%
1236	0	0	0	0	0	0													0	6	0.00
619		0	0	0	0	0													0	6	0.00
312	0	1	0	0	0	1	0	1	0	1	0	1							5	12	41.67
157	0	1	0	1	0	1	0	1	0	1	0	1	0	1	0	1	0	1	9	18	50.00
57	0	1	0	1	0	1	0	1	0	1	1	1							7	12	58.33
36	0	1	0	1	1	1	1	1	1	1	1	1							10	12	83.33
19	1	1	1	1	1	1													6	6	100.00
Annoyance																					
Dilution	1	2	3	4	5	6	7	8	9	10	11	12	13	14	15	16	17	18	Total	No. of measurements	Average
1236	0	0	0	0	0	0													0	6	0.00
619	0	0	0	0	0	0													0	6	0.00
312	0	0.5	0	0	0	4	0	0.5	0	1		8							14	12	1.17
157	0	4	0	3	0	5	0	2	0	2	0	8	0	1	0	3	0	5	33	18	1.83
57	0	9	0	5	0	8	0	6	0	5	5	10							48	12	4.00
36	0	10	0	8	6	10	6	10	8.5	8	5	10							81.5	12	6.79
19	8	8	8	8	6	10													48	6	8.00

Figure B.2: Probability of response and dilution-to-threshold of the fosse sample in the first experiment..

Table B.3: Determination of probability of response and annoyance for each dilution of sample 300C in the first experiment.

Dilutions	1	2	3	4	5	6	7	8	9	10	11	12	13	14	15	16	17	18	Total	No. of measurements	%
2556	0	0	0	0	0	0													0	6	0.00
1236	0	0	1	0	0	1	0	1	1	0	0	1							5	12	41.67
619	0	0	1	0	0	1	0	1	1	0	0	1							5	6	83.33
312	1	1	1	1	0	1	1	1	1	1	0	1							10	12	83.33
157	1	1	1	1	0	1	1	1	1	1	0	1	1	1	1	1	1	1	16	18	88.89
57	1	1	1	1	1	1	1	1	1	1	1	1							12	12	100.00
36	1	1	1	1	1	1													6	6	100.00
19	1	1	1	1	1	1													6	6	100.00
9	1	1	1	1	1	1													6	6	100.00

Header spanning all response columns: Probability of Response

Table B.3 (continued): Determination of probability of response and annoyance for each dilution of sample 300C in the first experiment.

Annoyance																					
Dilution	1	2	3	4	5	6	7	8	9	10	11	12	13	14	15	16	17	18	Total	No. of measurements	Average
2556	0	0	0	0	0	0													0	6	0.00
1236	0	0	0.5	0	0	1													1.5	12	0.13
619	0	0	1	0	0	2	0	0.5	1	0	0	1							5.5	6	0.92
312	1	0.5	2	1	0	2	1	1	3	2	0	7							20.5	12	1.71
157	2	1	4	1	0	2	1	1	6	3	0	4	2	1	5	3	3	5	44	18	2.44
57	5	4	6.5	5	4	6	4	4	8	8	5	10							69.5	12	5.79
36	3	6	8	4	5	7													33	6	5.50
19	5	7	9	8	8	9													46	6	7.67
9	4	8	10	9	9	10													50	6	8.33

Figure B.3: Probability of response and dilution-to-threshold of the 300C sample in the first experiment.

Table B.4: Determination of probability of response and annoyance for each dilution of sample 300F in the first experiment..

Probability of Response															
Dilution	1	2	3	4	5	6	7	8	9	10	11	12	Total	No. of measurements	%
1236	0	0	0	0	0	0							0	6	0
619	0	0	1	0	0	1							2	6	33
312	1	0	1	1	0	1	1	0	1	1	0	1	8	12	67
157	1	1	1	1	0	1	1	1	1	1	0	1	10	12	83
57	1	1	1	1	1	1	1	1	1	1	1	1	12	12	100
36	1	1	1	1	1	1							6	6	100
19	1	1	1	1	1	1							6	6	100
9	1	1	1	1	1	1							6	6	100

Annoyance															
Dilution	1	2	3	4	5	6	7	8	9	10	11	12		No. of measurements	Average
1236	0	0	0	0	0	0							0	6	0
619	0	0	1	0	0	1							2	6	0.3
312	1	0	3	1	0	4	1		3			2	15	12	1.3
157	4	0.5	4	2	0	4	1	1	4	2	0	6	29	12	2.4
57	4	4	6	6	2	8	6	6	8.5	8	6	10	75	12	6.2
36	9	6	8	7	8	8							46	6	7.7
19	9	8	9	8	7	10							51	6	8.5
9	6	10	10	9	9	10							54	6	9
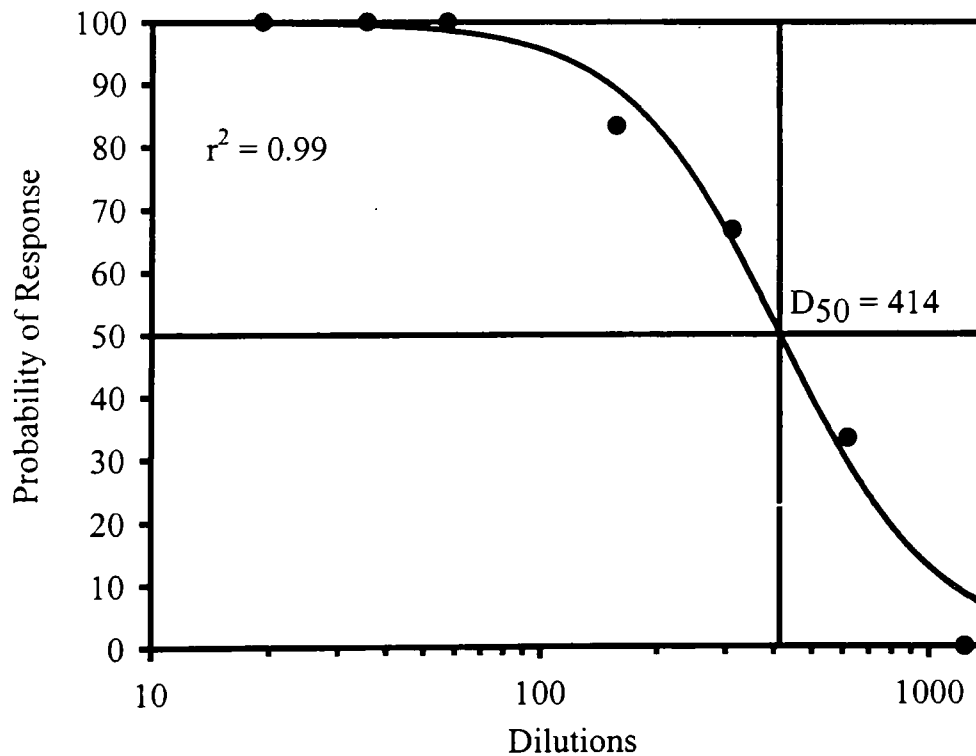
Figure B.4: Probability of response and dilution-to-threshold of the 300F sample in the first experiment.

Table B.5: Probability of response and degree of annoyance for the combined olfactometry results of the samples 299F, 300C, and 300F in the first experiment..

Dilutions	Total no. Of measurements	Probability of Response		Annoyance	
		Total	%	Total	Average
2556	12	0	0	0	0
1236	18	3	17	1.5	0.03
619	24	8	33	9	0.4
312	36	22	61	48	1.3
157	42	38	90	106.5	2.5
57	36	36	100	219.5	6.1
36	24	24	100	164.5	6.9
19	18	18	100	143.5	8.0
9	18	18	100	151.5	8.4
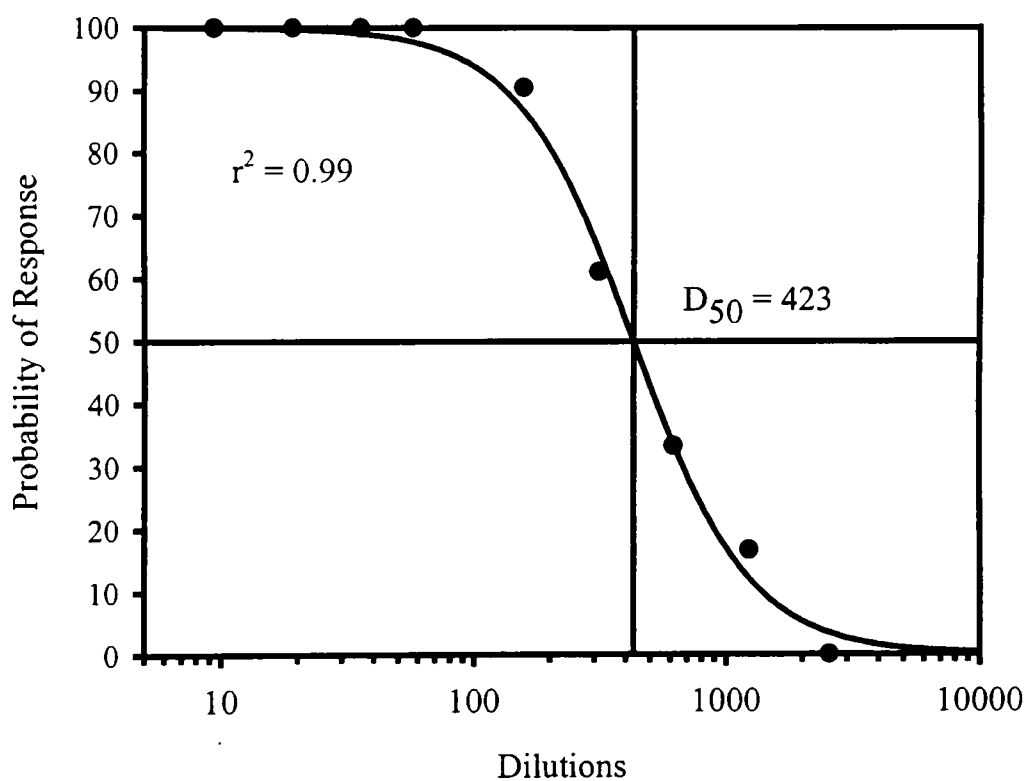
Figure B.5: Probability of response and dilution-to-threshold for the combined olfactometry results of the samples 299F, 300C, and 300F in the first experiment.

Second Experiment

Table B.6: Determination of probability of response and annoyance for each dilution of sample 299C in the second experiment.

Probability of Response															
Dilutions	1	2	3	4	5	6	7	8	9	10	11	12	Total	No. of measurements	%
2557.5	0	0	0	0	0	0							0	6	0.00
1235.6	0	0	0	0	0	0	0	0	0	0	1	0	1	12	8.33
618.9	0	0	0	0	1	0	0	0	0	1	1	0	3	12	25.00
312.2	1	1	0	1	1	0	1	1	1	1	1	0	9	12	75.00
157.2	1	1	1	1	1	1	1	1	1	1	1	1	12	12	100.00
57.3	1	1	1	1	1	1	1	1	1	1	1	1	12	12	100.00
36.6	1	1	1	1	1	1							6	6	100.00
19.2	1	1	1	1	1	1							6	6	100.00

Annoyance															
Dilutions	1	2	3	4	5	6	7	8	9	10	11	12	Total	No. of measurements	Average
2557.5	0	0	0	0	0	0							0	6	0.00
1235.6	0	0	0	0	0	0	0	0	0	0	2	0	2	12	0.17
618.9	0	0	0	0	1	0	0	0	0	1	7	0	9	12	0.75
312.2	7	4	0	4	3	0	1	4	1	3	7	0	34	12	2.83
157.2	8	5	5	8	4	4	5	2	1	6	7	1	56	12	4.67
57.3	9	8	6	8	5	4	8	5	4	7	4	4	72	12	6.00
36.6	10	8	8	10	5	5							46	6	7.67
19.2	9	9	9	10	5	5							47	6	7.83

Figure B.6: Probability of response and dilution-to-threshold of the 299C sample in the second experiment.

Table B.7: Determination of probability of response and annoyance for each dilution of sample 299F in the second experiment.

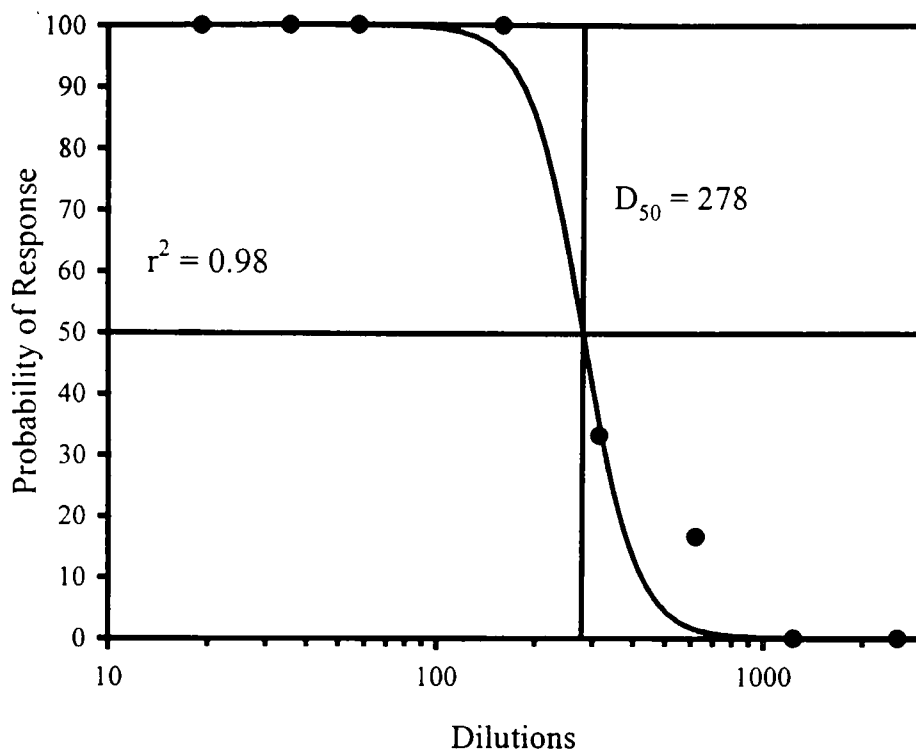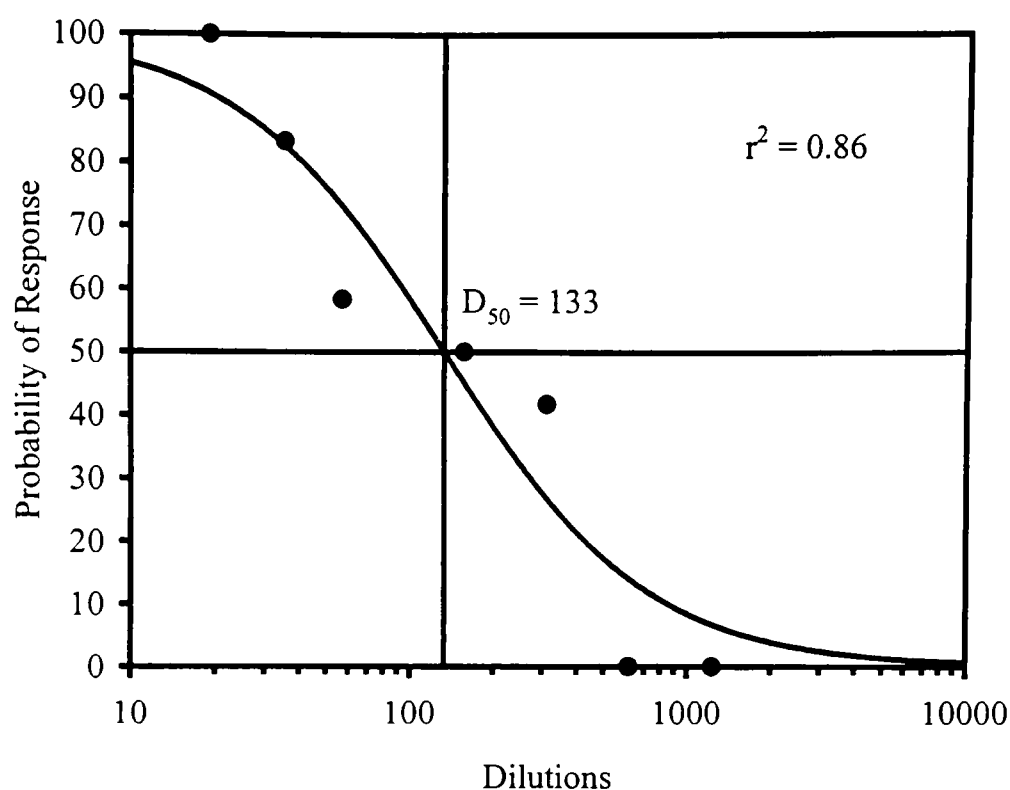| Probability of Response | | | | | | | | | | | | | | | |
Dilutions	1	2	3	4	5	6	7	8	9	10	11	12	Total	No. of measurements	%
2557.5	0	0	0	0	0	0							0	6	0.00
1235.6	1	0	0	0	0	0							0	6	16.67
618.9	1	1	0	1	0	0	1	1	1	1	1	0	8	12	66.67
312.2	1	1	1	1	1	1	1	1	1	1	1	1	12	12	100.00
157.2	1	1	1	1	1	1	1	1	1	1	1	1	12	12	100.00
57.3	1	1	1	1	1	1	1	1	1	1	1	1	12	12	100.00
36.6	1	1	1	1	1	1							6	6	100.00
19.2	1	1	1	1	1	1							6	6	100.00
9.4	1	1	1	1	1	1							6	6	100.00
Annoyance															
Dilutions	1	2	3	4	5	6	7	8	9	10	11	12	Total	No. of measurements	Average
2557.5	0	0	0	0	0	0							0	6	0.00
1235.6	1	0	0	0	0	0							1	6	0.17
618.9	1	1	0	2	0	0	2	2	2	8.5	4	0	22.5	12	1.88
312.2	3	7	4	4	3	5	2	4	6	7	5	2	52	12	4.33
157.2	5	8	7	6	5	6	5	6	5	8	7	5	73	12	6.08
57.3	8	10	9.5	8	8	7	8	7	9	10	7	5	96.5	12	8.04
36.6	9	10	10	10	8	7							54	6	9.00
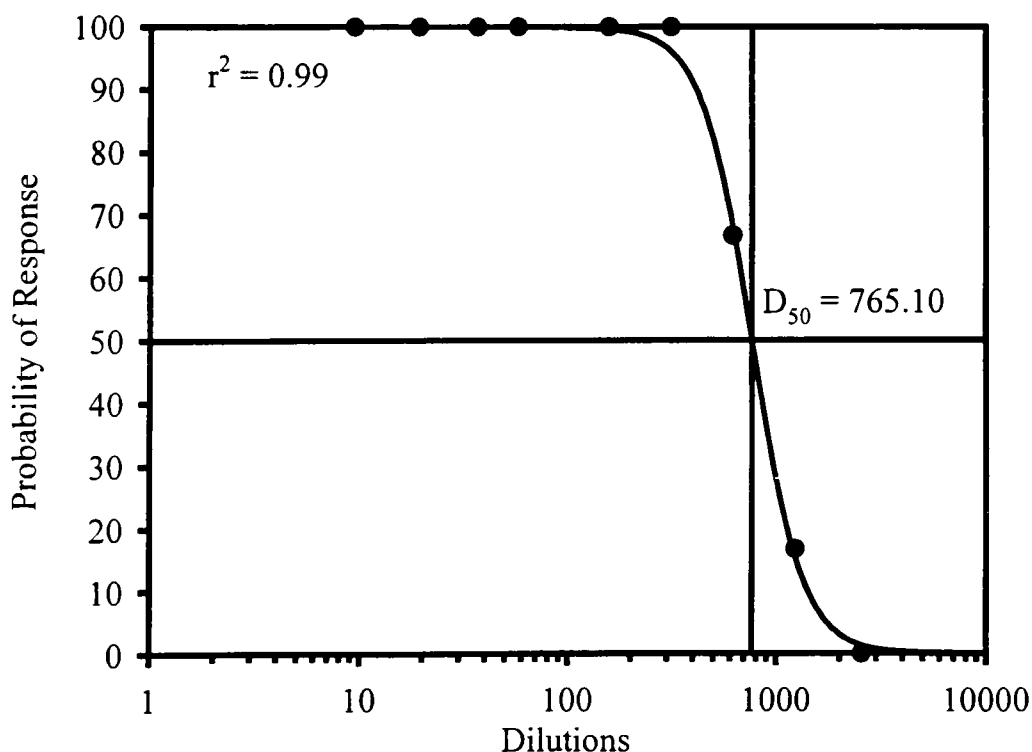
Figure B.7: Probability of response and dilution-to-threshold of the 299F sample in the second experiment.

Table B.8: Determination of probability of response and annoyance for each dilution of sample 300C in the second experiment.

Probability of Response															
Dilutions	1	2	3	4	5	6	7	8	9	10	11	12	Total	No. of measurements	%
2557.5	0	0	0	0	0	0							0	6	0
1235.6	0	1	0	0	0	0							1	6	16.67
618.9	1	1	0	1	0	1							4	6	66.67
312.2	1	1	1	1	1	1							6	6	100
157.2	1	1	1	1	1	1	1	1	1	1	1	1	12	12	100
57.3	1	1	1	1	1	1							6	6	100
36.6	1	1	1	1	1	1							6	6	100
19.2	1	1	1	1	1	1							6	6	100

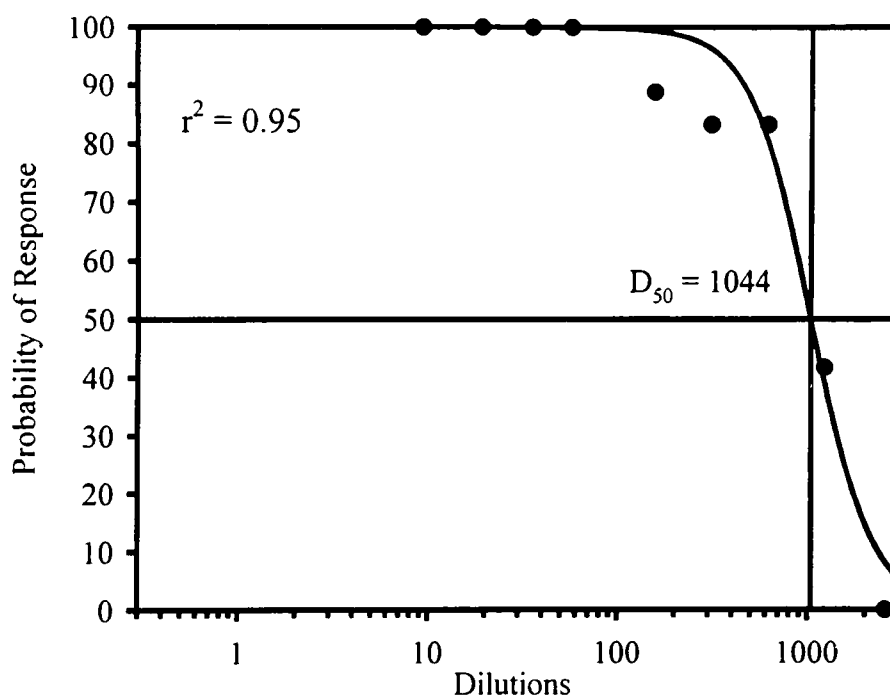| Annoyance															
Dilutions	1	2	3	4	5	6	7	8	9	10	11	12	Total	No. of measurements	Average
2557.5	0	0	0	0	0	0							0	6	0
1235.6	0	1	0	0	0	0							1	6	0.17
618.9	1	2	0	1	0	1							5	6	0.83
312.2	6	8	7	4	8	3							36	6	6.00
157.2	7	10	8	4	8	5	5	6	3	6	4	2	65	12	5.67
57.3	9	10	8	6	9	7							49	6	8.17
36.6	9	10	9	7	10	8							45	6	8.83
19.2	9	10	10	10	10	9							58	6	9.67

$r^2 = 0.99$

$D_{50} = 765.10$

Figure B.8: Probability of response and dilution-to-threshold of the 300C sample in the second experiment.

Table B.9: Determination of probability of response and annoyance for each dilution of sample 300F in the second experiment.

	Probability of Response																				
Dilutions	1	2	3	4	5	6	7	8	9	10	11	12	13	14	15	16	17	18	Total	No. of measurements	%
2557.5	0	0	0	0	0	0													0	6	0
1235.6	0	0	0	0	0	0	0	0	0	0	0	0							0	12	0
618.9	1	0	0	0	1	0	1	0	0	0	1	0							4	12	33.33
312.2	1	0	0	1	1	1	1	0	0	1	1	1							8	12	66.67
157.2	1	1	0	1	1	1	1	1	0	1	1	1	1	1	1	1	1	1	16	18	88.89
57.3	1	1	1	1	1	1	1	1	1	1	1	1							12	12	100
36.6	1	1	1	1	1	1													6	6	100
19.2	1	1	1	1	1	1													6	6	100
	Annoyance																				
Dilutions	1	2	3	4	5	6	7	8	9	10	11	12	13	14	15	16	17	18	Total	No. of measurements	Average
2557.5	0	0	0	0	0	0													0	6	0
1235.6	0	0	0	0	0	0	0	0	0	0	0	0							0	12	0
618.9	1	0	0	0	2	0	1	0	0	0	2	0							6	12	0.5
312.2	5	0	4	6	3	2	2	0	4	1	2	1							30	12	2.5
157.2	7	5	6	6	3	3	2	2	0	2	2	1	3	7	1	5	2	1	58	18	3.22
57.3	5	8	7	9	6	4	5	9	6	10	6	2							77	12	6.42
36.6	6	10	8	10	7	3													44	6	7.33
19.2	5	10	6	10	7	5													43	6	7.17

$r^2 = 0.99$

$D_{50} = 425$

Probability of Response
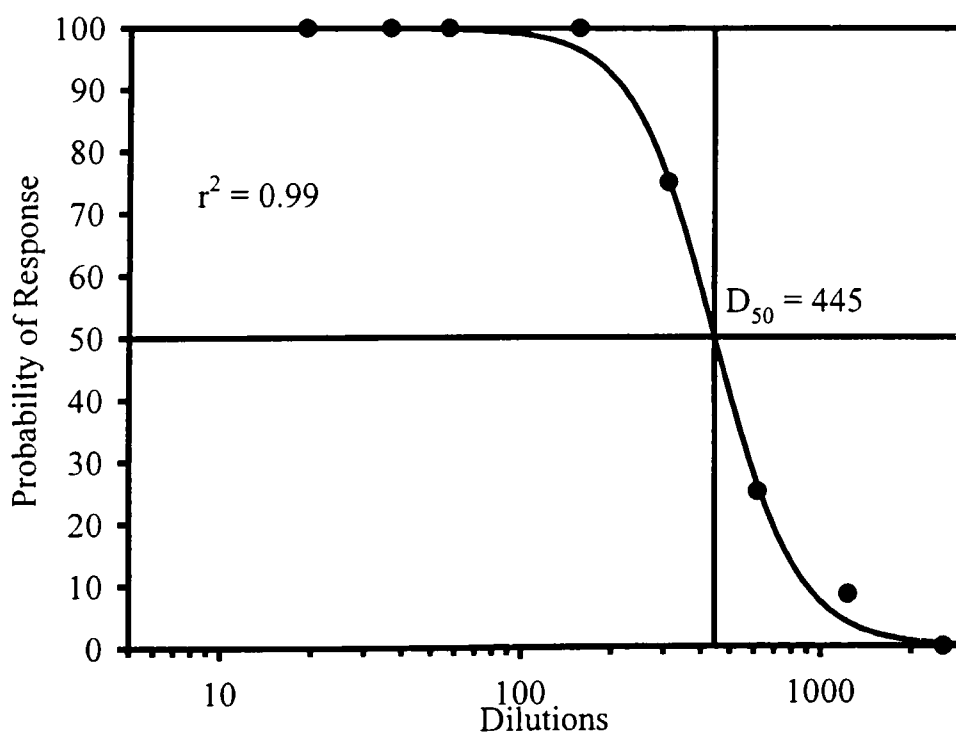
Diutions

Figure B.9: Probability of response and dilution-to-threshold of the 300F sample in the second experiment.

Table B.10: Determination of probability of response and annoyance for each dilution of Fosse ample in the second experiment.

Probability of Response									
Dilutions	1	2	3	4	5	6	Total	No. of measurements	%
2557.5	0	0	0	0	0	0	0	6	0
1235.6	0	0	0	0	0	0	0	6	0
618.9	1	0	1	0	0	0	2	6	33.33
312.2	1	1	1	0	1	0	4	6	66.67
157.2	1	1	1	1	1	0	5	6	83.33
57.3	1	1	1	1	1	1	6	6	100
36.6	1	1	1	1	1	1	6	6	100
19.2	1	1	1	1	1	1	6	6	100

Annoyance									
Dilutions	1	2	3	4	5	6	Total	No. of measurements	Average
2557.5	0	2	1	0	0	0	3	6	0.5
1235.6	1	0	0	0	0	0	1	6	0.17
618.9	1	0	1	0	0	0	2	6	0.33
312.2	1	3	1	0	2	0	7	6	1.17
157.2	1	4	1	1	4	0	11	6	1.83
57.3	4	4	2	3	4	2	19	6	3.17
36.6	4	7	4	2	5	1	23	6	3.83
19.2	5	9	1	3	5	3.5	26.5	6	4.42

Figure B.10: Probability of response and dilution-to-threshold of the Fosse sample in the second experiment.

Third Experiment

Table B.11: Determination of probability of response and annoyance for each dilution of 299F sample in the third experiment.

	Probability of Response														
Dilutions	1	2	3	4	5	6	7	8	9	10	11	12	Total	No. of measurements	%
2557.5	0	0	0	0	0	0							0	6	0
1235.6	0	0	0	0	1	1							2	6	33.33
618.9	1	0	1	1	1	1	1	0	1	1	1	1	10	12	83.33
312.2	1	1	1	1	1	1							6	6	100.0
157.2	1	1	1	1	1	1	1	1	1	1	1		11	11	100.0
57.3	1	1	1	1	1								5	5	100.0
36.6	1	1	1	1	1								5	5	100.0
19.2	1	1	1	1	1								5	5	100.0

	Annoyance														
Dilutions	1	2	3	4	5	6	7	8	9	10	11	12	Total	No. of measurements	Average
2557.5	0	0	0	0	0	0							0	6	0
1235.6	0	0	0	0	1	2							3	6	0.50
618.9	1	0	5	2	4	3	3	0	6	7	3	8	42	12	3.50
312.2	7	5	5	6	10	4							37	6	6.17
157.2	10	6	6	8	10	6	3	6	5	5	9		74	11	6.73
57.3	10	7	6		7	10							40	5	8.0
36.6	6	10	9	8	10								43	5	8.60
19.2	7	10	9	9	10								45	5	9.0

Figure B.11: Probability of response and dilution-to-threshold of the 299F sample in the second experiment in the third experiment.

Table B.12: Determination of probability of response and annoyance for each dilution of 299C sample in the third experiment.

Probability of Response															
Dilutions	1	2	3	4	5	6	7	8	9	10	11	12	Total	No. of measurements	%
2557.5	0	0	0	0	0	0							0	6	0
1235.6	1	0	0	0	0	0	1	0	0	0	1	0	3	6	50
618.9	1	0	1	0	1	1	1	1	1	1	1	1	10	12	83.33
312.2	1	1	1	1	1	1	1	1	1	1	1	1	12	12	100.0
157.2	1	1	1	1	1	1	1	1	1	1	1	1	12	12	100.0
57.3	1	1	1	1	1	1	1	1	1	1	1	1	12	12	100.0
36.6	1	1	1	1	1	1							6	6	100.0
19.2	1	1	1	1	1	1							6	6	100.0

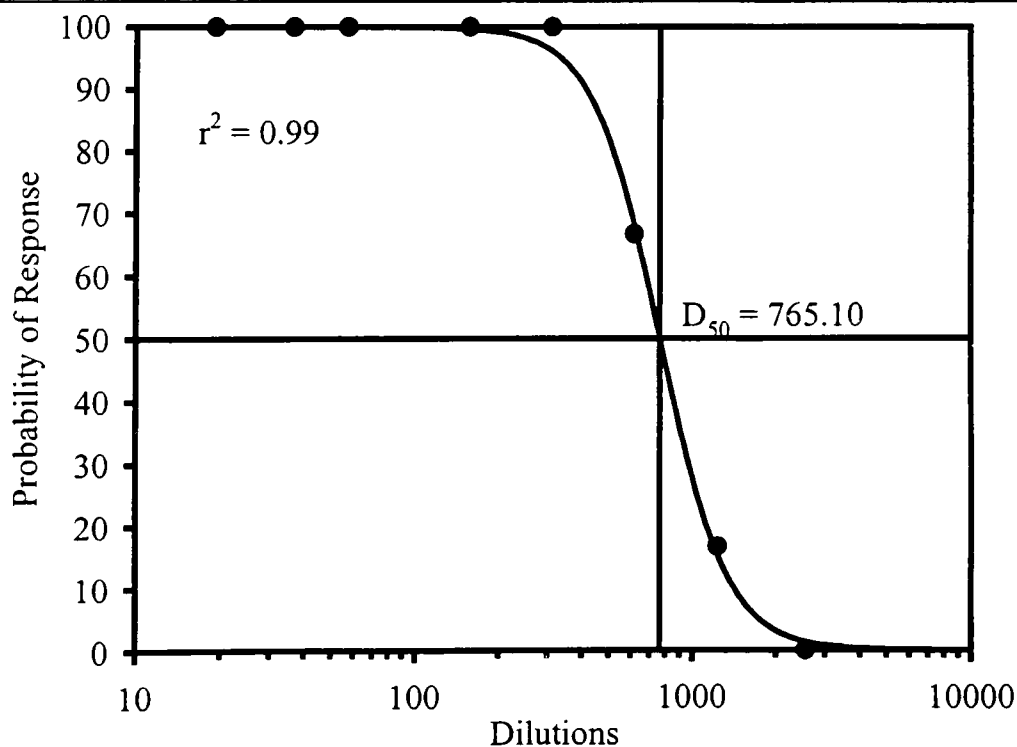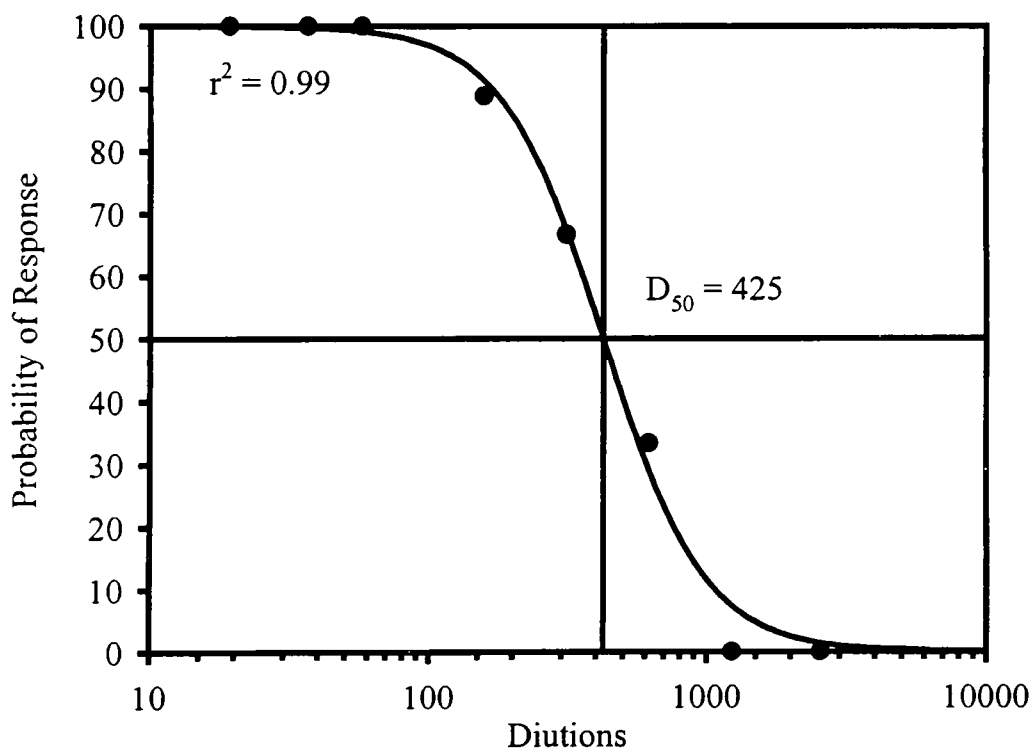| Annoyance															
Dilutions	1	2	3	4	5	6	7	8	9	10	11	12	Total	No. of measurements	Average
2557.5	0	0	0	0	0	0							0	6	0
1235.6	1	0	0	0	0	0	1	0	0	0	2	0	4	6	0.67
618.9	1	0	2	0	7	1	1	4	2	1	2	1	22	12	1.83
312.2	3	3	4	8	8	3	2	3	4	5	3	2	48	12	4.0
157.2	4	5	6	10	9	3	3	5	5	10	6	4	70	12	5.83
57.3	6	5	8	10	7	5	4	9	10	8	9	6	87	12	7.25
36.6	8	8	8	10	7	6							47	6	7.83
19.2	8	10	8	10	6	6							48	6	8.0

Figure B.12: Probability of response and dilution-to-threshold of the299C sample in the third experiment.

Table B.13: Determination of probability of response and annoyance for each dilution of 300C sample in the third experiment.

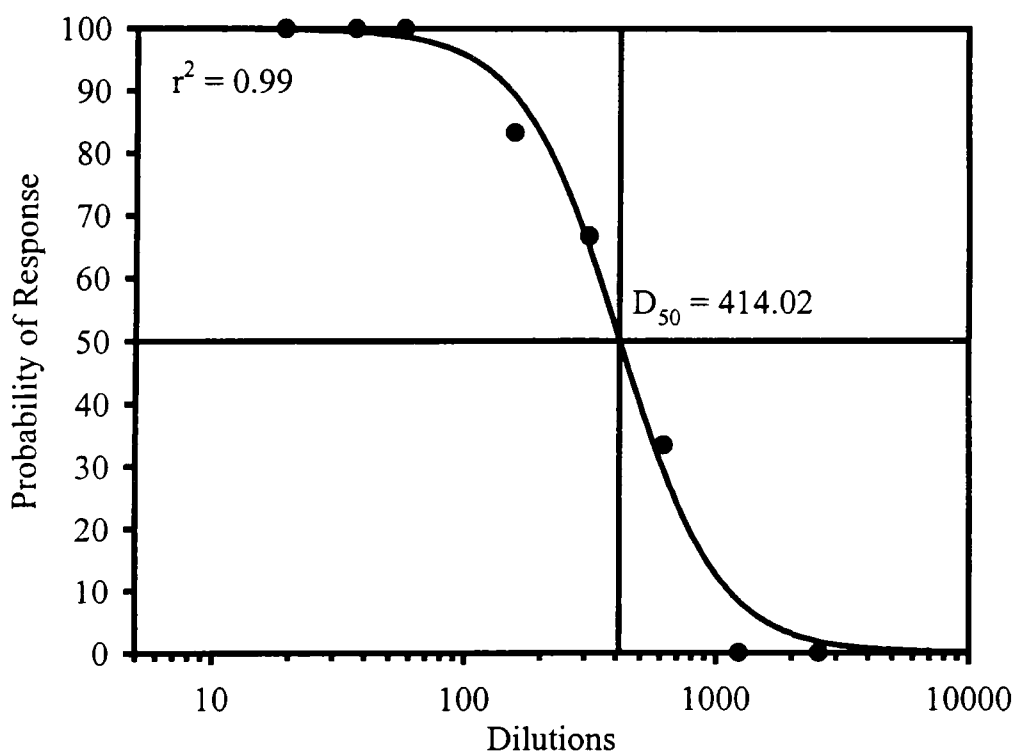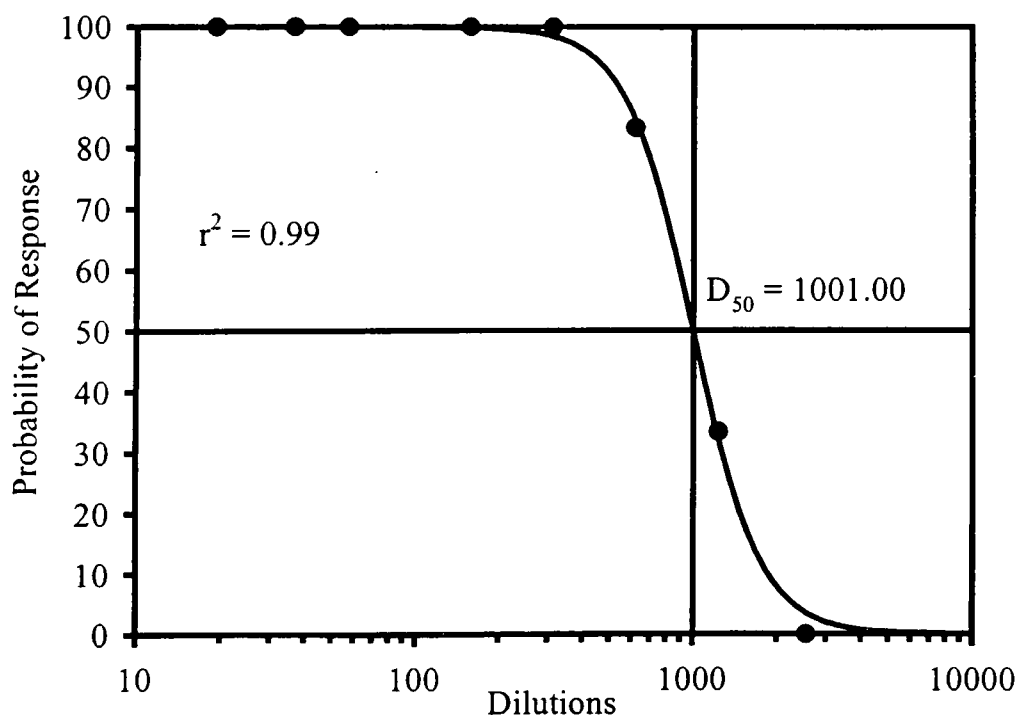| Probability of Response															
Dilutions	1	2	3	4	5	6	7	8	9	10	11	12	Total	No. of measurements	%
2557.5	0	0	0	0	0	0							0	6	0
1235.6	0	0	0	0	1	0							1	6	16.67
618.9	1	1	0	1	1	1	1	1	1	1	1	1	11	12	91.67
312.2	1	1	1	1	1	1	1	1	1	1	1	1	12	12	100
157.2	1	1	1	1	1	1	1	1	1	1	1	1	12	12	100
57.3	1	1	1	1	1	1							6	6	100
36.6	1	1	1	1	1	1							6	6	100
19.2	1	1	1	1	1	1							6	6	100
Annoyance															
Dilutions	1	2	3	4	5	6	7	8	9	10	11	12	Total	No. of measurements	Average
2557.5	0	0	0	0	0	0							0	6	0
1235.6	0	0	0	0	1	0							1	6	0.17
618.9	2	2	0	2	4	7	1	2	5	2	2	7	36	12	3
312.2	6	4	6	4	7	10	2	2	8	3	4	10	66	12	5.50
157.2	10	5	8	6	8	10	5	3	8	3	5	10	81	12	6.75
57.3	10	6	8	4	8	10							46	6	7.67
36.6	10	7	9	4	8	10							48	6	8
19.2	8	8	10	6	7	10							49	6	8.17

$r^2 = 0.99$

$D_{50} = 936.09$

Figure B.13: Probability of response and dilution-to-threshold of the 300C sample in the third experiment.

Table B.14: Determination of probability of response and annoyance for each dilution of 300F sample in the third experiment.

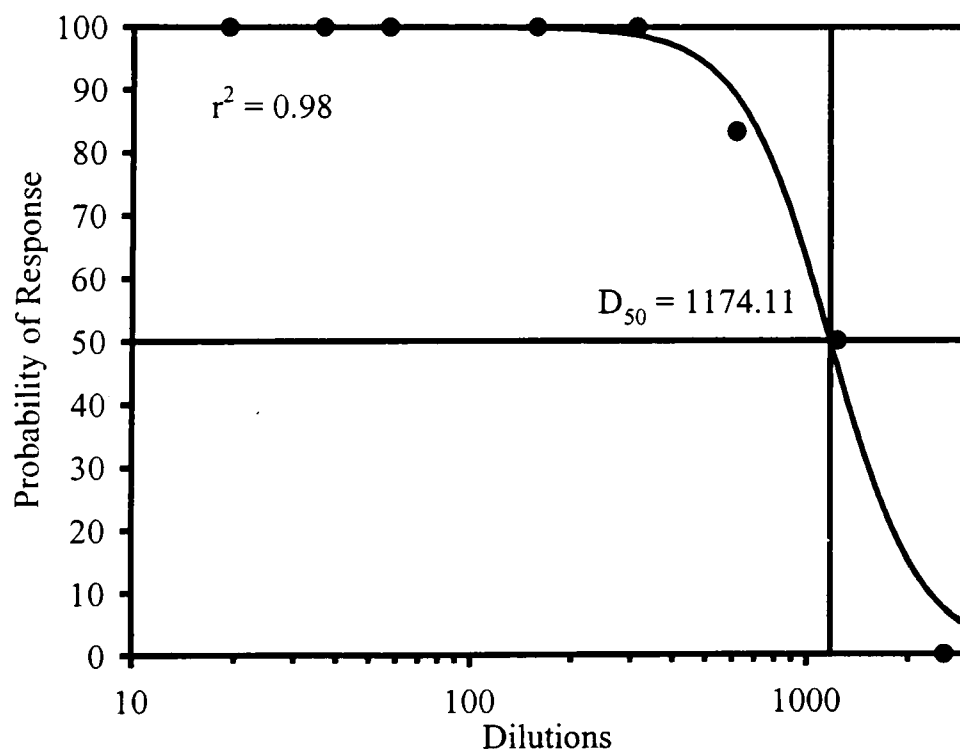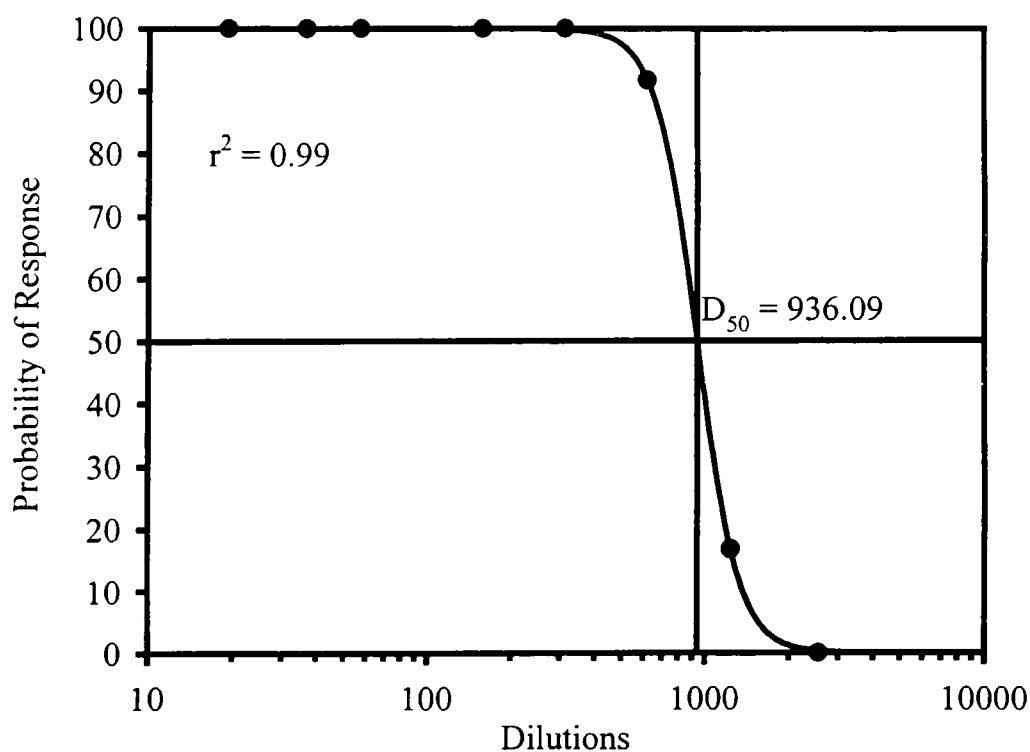| Probability of Response															
Dilution	1	2	3	4	5	6	7	8	9	10	11	12	Total	No. of measurements	%
2557.5	0	0	0	0	0	0							0	6	0
1235.6	0	0	0	0	0	1							1	6	16.67
618.9	1	1	0	0	1	1	1	1	0	0	1	1	8	12	66.67
312.2	1	1	1	1	1	1	1	1	1	1	1	1	12	12	100
157.2	1	1	1	1	1	1	1	1	1	1	1	1	12	12	100
57.3	1	1	1	1	1	1							6	6	100
36.6	1	1	1	1	1	1							6	6	100
19.2	1	1	1	1	1	1							6	6	100
Annoyance															
Dilution	1	2	3	4	5	6	7	8	9	10	11	12	Total	No. of measurements	Average
2557.5	0	0	0	0	0	0							0	6	0
1235.6	0	0	0	0	0	0.5							0.5	6	0.08
618.9	2	2	0	0	4	2	1	1	0	0	2	3	17	12	1.42
312.2	4	4	4	4	5	3	1	5	4	4	3	2	43	12	3.58
157.2	4	8	6	6	6	4	3	4	8	6	4	5	64	12	5.33
57.3	5	8	4	8	7	6							38	6	6.33
36.6	5	8	6	10	7	7							43	6	7.17
19.2	7	8	8	10	9	7							49	6	8.17
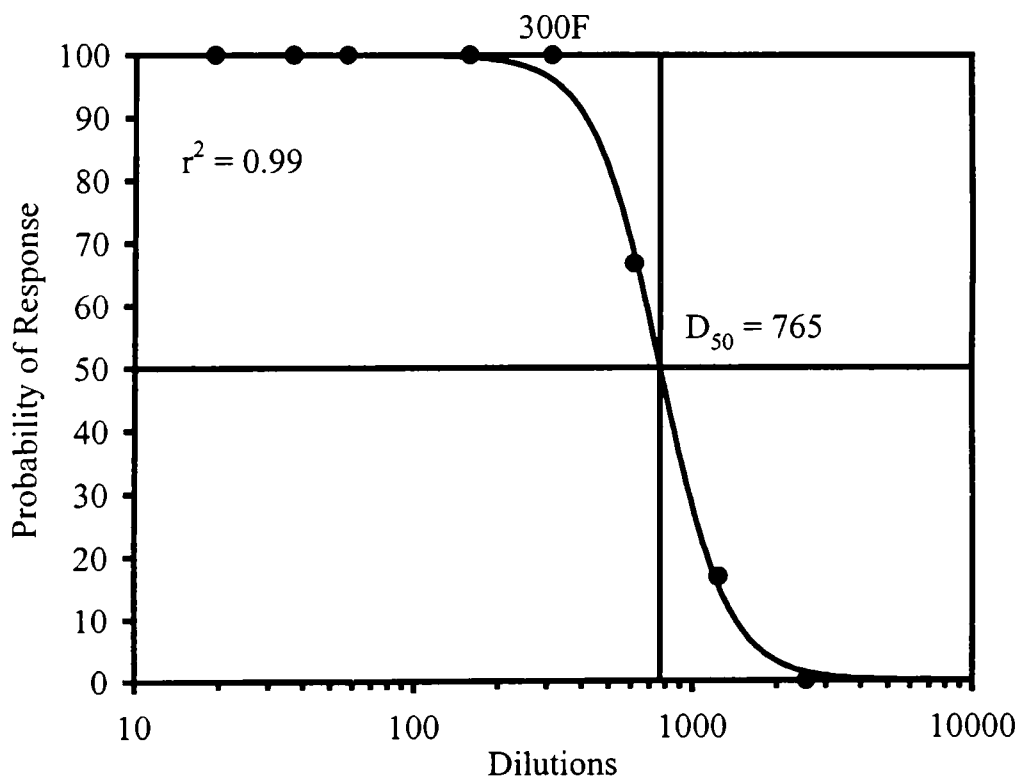
Figure B.14: Probability of response and dilution-to-threshold of the 300F sample in the third experiment.

Table B.15: Determination of probability of response and annoyance for each dilution of Fosse sample in the third experiment.

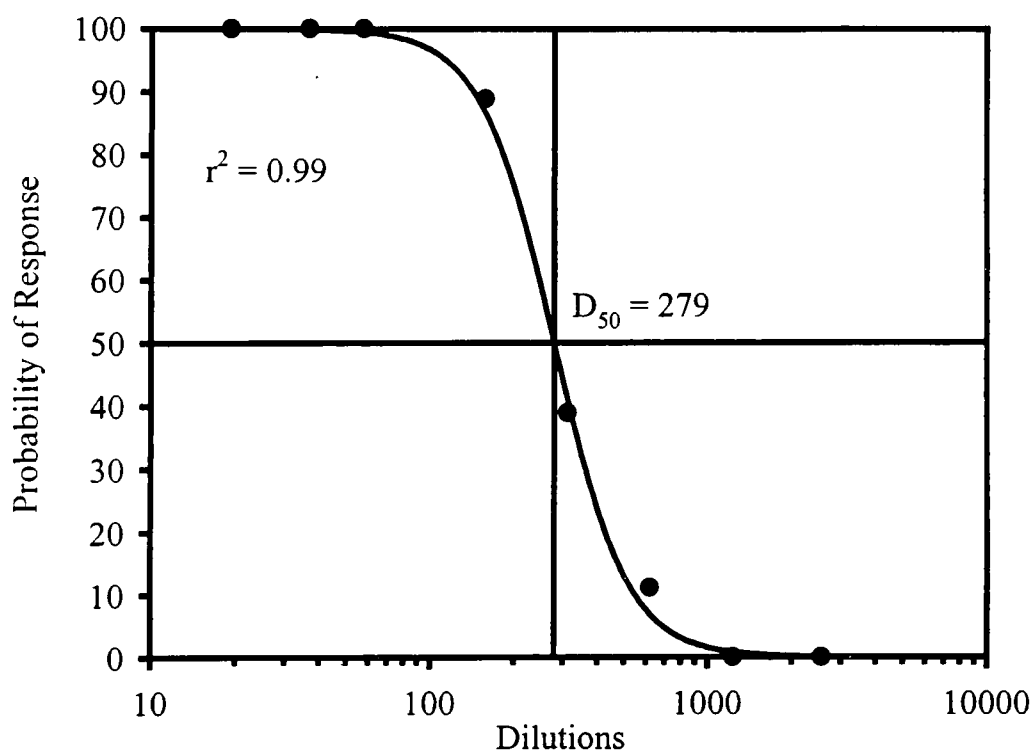|										Probability of Response											
Dilutions	1	2	3	4	5	6	7	8	9	10	11	12	13	14	15	16	17	18	Total	No. of measurements	%
2557.5	0	0	0	0	0	0	0	0	0	0	0	0							0	12	0
1235.6	0	0	0	0	0	0	0	0	0	0	0	0							0	12	0
618.9	0	1	0	0	0	1	0	0	0	0	0	0	0	0	0	0	0	0	2	18	11.11
312.2	1	1	0	1	0	1	1	0	0	0	0	0	1	1	0	0	0	0	7	18	38.89
157.2	1	1	1	1	1	1	1	1	1	1	1	0	1	1	1	1	1	0	16	18	88.89
57.3	1	1	1	1	1	1													6	6	100
36.6	1	1	1	1	1	1													6	6	100
19.2	1	1	1	1	1	1													6	6	100
										Annoyance											
Dilutions	1	2	3	4	5	6	7	8	9	10	11	12	13	14	15	16	17	18	Total	No. of measurements	Average
2557.5	0	0	0	0	0	0	0	0	0	0	0	0							0	12	0
1235.6	0	0	0	0	0	0	0	0	0	0	0	0							0	12	0
618.9	0	2	0	0	0	1	0	0	0	0	0	0	0	0	0	0	0	0	3	18	0.17
312.2	2	2	0	1	0	2	0	0	0	0	0	0	1	5	0	0	0	0	13	18	0.72
157.2	1	3	3	2	3	7	1	3	2	1	3	0	1	4	2	1	2	0	39	18	2.17
57.3	2	5	4	4	4	1													20	6	3.33
36.6	4	5	4	6	6	3													28	6	4.67
19.2	5	6	6	3	5	4													29	6	4.83

$r^2 = 0.99$

$D_{50} = 279$

Figure B.15: Probability of response and dilution-to-threshold of the Fosse sample in the third experiment.

Appendix C

Source Parameters

Point Sources

First Experiment

Table C.1: Coordinates of point sources and emission characteristics in the first experiment.

Source I.D	x-coordinates	y-coordinates	Diameter (m)	Exit Velocity	Emission rate	Exit Temp. (K)	Release Height (m)
A1	682530.9	5107388	0.5	7.8	745.6	305	2.17
A2	682533.1	5107386	0.4	8.4	468.7	305	2.14
A3	682535.3	5107383	0.6	7.0	888.4	305	2.22
A4	682537.5	5107381	0.5	7.8	745.6	305	2.17
A5	682539.7	5107379	0.4	8.4	468.7	305	2.14
A6	682541.9	5107377	0.6	7.0	888.4	305	2.22
A7	682544.1	5107375	0.5	7.8	745.6	305	2.17
A8	682546.3	5107373	0.4	7.8	468.7	305	2.14
A9	682548.5	5107370	0.6	7.0	888.4	305	2.22
A10	682550.7	5107368	0.5	7.8	745.6	305	2.17
A11	682552.9	5107366	0.4	8.4	468.7	305	2.14
A12	682555.1	5107364	0.6	7.0	888.4	305	2.22
A13	682561	5107358	0.5	7.8	745.6	305	2.17
A14	682563.2	5107356	0.4	8.4	468.7	305	2.14
A15	682565.4	5107354	0.6	7.0	888.4	305	2.22
A16	682567.7	5107351	0.5	7.8	745.6	305	2.17
A17	682569.9	5107349	0.4	8.4	468.7	305	2.14
A18	682572.1	5107347	0.6	7.0	888.4	305	2.22
A19	682574.3	5107345	0.5	7.8	745.6	305	2.17
A20	682576.5	5107343	0.4	8.4	468.7	305	2.14
A21	682578.7	5107340	0.6	7.0	888.4	305	2.22
A22	682580.9	5107338	0.5	7.8	745.6	305	2.17
A23	682583.1	5107336	0.4	8.4	468.7	305	2.14
A24	682585.3	5107334	0.6	7.0	888.4	305	2.22
B1	682659.9	5107260	0.5	7.8	745.6	305	2.17
B2	682662.1	5107258	0.4	8.4	468.7	305	2.14
B3	682664.3	5107255	0.6	7.0	888.4	305	2.22
B4	682666.5	5107253	0.5	7.8	745.6	305	2.17
B5	682668.7	5107251	0.4	8.4	468.7	305	2.14
B6	682670.9	5107249	0.6	7.0	888.4	305	2.22
B7	682673.1	5107247	0.5	7.8	745.6	305	2.17
B8	682675.3	5107245	0.4	8.4	468.7	305	2.14
B9	682677.5	5107242	0.6	7.8	888.4	305	2.22
B10	682679.7	5107240	0.5	7.8	745.6	305	2.17
B11	682681.9	5107238	0.4	8.4	468.7	305	2.14

Table C.1 (continued): Coordinates of point sources and emission characteristics in the first experiment.

Source I.D	x-coordinates	y-coordinates	Diameter (m)	Exit Velocity	Emission rate	Exit Temp. (K)	Release Height (m)
B12	682684.1	5107236	0.6	7.0	888.4	305	2.22
B13	682690	5107230	0.5	7.8	745.6	305	2.17
B14	682692.2	5107228	0.4	8.4	468.7	305	2.14
B15	682694.4	5107226	0.6	7.8	888.4	305	2.22
B16	682696.7	5107223	0.5	7.8	745.6	305	2.17
B17	682698.9	5107221	0.4	8.4	468.7	305	2.14
B18	682701.1	5107219	0.6	7.0	888.4	305	2.22
B19	682703.3	5107217	0.5	7.8	745.6	305	2.17
B20	682705.5	5107215	0.4	8.4	468.7	305	2.14
B21	682707.7	5107212	0.6	7.0	888.4	305	2.22
B22	682709.9	5107210	0.5	7.8	745.6	305	2.17
B23	682712.1	5107208	0.4	8.4	468.7	305	2.14
B24	682714.3	5107206	0.6	7.0	888.4	305	2.22

Second Experiment

Table C.2: Coordinates of point sources and emission characteristics in the second experiment.

Source I.D	x-coordinates	y-coordinates	Diameter (m)	Exit Velocity	Emission rate	Exit Temp. (K)	Release Height (m)
A1	682530.9	5107388	0.5	1.2	121.6	296	2.17
A2	682533.1	5107386	0.4	1.3	76.4	296	2.14
A3	682535.3	5107383	0.6	1.1	144.8	296	2.22
A4	682537.5	5107381	0.5	1.2	121.6	296	2.17
A5	682539.7	5107379	0.4	1.3	76.4	296	2.14
A6	682541.9	5107377	0.6	1.1	144.8	296	2.22
A7	682544.1	5107375	0.5	1.2	121.6	296	2.17
A8	682546.3	5107373	0.4	1.3	76.4	296	2.14
A9	682548.5	5107370	0.6	1.1	144.8	296	2.22
A10	682550.7	5107368	0.5	1.2	121.6	296	2.17
A11	682552.9	5107366	0.4	1.3	76.4	296	2.14
A12	682555.1	5107364	0.6	1.1	144.8	296	2.22
A13	682561	5107358	0.5	1.2	208.9	296	2.17
A14	682563.2	5107356	0.4	1.3	131.3	296	2.14
A15	682565.4	5107354	0.6	1.1	248.9	296	2.22
A16	682567.7	5107351	0.5	1.2	208.9	296	2.17
A17	682569.9	5107349	0.4	1.3	131.3	296	2.14
A18	682572.1	5107347	0.6	1.1	248.9	296	2.22
A19	682574.3	5107345	0.5	1.2	208.9	296	2.17
A20	682576.5	5107343	0.4	1.3	131.3	296	2.14
A21	682578.7	5107340	0.6	1.1	248.9	296	2.22
A22	682580.9	5107338	0.5	1.2	208.9	296	2.17

Table C.2 (continued): Coordinates of point sources and emission characteristics in the second experiment.

Source I.D	x-coordinates	y-coordinates	Diameter (m)	Exit Velocity	Emission rate	Exit Temp. (K)	Release Height (m)
A23	682583.1	5107336	0.4	1.3	131.3	296	2.14
A24	682585.3	5107334	0.6	1.1	248.9	296	2.22
B1	682659.9	5107260	0.5	1.1	194.0	296	2.17
B2	682662.1	5107258	0.4	1.2	122.0	296	2.14
B3	682664.3	5107255	0.6	1.0	231.1	296	2.22
B4	682666.5	5107253	0.5	1.1	194.0	296	2.17
B5	682668.7	5107251	0.4	1.2	122.0	296	2.14
B6	682670.9	5107249	0.6	1.0	231.1	296	2.22
B7	682673.1	5107247	0.5	1.1	194.0	296	2.17
B8	682675.3	5107245	0.4	1.2	122.0	296	2.14
B9	682677.5	5107242	0.6	1.0	231.1	296	2.22
B10	682679.7	5107240	0.5	1.1	194.0	296	2.17
B11	682681.9	5107238	0.4	1.2	122.0	296	2.14
B12	682684.1	5107236	0.6	1.0	231.1	296	2.22
B13	682690	5107230	0.5	1.1	107.7	296	2.17
B14	682692.2	5107228	0.4	1.2	67.7	296	2.14
B15	682694.4	5107226	0.6	1.0	128.3	296	2.22
B16	682696.7	5107223	0.5	1.1	107.7	296	2.17
B17	682698.9	5107221	0.4	1.2	67.7	296	2.14
B18	682701.1	5107219	0.6	1.0	128.3	296	2.22
B19	682703.3	5107217	0.5	1.1	107.7	296	2.17
B20	682705.5	5107215	0.4	1.2	67.7	296	2.14
B21	682707.7	5107212	0.6	1.0	128.3	296	2.22
B22	682709.9	5107210	0.5	1.1	107.7	296	2.17
B23	682712.1	5107208	0.4	1.2	67.7	296	2.14
B24	682714.3	5107206	0.6	1.0	128.3	296	2.22

Experiment 3

Table C.3: Coordinates of point sources and emission characteristics in the third experiment.

Source I.D	x-coordinates	y-coordinates	Diameter (m)	Exit Velocity	Emission rate	Exit Temp. (K)	Release Height (m)
A1	682530.9	5107388	0.5	1.1	293.1	298	2.17
A2	682533.1	5107386	0.4	1.2	184.2	298	2.14
A3	682535.3	5107383	0.6	1.0	349.1	298	2.22
A4	682537.5	5107381	0.5	1.1	293.1	298	2.17
A5	682539.7	5107379	0.4	1.2	184.2	298	2.14
A6	682541.9	5107377	0.6	1.0	349.1	298	2.22

Table C.3 (continued): Coordinates of point sources and emission characteristics in the third experiment.

Source I.D	x-coordinates	y-coordinates	Diameter (m)	Exit Velocity	Emission rate	Exit Temp. (K)	Release Height (m)
A7	682544.1	5107375	0.5	1.1	293.1	298	2.17
A8	682546.3	5107373	0.4	1.2	184.2	298	2.14
A9	682548.5	5107370	0.6	1.0	349.1	298	2.22
A10	682550.7	5107368	0.5	1.1	293.1	298	2.17
A11	682552.9	5107366	0.4	1.2	184.2	298	2.14
A12	682555.1	5107364	0.6	1.0	349.1	298	2.22
A13	682561	5107358	0.5	1.1	249.8	298	2.17
A14	682563.2	5107356	0.4	1.2	157.1	298	2.14
A15	682565.4	5107354	0.6	1.0	297.6	298	2.22
A16	682567.7	5107351	0.5	1.1	249.8	298	2.17
A17	682569.9	5107349	0.4	1.2	157.1	298	2.14
A18	682572.1	5107347	0.6	1.0	297.6	298	2.22
A19	682574.3	5107345	0.5	1.1	249.8	298	2.17
A20	682576.5	5107343	0.4	1.2	157.1	298	2.14
A21	682578.7	5107340	0.6	1.0	297.6	298	2.22
A22	682580.9	5107338	0.5	1.1	249.8	298	2.17
A23	682583.1	5107336	0.4	1.2	157.1	298	2.14
A24	682585.3	5107334	0.6	1.0	297.6	298	2.22
B1	682659.9	5107260	0.5	1.0	172.7	298	2.17
B2	682662.1	5107258	0.4	1.1	108.5	298	2.14
B3	682664.3	5107255	0.6	0.9	205.7	298	2.22
B4	682666.5	5107253	0.5	1.0	172.7	298	2.17
B5	682668.7	5107251	0.4	1.1	108.5	298	2.14
B6	682670.9	5107249	0.6	0.9	205.7	298	2.22
B7	682673.1	5107247	0.5	1.0	172.7	298	2.17
B8	682675.3	5107245	0.4	1.1	108.5	298	2.14
B9	682677.5	5107242	0.6	0.9	205.7	298	2.22
B10	682679.7	5107240	0.5	1.0	172.7	298	2.17
B11	682681.9	5107238	0.4	1.1	108.5	298	2.14
B12	682684.1	5107236	0.6	0.9	205.7	298	2.22
B13	682690	5107230	0.5	1.0	211.3	298	2.17
B14	682692.2	5107228	0.4	1.1	132.7	298	2.14
B15	682694.4	5107226	0.6	0.9	251.6	298	2.22
B16	682696.7	5107223	0.5	1.0	511.3	298	2.17
B17	682698.9	5107221	0.4	1.1	132.7	298	2.14
B19	682703.3	5107217	0.5	1.0	211.3	298	2.17
B20	682705.5	5107215	0.4	1.1	132.7	298	2.14
B21	682707.7	5107212	0.6	0.9	251.6	298	2.22
B22	682709.9	5107210	0.5	1.0	211.3	298	2.17
B23	682712.1	5107208	0.4	1.1	132.7	298	2.14
B24	682714.3	5107206	0.6	0.9	251.6	298	2.22

Area Sources

Table C.4: Coordinates of the area sources and their emission characteristics.

Source ID	x-coordinates.	y-coordinates	Length of side X	Length of side Y	Release Ht. (m)	Emission Rate		
						Exp. 1	Exp.2	Exp.3
A1	682530.6	5107387	3.4	0.52	2.18	490.2	78.2	188.4
A2	682533	5107385	3.4	0.52	2.18	490.2	78.2	188.4
A3	682535.4	5107383	3.4	0.52	2.18	490.2	78.2	188.4
A4	682537.8	5107380	3.4	0.52	2.18	490.2	78.2	188.4
A5	682540.2	5107378	3.4	0.52	2.18	490.2	78.2	188.4
A6	682542.6	5107375	3.4	0.52	2.18	490.2	78.2	188.4
A7	682545	5107373	3.4	0.52	2.18	490.2	78.2	188.4
A8	682547.4	5107371	3.4	0.52	2.18	490.2	78.2	188.4
A9	682573.1	5107346	3.4	0.52	2.18	490.2	78.2	188.4
A10	682552.2	5107366	3.4	0.52	2.18	490.2	78.2	188.4
A11	682561	5107358	3.4	0.52	2.18	490.2	134.3	160.6
A12	682563.5	5107356	3.4	0.52	2.18	490.2	134.3	160.6
A13	682565.9	5107353	3.4	0.52	2.18	490.2	134.3	160.6
A14	682568.3	5107351	3.4	0.52	2.18	490.2	134.3	160.6
A15	682570.7	5107348	3.4	0.52	2.18	490.2	134.3	160.6
A16	682577.9	5107341	3.4	0.52	2.18	490.2	134.3	160.6
A17	682575.5	5107344	3.4	0.52	2.18	490.2	134.3	160.6
A18	682580.3	5107339	3.4	0.52	2.18	490.2	134.3	160.6
A19	682582.7	5107336	3.4	0.52	2.18	490.2	134.3	160.6
A20	682549.8	5107368	3.4	0.52	2.18	490.2	134.3	160.6
B1	682659.6	5107259	3.4	0.52	2.18	490.2	124.7	111.0
B2	682662	5107257	3.4	0.52	2.18	490.2	124.7	111.0
B3	682664.4	5107255	3.4	0.52	2.18	490.2	124.7	111.0
B4	682666.8	5107252	3.4	0.52	2.18	490.2	124.7	111.0
B5	682669.2	5107250	3.4	0.52	2.18	490.2	124.7	111.0
B6	682671.6	5107247	3.4	0.52	2.18	490.2	124.7	111.0
B7	682674	5107245	3.4	0.52	2.18	490.2	124.7	111.0
B8	682676.4	5107243	3.4	0.52	2.18	490.2	124.7	111.0
B9	682678.8	5107240	3.4	0.52	2.18	490.2	124.7	111.0
B10	682681.2	5107238	3.4	0.52	2.18	490.2	124.7	111.0
B11	682689.7	5107230	3.4	0.52	2.18	490.2	69.2	135.8
B12	682692.1	5107227	3.4	0.52	2.18	490.2	69.2	135.8
B13	682694.5	5107225	3.4	0.52	2.18	490.2	69.2	135.8
B14	682696.9	5107222	3.4	0.52	2.18	490.2	69.2	135.8
B15	682699.3	5107220	3.4	0.52	2.18	490.2	69.2	135.8
B16	682701.7	5107218	3.4	0.52	2.18	490.2	69.2	135.8

Table C.4 (continued): Coordinates of the area sources and their emission characteristics.

Source ID	x-coordinates	y-coordinates	Length of side X	Length of side Y	Release Ht. (m)	Emission Rate		
						Exp.1	Exp.2	Exp.3
B17	682704.1	5107215	3.4	0.516	2.18	490.2	69.2	135.8
B18	682706.5	5107213	3.4	0.516	2.18	490.2	69.2	135.8
B19	682708.9	5107210	3.4	0.516	2.18	490.2	69.2	135.8
B20	682711.3	5107208	3.4	0.516	2.18	490.2	69.2	135.8

Volume Sources

Table C.5: Coordinates of nodes of the volume sources and their emission characteristics.

		299C	299F	300C	300F
Node 1	x-coordinates	682530.74	682560.87	682659.74	682689.86
	y- coordinates	5107387.63	5107357.77	5107259.63	5107229.77
Node 2	x- coordinates	682554.96	682585.08	682683.96	682714.08
	y- coordinates	5107363.62	5107333.77	5107235.62	5107205.77
Width (m)		0.52	0.52	0.52	0.52
Emission Rate (OU·m^3/s)	1st Experiment	8406.30	8406.30	8406.30	8406.30
	2nd Experiment	1371.08	2356.49	2188.17	1214.62
	3rd Experiment	3305.13	2817.81	1947.17	2382.34

Manure Storage Tank

Table C.6: Input parameters of the manure storage tank.

Source	x-coordinate	y-coordinate	Release ht. (m)	Velocity (m/s)	Diameter (m)	Emission rate (OU·m^3/s)		
						1st Exp.	2nd Exp.	3rd Exp.
Point	682631.25	5107293.00	2.6	66.2	0.2	433	1346	908
Area	682626.89	5107301.22	2.44	N/R	32	2	2	1.1

N/R: not required

Appendix D

Normalized Probability of Response and Degree of Annoyance Curves

First Experiment
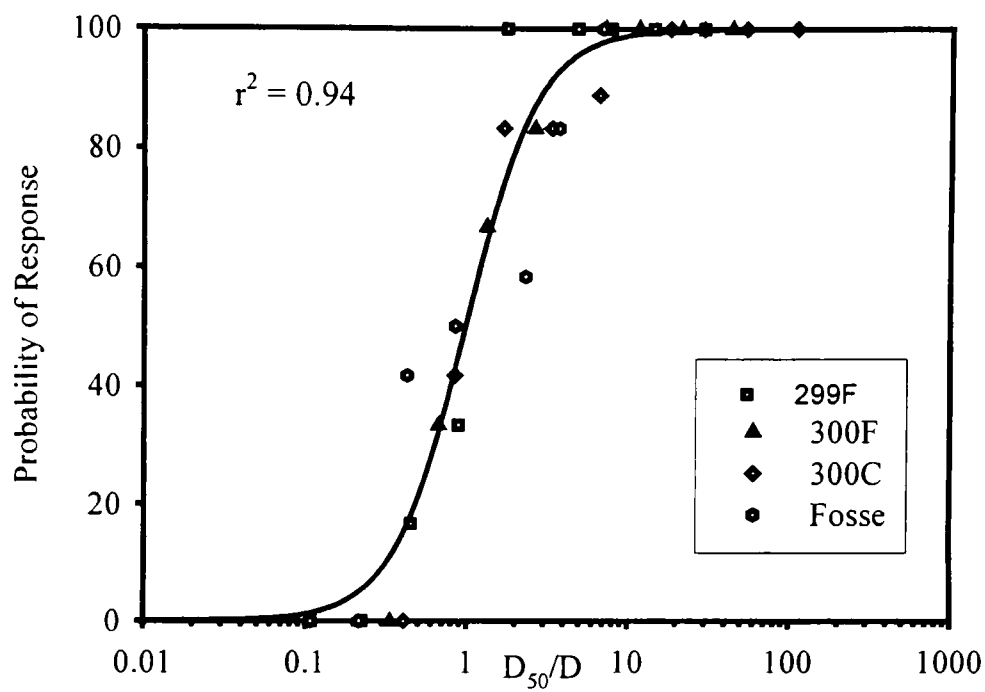
Figure D.1: Normalized probability of response in the first experiment.
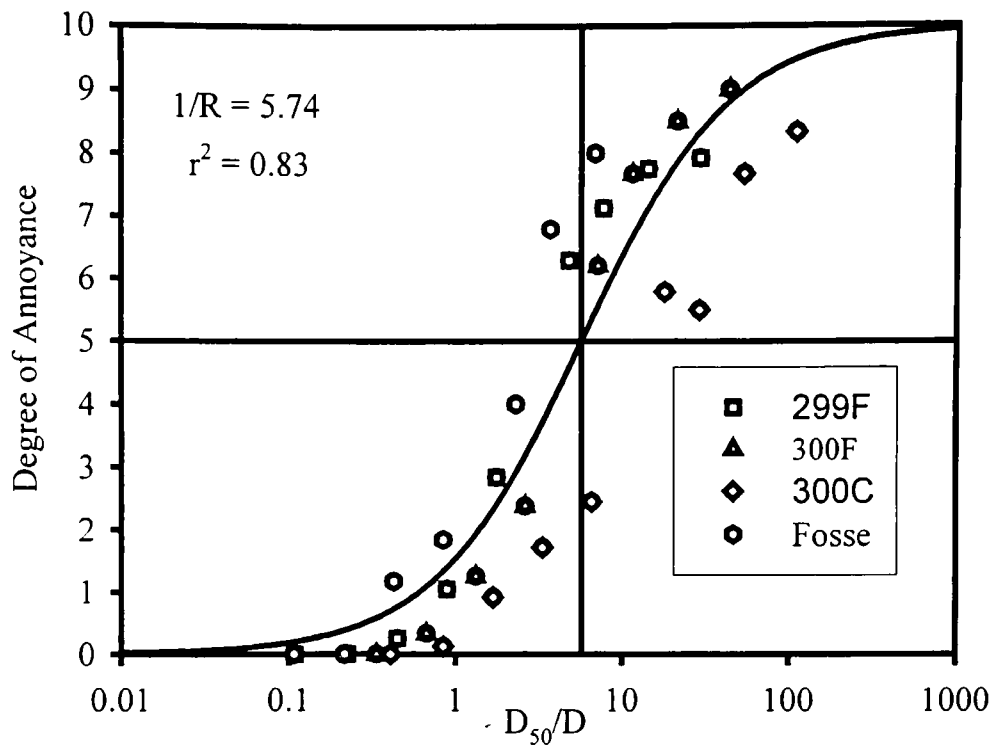
Figure D.2: Normalized degree of annoyance in the first experiment.
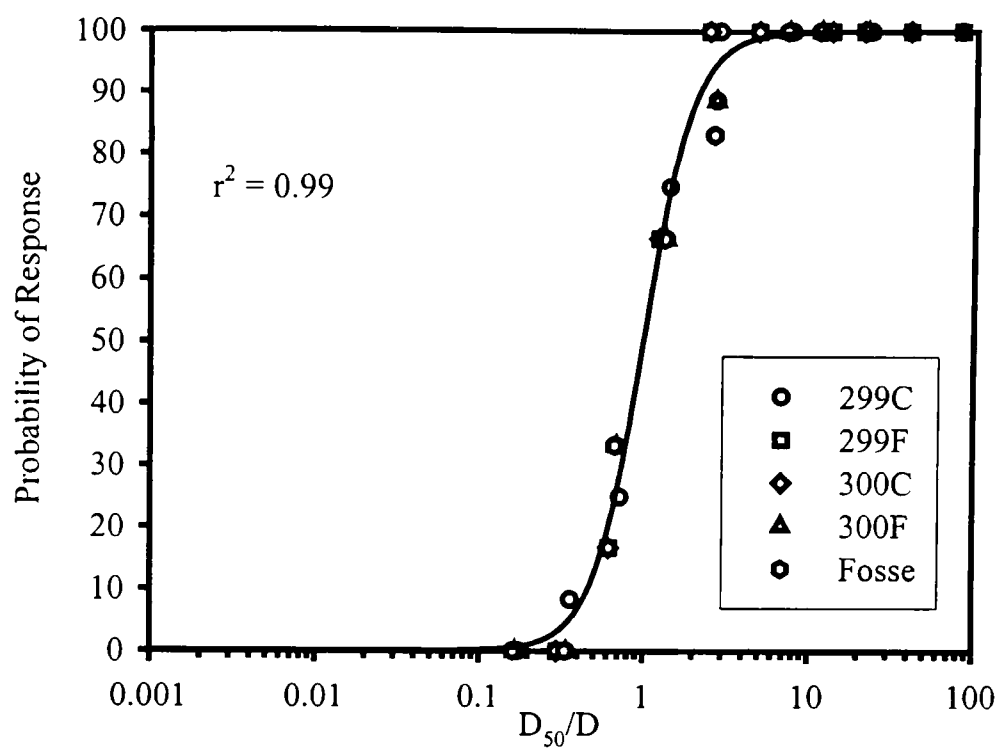
Second Experiment

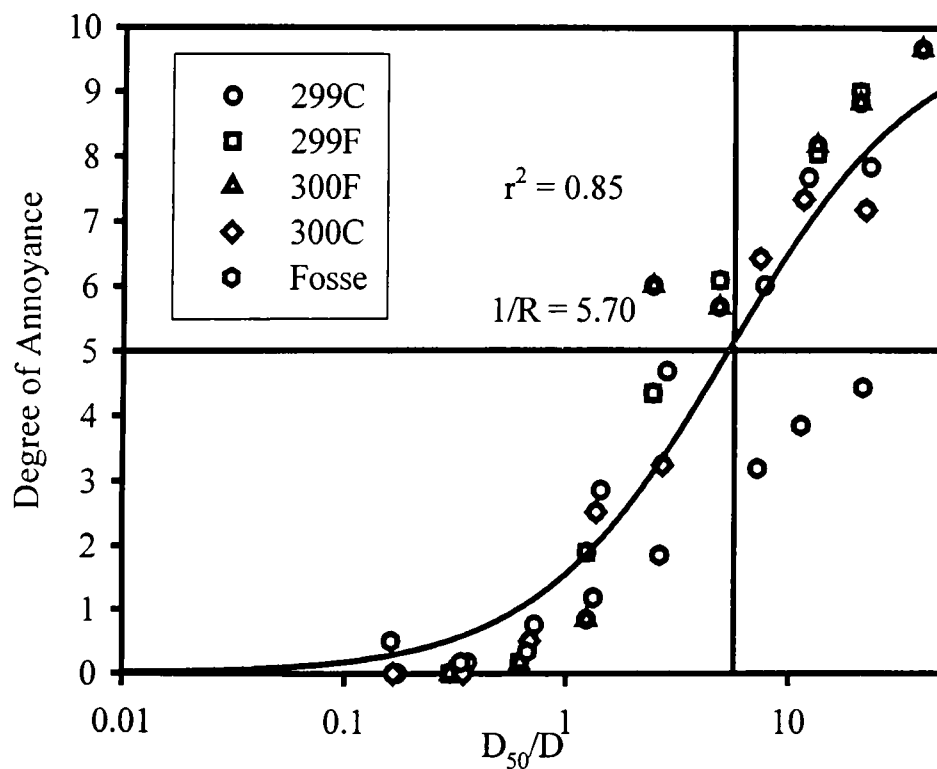Figure D.3: Normalized probability of response in the second experiment.
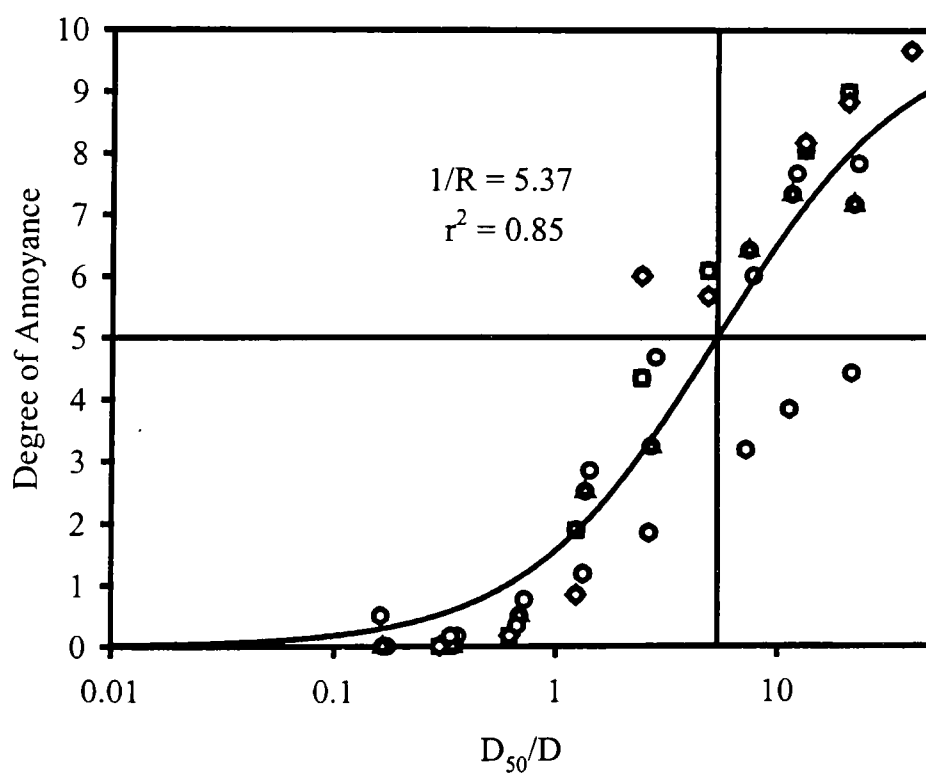
Figure D.4: Normalized degree of annoyance in the second experiment.
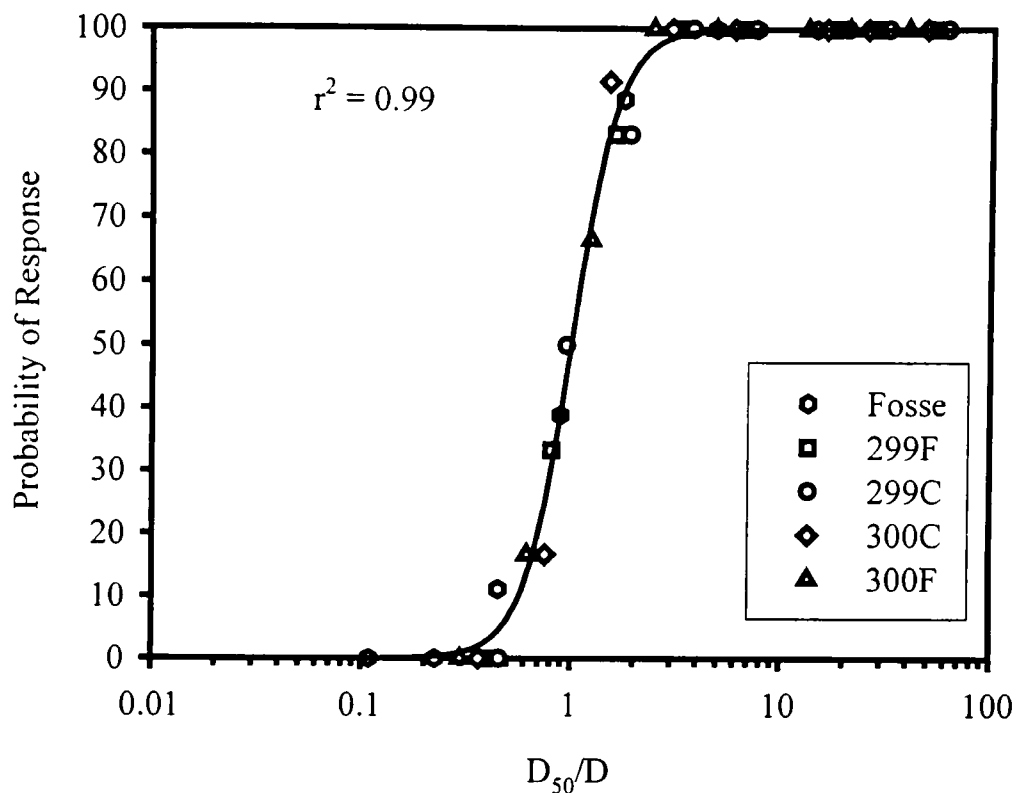
Third Experiment

Figure D.5: Normalized probability of response in the third experiment.

Figure D.6: Normalized degree of annoyance in the third experiment.

Appendix E

Highest Coefficients of Correlation for All Experiments

First Experiment
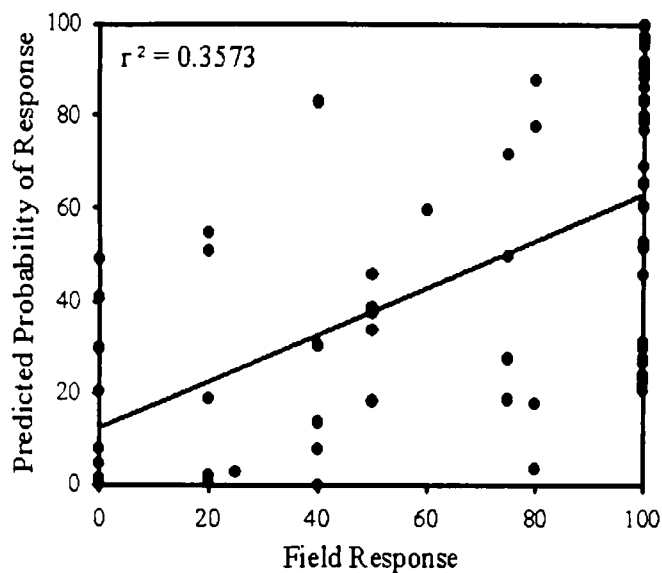
Figure E.1: Highest coefficient of correlation for 1-hour average probability of response occurring for ground level area sources & 1.5m receptors
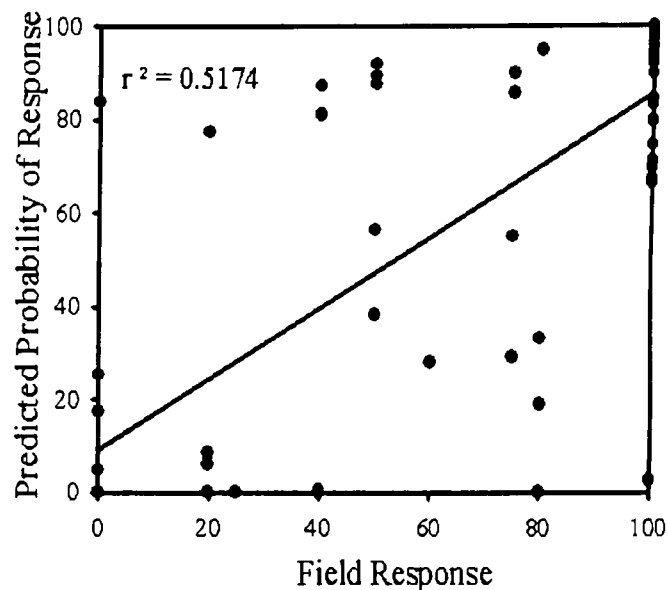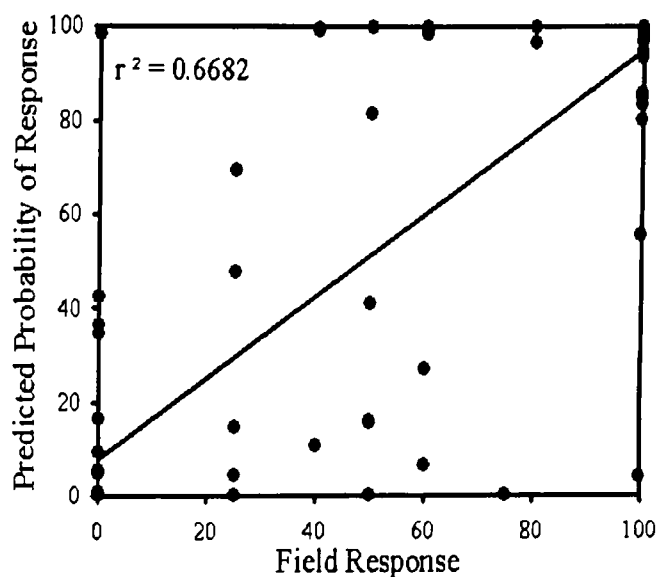

Figure E.2: Highest coefficient of correlation for 1-minute average probability of response occurring for ground level point sources & 1.5m receptors
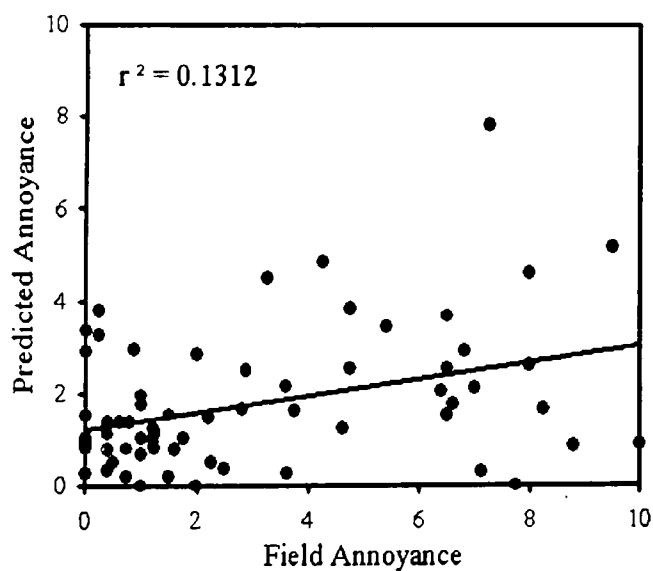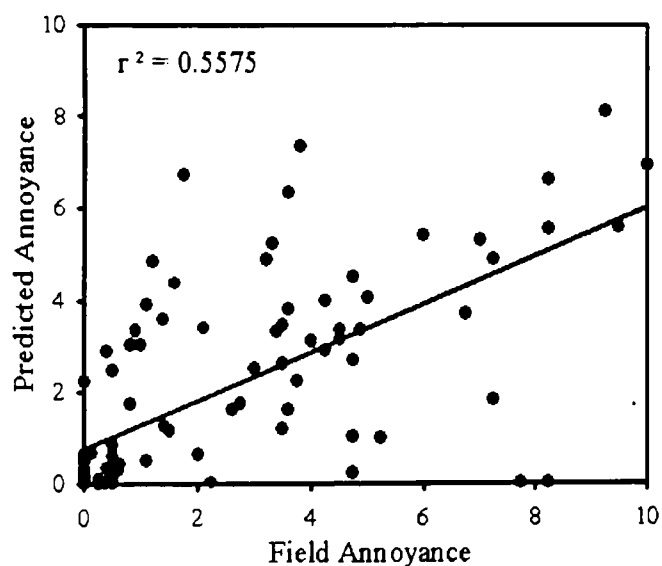

Figure E.3: Highest coefficient of correlation for 1-hour average annoyance occurring for area sources with release height & ground level receptors
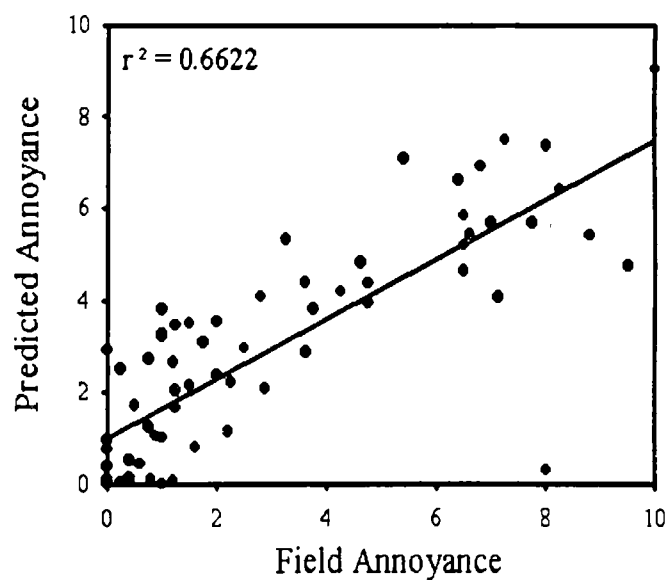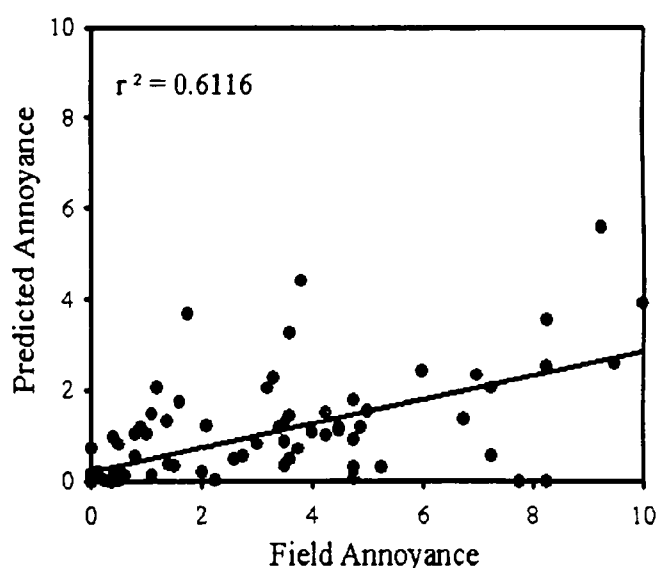

Figure E.4: Highest coefficient of correlation for 1-minute average annoyance occurring for ground level point sources & 1.5m receptors
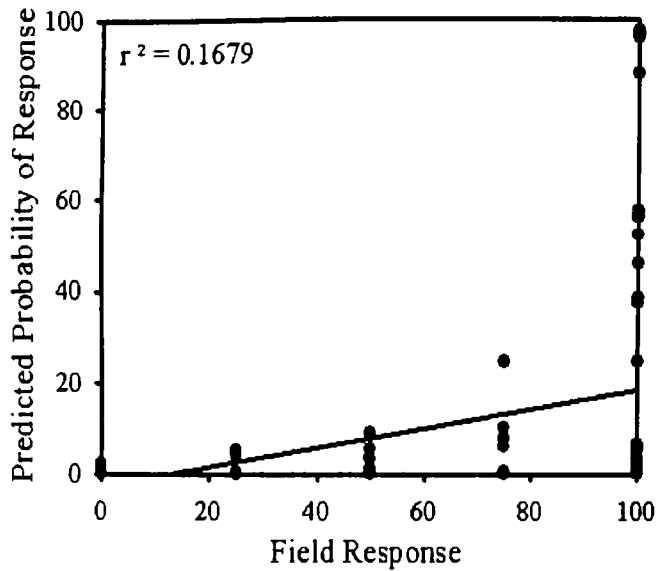
Second Experiment
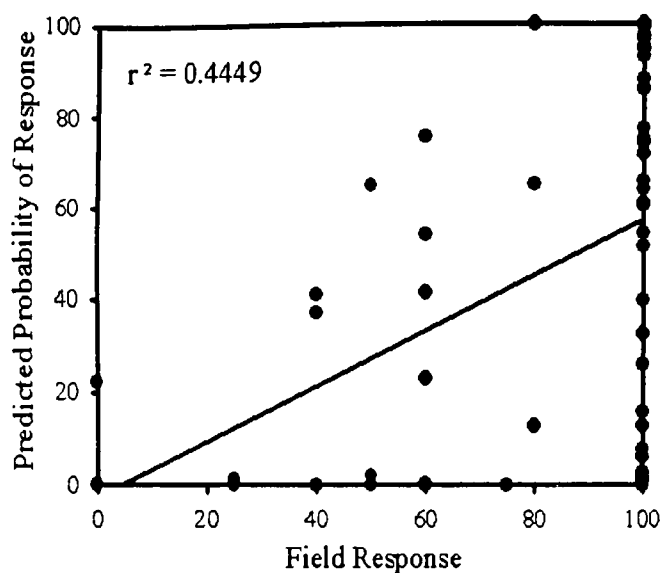
Figure E.5: Highest coefficient of correlation for 1-hour average probability of response occurring for ground level area sources & ground level receptors.

Figure E.6: Highest coefficient of correlation for 1-minute average probability of response occurring for volume sources with release height & ground level receptors.

Figure E.7: Highest coefficient of correlation for 1-hour average annoyance occurring for volume sources with release height & 1.5m receptors.

Figure E.8: Highest coefficient of correlation for 1-minute average annoyance occurring for ground level volume sources & 1.5m receptors.

Third Experiment

Figure E.9: Highest coefficient of correlation for 1-hour average probability of response occurring for ground level area sources & ground level receptors.
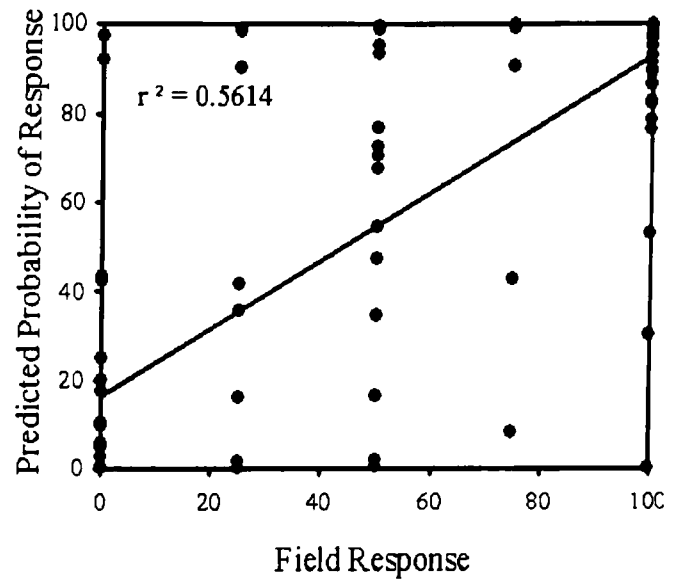

Figure E.10: Highest coefficient of correlation for 1-minute average probability of response occurring for Point sources with release height & ground level receptors.
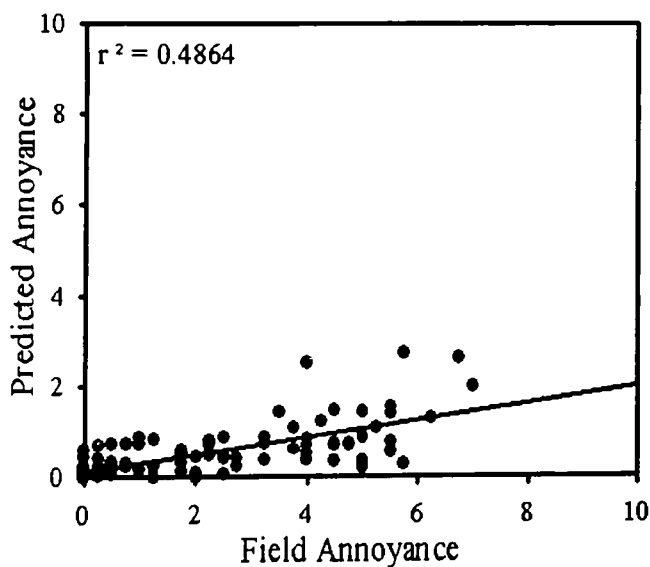

Figure E.11: Highest coefficient of correlation for 1-hour average annoyance occurring for point sources with release height & 1.5m receptors.
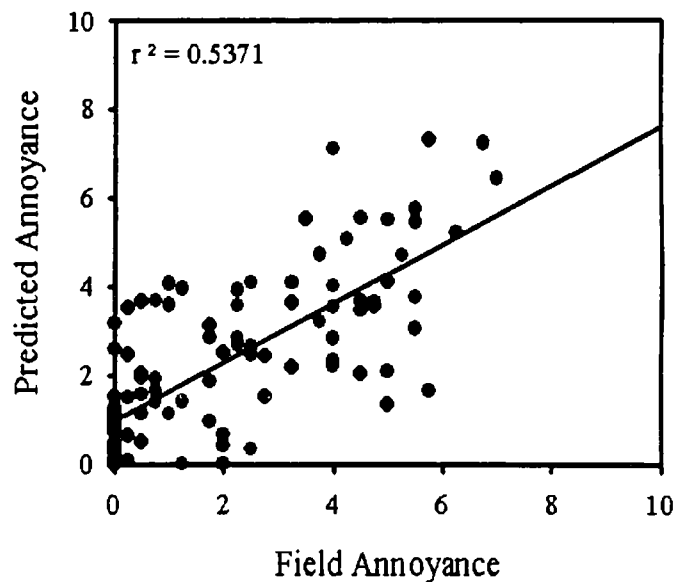

Figure E.12: Highest coefficient of correlation for 1-minute average annoyance occurring for point sources with release height & ground level receptors.

Appendix F

Research Compliance Certificate

McGill University
Faculty of Agricultural and Environmental Sciences

Certificate of Ethical Acceptability for
Research Involving Humans (Revised September 1999)

The Faculty of Agricultural and Environmental Sciences Ethics Review Committee consists of 4 members nominated by the Faculty of Agricultural and Environmental Sciences Nominating Committee and elected by Faculty, an appointed member from the community and an individual versed in ethical issues.

The undersigned considered the application for certification of the ethical acceptability of the project entitled: *TESTING VARIOUS ODOR DISPERSION MODELS FOR THEIR EFFICACY*
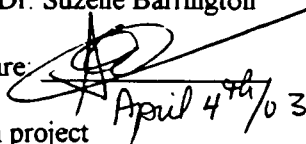
As proposed by:

Applicant's name: Dr. Suzelle Barrington   Supervisor's Name:

Applicant's signature: *[signature] April 4th/03*   Supervisor's Signature: _____

Program: Research project   Company: Ontario Ministry of Agriculture, Food and Rural Affairs (OMAFRA), Conseil du développement du Québec (CDAQ), and Ministère de l'Agriculture, des Pêcheries et de l'Alimentation du Québec (MAPAQ).

The applicant is considered to be:

A full review _____X_____   An expedited review _____

A renewal for an approved project_____   A departmental level review_____
Signature of the chair / Designate

The review committee considers the research procedure and practices by the applicant in this application, to be acceptable on ethical grounds.

1. Prof. Robin Beech
   Department of parasitology
   Psychology

   _____
   signature / date

2. Prof. Peter Jones
   School of dietetics and Human Nutrition

   _____
   signature / date

3. Prof. Harriet Kuhnlein
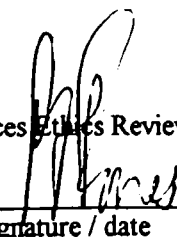   Department of Dietetics and Human Nutrition

   _____
   signature / date

4. Dr. W. Parsons
   Ste. Anne's Hospital

   _____
   signature / date

5. Member of the community – L. Prichard

   _____
   signature / date

Paula Ribeiro
Chair, Faculty of Agricultural and Environmental Sciences Ethics Review Committee
Institute of Parasitology
Tel: (514) 398-7607; Fax: (514) 398-7857

_____   *CHAIR APR 9 '03*
Signature / date

 # 818